LOSSLESS CONVERSION BETWEEN SIGMA-DELTA AND PCM CONVERTERS FOR DIGITAL AUDIO APPLICATIONS, WITH HUMAN AUDIBLE RANGE ANALYSIS

By

Edward M. Latorre Navarro

A thesis submitted in partial fulfillment of the requirements for the degree of

MASTER OF SCIENCE
IN
ELECTRICAL ENGINEERING

UNIVERSITY OF PUERTO RICO
MAYAGÜEZ CAMPUS
2004

Approved by:

Domingo Rodríguez, Ph.D. Member, Graduate Committee	Date
Jorge A. Cruz Emeric, Ph.D. Member, Graduate Committee	Date
Shawn D. Hunt, Ph.D. Chairperson, Graduate Committee	Date
Dana L. Collins, Ph.D. Representative of Graduate Studies	Date
Isodoro Couvertier, Ph.D. Chairperson of the Department	Date

Abstract

Pulse Code Modulation (PCM) has been the dominant format for signal representation since the early days of digital audio. This has come about because the compact disc (CD) uses PCM to encode audio. Recently, two high-resolution audio encoding formats have emerged and attempt to replace the CD as the dominant digital audio medium, DVD-Audio and SACD. DVD-A continues the CD tradition by using the same PCM digital audio technology, albeit with improved resolution. The other medium, SACD, encodes the signal in a one-bit format publicly named DSD. Presently, the technique used to encode the signal in DSD is based on Sigma-Delta Modulation (SDM). While both formats offer increased resolution over CD, the argument over which format is better is yet to be resolved at this point. Also, it remains unclear if conversions between these formats cause any audible effect. If an audibly lossless conversion between formats is possible, the argument over which is better would be mute. The thesis of this work is to try to answer these questions, in an attempt to perform lossless conversions between signals modulated in PCM and SDM. Conversions were made using lossless and lossy techniques. Lossless techniques proved unsuitable for audio applications and one-bit signal reconstruction. Lossy techniques were studied using both typical audio signal analysis and listening tests. The listening tests verified that conversions between both formats are indeed audibly lossless. The listening tests also determined the high-resolution formats do not offer significant audible improvements over CD quality. These results lead to the conclusion that current high-resolution formats surpass human audible perception and offer higher quality representation than the accompanying analog hardware in the audio chain.

Resumen

Pulse Code Modulation o PCM, ha sido el formato adoptado para representar las señales de audio desde el comienzo de la era de audio digital. Esto se debe a que el disco compacto (CD) utiliza PCM para codificar el audio digital. Recientemente han salido al mercado dos formatos de alta resolución, en un intento de reemplazar al CD como el medio dominante de audio digital, estos son DVD-Audio y SACD. DVD-A continúa la tradición del CD utilizando la misma tecnología PCM, pero con mayor resolución. El otro medio, SACD, codifica la señal en un formato de un bit, públicamente llamado DSD. Al día de hoy la técnica utilizada para codificar la señal DSD esta basada en Sigma-Delta Modulation o SDM. Aunque ambos formatos ofrecen mayor resolución que la del CD, al día de hoy todavía no se ha solucionado el argumento acerca de cual formato es mejor. Tampoco existe conclusión alguna acerca de si el cambio entre un formato y otro causa algún efecto audible. Si se puede lograr una conversión sin perdidas auditivas entre estos formatos de alta-resolución, el argumento acerca de cual es mejor quedaría sin efecto. La tesis de este trabajo es intentar resolver estas incógnitas por medio de un sistema que haga conversiones sin perdidas entre señales moduladas en ambos formatos, PCM y SDM. Las conversiones fueron hechas con sistemas sin perdidas y con perdidas. Las técnicas de conversiones sin pérdidas no resultaron ser efectivas para aplicaciones de audio, ni para aplicaciones que envolvieran reconstrucción de señales de un bit. Las técnicas de conversiones con pérdidas fueron examinadas utilizando típico análisis de señales de audio y pruebas de audio. Las pruebas de audio aseveraron que las conversiones entre los formatos de alta resolución no son perceptibles. Las pruebas de audio también determinaron que estos formatos de alta resolución no ofrecen mejoras de audio significativas sobre la calidad del CD. Con estos resultados se llegó a la conclusión de que los formatos modernos de alta resolución sobrepasan los niveles de percepción audible de los humanos y ofrecen una calidad de representación de la señal mayor a la del acompañante equipo análogo de la cadena de reproducción de audio.

This thesis is dedicated to my family and my girlfriend.

My family somehow led me here.

My girlfriend finished the job.

Acknowledgments

Thank you, my family and my girlfriend Jennifer Jiménez, for putting up with me during the most stressful years of my life (though the worst is still to come ☺). I love you all.

I must thank my advisor, Dr. Shawn D. Hunt. His support is a vital reason this thesis was finished. He taught me how to learn anything. Thank you.

I want to thank Mr. Todd W. Brown from ©Telarc International Corporation, for giving me his time and best efforts to answer all my emails and send me, various times, all the data I needed for the thesis. Thank you.

Thanks to Nelson Alicea and Javier Malavé for taking the time to compose and play the great melody used in the listening tests. Also thanks to all the people who participated in the listening tests. Long and demanding, I know, but you all did it. Thanks.

Thanks to Dr. Domingo Rodríguez Rodríguez and Dr. Jorge Cruz Emeric for being in my committee. Thanks to Rafael Medina, a pleasure working with you. Thanks a lot to all my friends, for giving me the best times; helping me survive. And all those ECE staff, professors and students with whom one-way or another I worked with, Thanks. Hope to see you around.

Table of Contents

List of Tables

List of Figures

List of Abbreviations

Σ-Δ	Sigma-Delta
ADC	Analog to Digital Converter
CD	Compact Disc
CMQ	Classical model of Quantization
CQF	Conjugate Quadrature Filters
DAC	Digital to Analog Converter
DSD	Direct Stream Digital
DVD-A	Digital Versatile Disc for Audio
FIR	Finite Impulse Response
IIR	Infinite Impulse Response
IMD	Intermodulation Distortion
LSB	Least Significant Bit
MMS	Multi-rate Modulation System
NTF	Noise Transfer Function
PCM	Pulse Code Modulation
QMF	Quadrature Mirror Filter
RPDF	Rectangular Probability Density Function
SACD	Super-Audio Compact Disc
SDM	Sigma-Delta Modulation
SDPC	Sigma-Delta Pre-Correction
SNR	Signal to Noise Ratio
STF	Signal Transfer Function
THD	Total Harmonic Distortion
TPDF	Triangular Probability Density Function

I. Introduction

With the ever-increasing development in digital audio technology, the argument about the "best" audio quality is a never-ending dispute for audiophiles everywhere, whilst, for the digital audio industry, the dispute for the best digital audio system may be the difference between the new standard and a commercial bomb. Presently, the new wave of high resolution digital audio formats most likely to succeed include the Super Audio Compact Disc (SACD) and the Digital Versatile Disc for audio (DVD-A). These formats are respectively, Direct Stream Digital (DSD) and Pulse Code Modulation (PCM). The purpose of this work is to investigate the relative merits of each, to determine if a direct relationship (lossless conversion) between the audio format of the Super Audio Compact Disc (SACD) and the audio format of the Digital Versatile Disc (DVD-A) exists, and justify the need for these high definition (quality) audio mediums based on the response of the human auditory system.

The first format, DSD, is a 1-bit representation of the audio waveform with a sampling frequency of 2.8224 MHz. Presently the most widely used process to encode the signal in DSD is Sigma-Delta Modulation (SDM). DVD-A encodes the signal using Pulse Code Modulation (PCM). PCM works by sampling an analog signal at regular intervals and encoding the amplitude value of the analog signal in a digital word. The DVD-A standard can represent the signal using from 16 to 24 bits per sample, and sampling frequencies of 44.1 kHz, 48 kHz, 88.2 kHz, 96 kHz, 176.4 kHz or 192 kHz.

Proponents of each format claim, with strong arguments related to audio quality, the advantages of each system [1]–[3], [5]–[6]. Supporters argue over which format offers significantly superior sound, better high frequency performance, added detail and overall clarity. While each format has advantages and disadvantages, the proposed work will deal with input vs. output measures of the quality of the audio signal.

There have been many papers presented which debate whether or not any one of these two formats should be standardized as the next dominant audio format [10]–[12],[16]. Yet given the improvement in digital signal processing technology, the need for a standard basis for digital audio performance, which specifies the requirements for an adequate audio format, is far overdue. Many audio societies worldwide have stated what they believe should be the standards of audio recordings, but a consensus has yet to be agreed on. Given the high quality standards offered in these two new formats, now appears to be a great moment to determine this standard based on audio quality. It is believed that both formats offer enough resolution to comply with what technical societies have proposed as the audio standard [10].

The process of quantization, for instance 1-bit vs. multi-bit, in essence regulates the precision of every digital audio system. Additional essentials, such as filtering, are designed accordingly to comply with the desired results. Also, both formats, SACD and DVD-A, incorporate lossless compression; lossless compression is simply a method of delivering bit-accurate output data while reducing the quantity of data stored or the rate transmitted in the channel. Since both formats have lossless compression as a feature we bypass this aspect. This work does not cover the details concerning distribution limitations.

Working with the previous facts leads us to work with only the digital-to-analog conversion, DSD or PCM, which allow for improvements in system related errors in exchange for better audio quality. The theory presented states that if these processes are combined with auditory data to form models of human hearing, then there is an opportunity to achieve optimum performance for a given data rate, which at one extreme can lead to a performance beyond the requirement for human hearing, or at the other extreme, reasonable audio quality with a low data rate [17]. Therefore, if a direct relationship between the audio format of the SACD and the audio format of the DVD-A exists at a level high enough to be undetectable by human hearing, it would provide the standard for digital audio excellence, given we have reached a level of audio quality strict enough in order to discriminate between what is needed in a format and overkill.

To accomplish the goal of comparing these systems, a full background study on both digital to analog conversion methods, SDM and PCM, is given first. The research involves studies on linear and non-linear systems, random signals and error moments (for dithering applications).

After the study on each modulation process, additional study comprises methods for conversion between signals, specifically multirate systems. The processing required for conversions between various word length signals involves signal and noise analysis with the aim of finding lossless conversions in the audio spectrum. Conventional multirate systems do not perform lossless conversions between signals; therefore, additional multirate options were investigated.

The research carried out here indicated a lossless conversion between formats is not possible. Because of this, a thorough signal analysis was completed in order to determine the effects of the lossy process. Various methods for signal analysis were performed to fairly judge the quality of the audio content. The analysis methods must be equivalent to methods customarily employed by the digital audio industry with the intention of publication in the same community.

II. Theory

A. Pulse Code Modulation

Since the introduction of the Compact Disc (CD) in 1982, Pulse Code Modulation (PCM) has been the dominant technique for digital music recording. In essence, PCM involves sampling the analog signal (conforming to the Nyquist criteria) and coding the signal into a finite sequence of numbers. Therefore, the quality of the output signal depends on the sampling frequency, F_S and the number of bits or quantization levels. For digital audio, signal levels are represented by binary numbers, so throughout this thesis binary coding will be assumed. Figure 1 shows the block diagram of a PCM analog-to-digital converter.

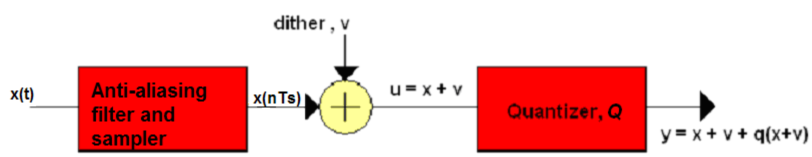

Figure 1: Block diagram of a PCM converter.

In the sampling process, the input signal $x(t)$, is sampled at uniformly spaced time intervals, T_s, creating $x[n] = x(nT_s)$, where n is an integer. In the frequency domain, the sampled signal contains periodic versions of the signal spectrum at multiples of the sampling frequency $F_s = 1/T_s$. The input signal can be reconstructed, with no loss of information, only if the repeated versions of the signal spectrum do not overlap, or in other words, if aliasing does not occur. In order to prevent the periodic signal spectrums from overlapping, the sampling frequency must be at least twice as large as the signal bandwidth; $F_s \geq 2F_B$, where F_B is the bandwidth of $x(t)$. Clearly, increasing the sampling frequency, or the rate of signal samples per time, allows the signal to contain higher frequencies. Usually an anti-aliasing filter, placed before the sampler, is used to guarantee the signal is indeed band limited.

The second process involved in PCM is quantization in amplitude. Quantization takes place to map the infinite number of input amplitude values of the continuous signal, into a finite (fixed) number of output amplitude values. Because infinite precision is lost, quantization is an irreversible process. The quantized values are then represented in binary digital code words composed of a finite number of bits, hence the term, Pulse Code Modulation. A quantizer with N bits resolution will have 2^N output levels, or N digital bits are needed to encode each codeword corresponding to each output level.

Figure 2 shows the transfer characteristics for a mid-tread and mid-riser quantizer. These quantizers have two fundamental differences. The first one is a DC offset present in the mid-riser quantizer since it is not capable of representing a zero value. The other one is that a mid-riser must have an even number of output levels to produce a completely symmetric transfer curve, while the mid-tread needs an odd number of output levels. Though each configuration has its own advantages [19], all follow-up discussion assumes a mid-tread quantizer since a DC offset is often not desired in audio signals. In any case, all statements have equivalent results for the mid-riser.

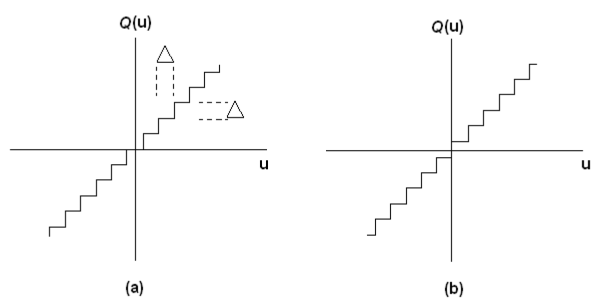

Figure 2: Quantizer transfer characteristics where Δ denotes the size of one bit. (a) Mid-tread (b) Mid-riser.

The relation between quantizer input u and output y can be described as

$$y = Q(u) = \Delta\left\langle \frac{u}{\Delta} \right\rangle, \tag{1}$$

where $\langle\ \rangle$ is the standard rounding to the nearest integer operation and Δ is the quantizer step size, as in Figure 2, which represents one bit. The step size is generally identified as the Least Significant Bit (LSB), since it represents the difference between the binary digital codes for two adjacent output levels. Accordingly, a difference in input amplitudes corresponds to one LSB difference in output code words.

The quantization process introduces an error signal e, which is the difference between the quantizer input and output, and whose magnitude does not exceed half a LSB. This error e is defined as

$$e = y - u\,, \tag{2}$$

where,

$$|e| \leq \Delta/2\,. \tag{3}$$

A quantizer that acts in accordance with (3) is said not to overload.

The classical model of quantization (CMQ) states that the quantization error can be modeled as an additive random process that is uncorrelated to the system input and independently and identically distributed (iid) [26]. The CMQ also postulates the error follows a uniform probability density function (pdf), such that p_e of e is

$$p_e(e) = \begin{cases} \frac{1}{\Delta}, -\frac{\Delta}{2} < e < \frac{\Delta}{2} \\ 0, \quad otherwise \end{cases}. \tag{4}$$

Therefore, to represent the quantizer in a linearized model and simplify the analysis of the system, one can interchange the quantizer for an additive white noise source $e[n]$ added to the input signal. Equation (2) is now

$$e[n] = y[n] - u[n]\,. \tag{5}$$

Under these conditions the m error signal moments are

$$E[e] = 0\,, \tag{6}$$

$$E\left[e^2\right]=\frac{\Delta^2}{12}, \tag{7}$$

and the *m*-th moment is

$$E\left[e^m\right]=\begin{cases}\dfrac{1}{m+1}\left(\dfrac{\Delta^2}{12}\right)^m, & m\ even\\ 0, & m\ odd\end{cases}. \tag{8}$$

The error signal variance (7) is also the noise power. This noise power is uniformly distributed between zero and F_s.

The CMQ is valid only if all preceding statements comply. For very small signals and many simple signals (e.g. sinusoidal signals) however, the quantization error preserves the nature of input-dependent distortion, and thus cannot be modeled as a noise source. For such cases, some statistical properties of the error signal can be mitigated by the application of a random noise process added to the input signal, prior to the quantization, called dithering.

In the dithering process, random noise signal added to the input signal is a white noise signal (v, in Figure 1) independent of the input. This type of dither, which remains in the output signal, is known as nonsubtractive dither. Subtractive dither requires the same dither signal at the output end for subsequent subtraction from the output signal. Nonsubtractive dither, with a rectangular pdf (RPDF) of one LSB peak-to-peak amplitude,

$$p_v(v)=\Delta(e), \tag{9}$$

can render the first statistical moment of the quantization error signal e independent of the input [25]. Therefore the first moment of $e[n]$ (5), is independent of the input. The second moment (7) is still dependent, which means the quantization noise power varies with the input signal. In audio signals, this is often denoted as the unpleasant *noise modulation*. If the dither is iid, then temporally separated error values will be uncorrelated and the short-time error power spectra will be flat.

One way of realizing the second error moment independent of the input signal, yet maintaining the first one independent, is by applying dither with a triangular pdf (TPDF) instead of RPDF. TPDF can be generated by summing two statistically independent RPDF random processes each of one LSB peak-to-peak amplitude; this is equivalent to convolving their pdf's. TPDF is the only zero-mean dither that renders the first and second moments of the total error independent of the input, such that the first moment is zero and the second is minimized [25]. The second moment of the error signal is manifested as audible distortion components in the output signal. The tradeoff in TPDF dither is that for properly TPDF dither error signals (7) is now

$$E\left[e^2\right] = \frac{3 \cdot \Delta^2}{12} = \frac{\Delta^2}{4}, \tag{10}$$

hence the signal to noise ratio has been slightly reduced.

Similar to the first case, with TPDF dither the third and higher moments of the error signal remain dependent of the input signal. Higher order pdf dithers can be generated by adding successive statistically independent RPDF random processes, e.g. n summed statistically independent RPDF random processes renders n independent moments. However, variations in these higher moments are believed to be inaudible [25].

One technique often used to improve the resolution of the quantization output signal is oversampling, i.e. sampling the signal at a rate significantly higher than needed

$$F_s = M \cdot F_B, \tag{11}$$

where M is an integer larger than 2 (physical, computational and practical limitations constrain F_S to values stated further on). The improvement comes from the quantization noise power (7) now being distributed over a larger sampling frequency. The benefit in resolution is such that for every doubling of the original sampling frequency, the SNR improves by about 3.01 dB. This amount is equivalent to improving the quantizer resolution by one-half bit. The noise power distributed over the "new" high frequency band can then be low pass filtered and downsampled to the original sampling frequency, or decimated.

Another significant benefit of oversampling is the relaxed specs of the cut-off frequency of all the system's filters; hence, the transition band of the filters can now be between F_B and $F_s/2$. This allows the use of lower order filters, for example, in a cascaded structure.

B. Sigma-Delta Modulation

Over the past two decades, sigma-delta (Σ–Δ) analog to digital converters (ADC) and digital to analog converters (DAC) have become widely available, particularly for low frequency applications such as high fidelity audio. Figure 3 shows the block diagram of a first-order Σ-Δ modulator (SDM) that accepts positive analog amplitudes (x) and produces sequences of impulses (y).

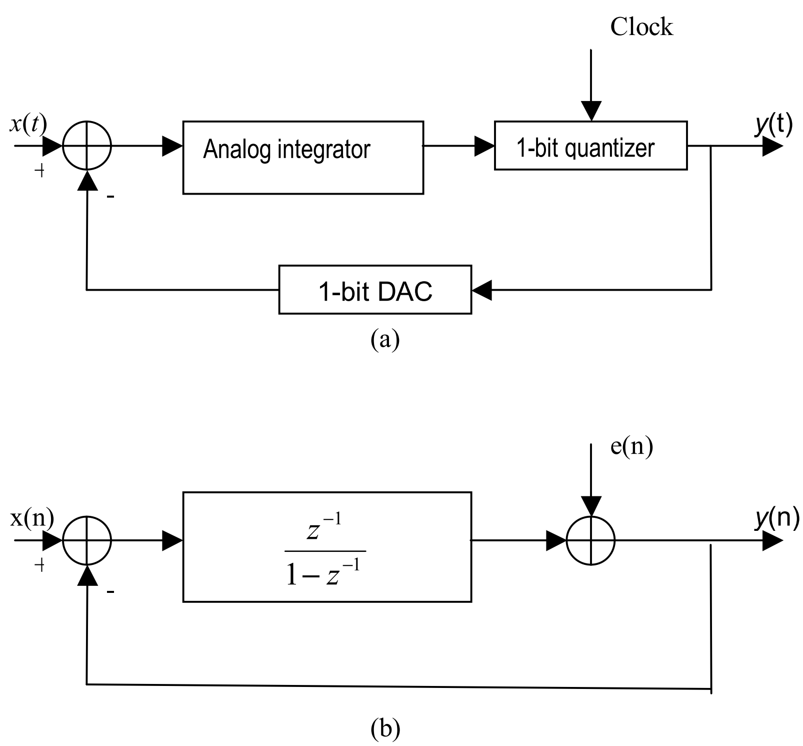

Figure 3: (a) First order Σ-Δ converter. (b) Digital model of first order Σ-Δ converter where the analog integrator and DAC are digital models and the quantizer is modeled as an additive white noise source.

An impulse is generated, in time with the clock, whenever the integrated difference between the input and the output is positive. This way the circuit regulates the rate at which impulses occur attempting to keep the average output equal to the average input. Zero input corresponds to no output impulses while maximum input corresponds to impulses generated at the clock rate. The output of the SDM is restricted to only two levels, thus forming a serial binary output code (a one-bit quantizer has two output levels, $\Delta/2$ and $-\Delta/2$).

By using negative feedback, if the input waveform accumulated over one sampling period (1/Fs) rises above the value accumulated in the negative feedback loop during previous input samples, the converter outputs a binary 1. If the waveform falls below the accumulated value, the converter outputs a binary 0. As a result, full positive waveforms will be all 1's. Full negative waveforms will be all 0's. Alternating 1's and 0's represent the zero point.

Sigma-delta modulators use oversampling and noise shaping (quantization) techniques. Oversampling offers two important advantages: the specification of the anti-alias filter is reduced from the Nyquist specification, and the N bits resolution obtained from the ADC can be increased to N+1 bits by oversampling the signal by a factor of four. Noise shaping is a technique in which the feedback architecture of a Σ-Δ converter allows the analog input signal of interest to pass unfiltered through the converter, while the quantization noise power is shifted to higher frequencies. Hence, if the quantization noise is high pass filtered, the baseband signal of interest can be extracted by digital low-pass filtering. Consequently, SDM demands a considerable increase in digital processing compared to traditional methods such as pulse code modulation. However, in many applications, the advantages for SDM over other methods far outweigh the disadvantages.

One significant advantage of sigma-delta modulation is that analog signals are converted using only a 1-bit ADC and analog signal processing circuits having a precision that is usually much less than the resolution of the overall converter. Furthermore, the circuitry of a Σ-Δ ADC only requires analog components of a comparator and an integrating component, making DSP-chip devices less costly.

For analysis, the 1-bit quantizer of the SDM is replaced by an additive white noise source as shown in Figure 3b. In practice, the quantizer is not linear and the quantization noise is not white. The effects of this approximation are considered later on. Following the model of Figure 3b, the modulator output $y(n)$ is given by:

$$y[n] = x[n-1] + e[n] - e[n-1]\,. \tag{12}$$

Its equivalent frequency domain representation is given by:

$$Y(z) = X(z)z^{-1} + E(z)(1 - z^{-1})\,. \tag{13}$$

Following Figure 1b and (13) the signal transfer function (STF) and noise transfer function (NTF) are respectively

$$H_x(z) = z^{-1}, \tag{14}$$

and

$$H_e(z) = 1 - z^{-1}, \tag{15}$$

From (13), (14) and (15) it is easily seen that the output of the SDM is a delayed input signal plus high-pass shaped quantization noise, hence the term noise shaping (Sigma Delta Modulators are often known as *Noise Shapers*). Since $H_e(z)$ contains a zero at $z = 1$, DC frequency, the NTF provides zero gain, or infinite attenuation at DC frequency. Figure 4 shows a typical output spectrum of an SDM of higher order.

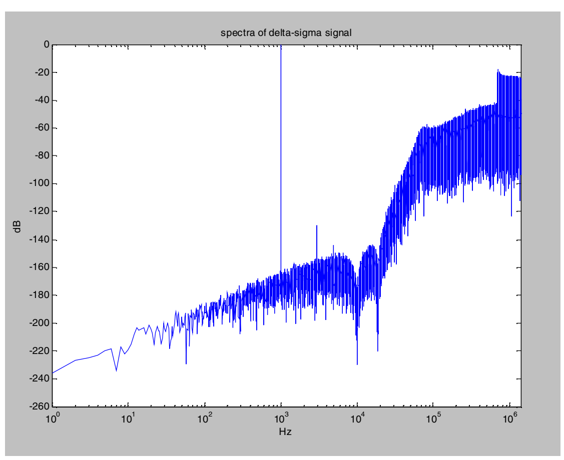

Figure 4: Typical output spectrum of an SDM (1 kHz, -6dB input).

To analyze the time domain behavior of the system, DC and sinusoidal signals are applied to the first-order SDM (Figure 3). Figure 5a shows that for a DC zero input, half the modulator output values are 1's, half are -1's. Figure 5b shows that for a DC input of 0.55, most of the modulator output values are 1's, while few values are -1's. Fig 5c and 5d compare sinusoidal inputs to their respective SDM output signals.

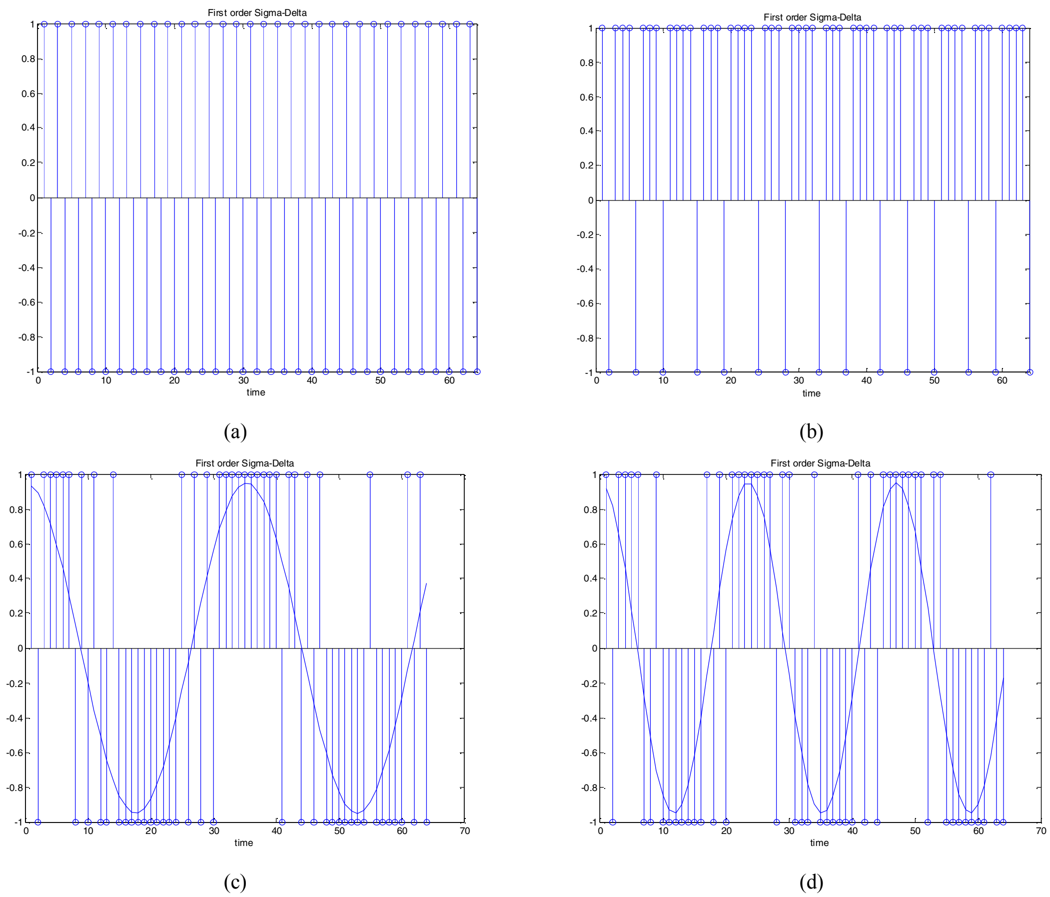

Figure 5: First-order SDM responding to various inputs with sampling frequency equal to 2.8224MHz: DC inputs, (a) amplitude = 0 (b) amplitude = .55; Sine inputs, (c) amplitude = .95 input, freq = 80 kHz (d) amplitude = .95 input, freq = 120 kHz.

As seen in the figures, when the input is positive most output values are positive, while the same goes for negative input values. In Figure 5a when the input is zero, half output values are positive, half are negative. Accordingly, the input signal can be approximated from the output signal by averaging the output over a period of time. Since we are interested in the low-frequency content of the signal, we implement the averaging process with a low-pass filter after the SDM. The chosen low-pass filter and cutoff frequency will affect the approximation of the SDM output.

Since the SDM only outputs ± 1s, its output signal will always have a constant power of one, and so the gain of the quantizer depends directly on its input, i.e. the smaller the input, the larger the gain. Because of the integrated feedback path in a non-linear SDM, the system is subject to the presence of periodic harmonic components in the output. The quantizer error spectrum is not truly white (conditions for white noise are not perfectly satisfied) [19],[37], the nonlinearity of a quantizer with only two output levels, and combined with oversampling, yields successive quantizer input samples with the probability of correlation, which leads to idle tones in the low frequency part of the signal. Higher order SDMs reflect this fault, though the tones are often embedded in large amounts of uncorrelated noise. Nonetheless, for low enough DC input amplitudes, typically under 10^{-3}, these idle tones have enough amplitude to appear above the noise floor. In [29] Ledzius and Irwin found a relationship between the DC input amplitude x_{DC} and the generated idle-tone frequency. If F_B is the signal bandwidth and OS is the oversampling rate, the first and largest idle tone f_{IT} occurs at

$$f_{IT} = 2 \cdot x_{DC} \cdot F_B \cdot OS\,. \tag{16}$$

For zero DC inputs, higher order SDMs may output a limit cycle. A limit cycle is a periodic pattern of certain length [24]. Figure 6 shows an example of a limit cycle from a 5th order SDM. Notice how limit cycles show no resemblance to a noise shaped system. Any distortion, non-signal component, which appears above the noise floor, will be audible. Subsequent explanation shall demonstrate methods for reducing distortions and eliminating these idle tones.

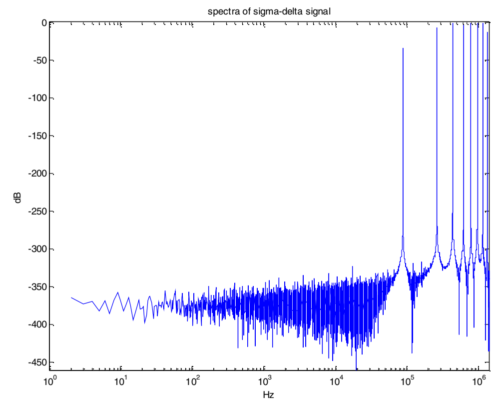

Figure 6: Example of a limit cycle from a 5th order SDM with input zero

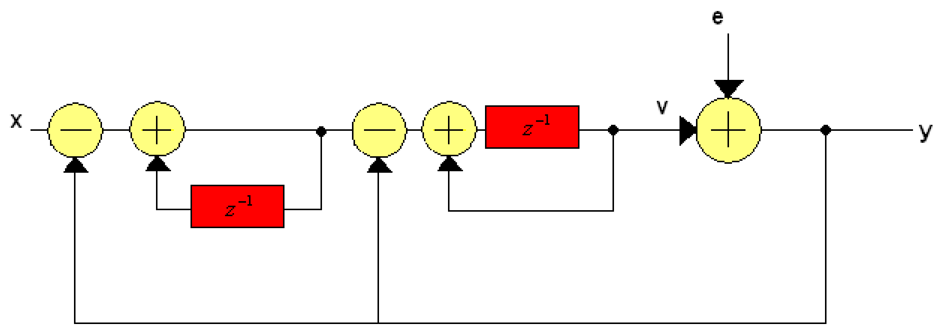

Figure 7: Second order SDM where quantizer is modeled as an additive white noise source.

Figure 7 shows a block diagram of a second order SDM where an additive white noise source represents the quantizer. All the fundamentals explained for the first order system apply to this modulator as well, as the new design only differs in the addition of an extra integrator loop. The transfer function of the first integrator is $\frac{1}{1-z^{-1}}$ and the transfer function of the second integrator is $\frac{z^{-1}}{1-z^{-1}}$. The system output is represented by the equation

$$Y(z) = X(z)z^{-1} + E(z)(1-z^{-1})^2. \tag{17}$$

The signal transfer function (STF) and noise transfer function (NTF) are respectively

$$H_x(z) = z^{-1}, \tag{18}$$

and

$$H_e(z) = \left(1 - z^{-1}\right)^2, \tag{19}$$

therefore, the only difference between the first and second order system is in the NTF.

Figure 8 compares the NTF of a first, second and third order modulator. Clearly the higher the order of the system, the more low frequency noise suppression it offers. Lower noise in the low frequency band means a better approximation of the input signal. Also clear from Figure 8 is the tradeoff between low frequency noise suppression and high frequency noise amplification. As the order of the system increases so does the relation between the suppression and amplification of quantization noise shaping.

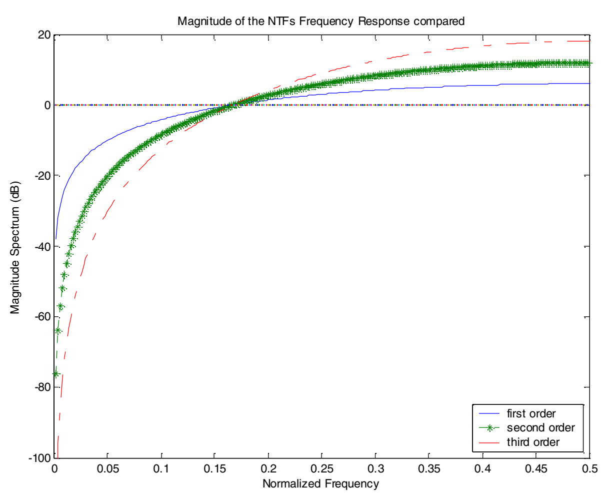

Figure 8: NTF for first, second and third order SDM

As the input amplitude of the second order modulator increases to levels approaching ± 1 (for a 1-bit quantizer), the quantizer reaches a level where it overloads. The quantizer is overloaded because the output of the second integrator may exceed the values of $\pm\Delta$, even though the modulator input is bounded by quantization levels of $\pm \Delta/2$ [19]. This overload causes serious problems such as the appearance of idle tones. If the input signal power increases to a level of quantizer overload, the increase in quantization noise power dominates the increase in signal power, thus reducing substantially the SNR or even driving the system to oscillation. As a result, the signal power must be limited to a value smaller to where the SNR will start to decrease. For this reason, stability is often described in the sense of the quantizer not being overloaded. For a second order modulator, this overload value is approximately -5 dB relative to full scale. Conversely, for low input signal power, the SNR also decreases due to the presence of idle tones from the non-linearity explained previously.

Figure 9 shows a linearized model of a SDM of arbitrary order, where $H(z)$ represents the same number of integrators as the order of the system. Notice how any order SDM may be represented by the same model as a first order system albeit the difference in $H(z)$.

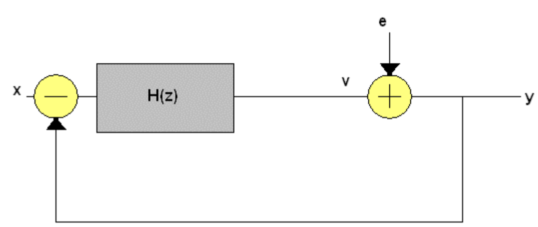

Figure 9: Linearized SDM where the quantizer is modeled as an additive white noise source.

The output of the system is defined by

$$Y(z) = STF(z)\cdot X(z) + NTF(z)\cdot E(z), \tag{20}$$

where

$$STF(z) = \frac{H(z)}{1+H(z)}, \tag{21}$$

and

$$NTF(z) = \frac{1}{1+H(z)}. \tag{22}$$

For higher order modulators it is more convenient to design the NTFs as IIR transfer functions instead of FIR, taking advantage of the better performance of IIR filters for lower orders versus FIR filters. The most popular modulator topology for DSD applications is the so-called feed-forward structure of Figure 10.

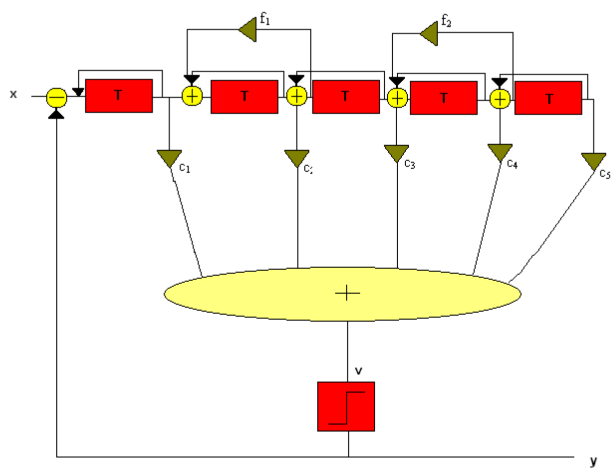

Figure 10: Fifth order feed-forward SDM

For this structure the loop filter $H(z)$ is given by

$$H(z)=c_1\frac{z^{-1}}{1-z^{-1}}+c_2\left(\frac{z^{-1}}{1-z^{-1}}\right)^2+c_3\left(\frac{z^{-1}}{1-z^{-1}}\right)^3+c_4\left(\frac{z^{-1}}{1-z^{-1}}\right)^4+c_5\left(\frac{z^{-1}}{1-z^{-1}}\right)^5, \qquad (23)$$

and so the NTF is given by

$$NTF(z)=\frac{\left(1-z^{-1}\right)^5}{\left(1-z^{-1}\right)^5+c_1z^{-1}\left(1-z^{-1}\right)^4+c_2z^{-2}\left(1-z^{-1}\right)^3+c_3z^{-3}\left(1-z^{-1}\right)^2+c_3z^{-4}\left(1-z^{-1}\right)+c_4z^{-5}},$$

$$NTF(z)=\frac{\left(1-z^{-1}\right)^5}{P_5\left(z^{-1}\right)}, \qquad (24)$$

which is equivalent to a Butterworth or a Chebyshev Type II filter where the term z^0 does not exist, so the system contains a delay in the closed loop and is realizable. Butterworth filters are characterized by a magnitude response that is maximally flat in the passband and monotonic overall. Chebyshev Type II filters are monotonic in the passband and equiripple in the stopband. The approach to obtain the feed-forward coefficients c_i is to design a high pass filter for $NTF(z)$, according to one these filter's rules and reorganize the terms such that it is in the shape of (23).

A Chebyshev Type II NTF design is accomplished by including the resonators (coefficients f_1 and f_2 in figure 10) in the SDM design. These coefficients are obtained by choosing the frequency where to place the poles [24]. Since the calculations only involve these integrators, the coefficients are independent of the rest of the design.

As with lower order systems, a fifth order modulator starts to overload at input signal power levels over -4 dB. For DSD signals, the maximum modulation depth of the modulator is 50%, meaning 0dB SACD is a ± 0.5 maximum amplitude input signal, i.e. $\Delta/4$. However, peaks in the signal of +3.1 dB are allowed for short periods of time. This requires the SDM to be stable for inputs up to 0.71. Therefore, it is necessary to enforce stability in the system for relatively large inputs. This situation is often resolved with the use of clippers in each integrator stage. Figure 11 shows the diagram of a clipped integrator.

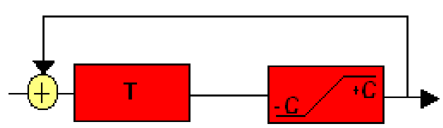

Figure 11: A clipped integrator, where the output of the integrator is limited to $\pm C$

In essence, the clippers saturate the output of the integrator, thus preventing it from outputting values that exceed the value $\pm C$; not to be confused with the coefficient values c_1, c_2, c_3, c_4, c_5. To obtain the values of the clippers, the integrator output levels are evaluated for sinusoidal and square wave inputs, with amplitudes reasonably close to system overload. Clippers C_1 and C_2 (from left to right in figure 10) are then set according to these values. If all clippers are set according to this method, the situation where all clippers will simultaneously activate might occur. Simultaneous activation of the clippers or, activation of the first clipper, will corrupt the signal, creating audible distortions. This problem may be resolved by choosing subsequent clippers such that for clipper C_i, the product of the clipper C_{i-1}, and the coefficient c_{i-1}, is reduced by about 1.5 – 2 times. For example, let clipper C_2 = 10, feed-forward coefficient c_2 = 0.24212 and c_3 = 0.05311, then $C_2 \cdot c_2 = 2.4212$, $\frac{2.4212}{1.6} = 1.5132$ and $C_3 = \frac{1.5132}{0.05311} = 28.49$.

There is a tradeoff of lower SNR for each time a clipper activates. For input levels close to overload without clippers, given the clippers should hardly activate, the tradeoff is minimum. For input levels above that threshold, up to where the clippers were designed to maintain stability, the tradeoff is such that SNR may be cut by more than half. Each design is a compromise between SNR and maximum allowable input.

As mentioned above, when the SDM inputs a DC signal with an amplitude below a certain threshold, idle tones and/or limit cycles appear (see Figure 6). As with PCM, SDMs can benefit from the use of dithering. However, due to the one-bit quantizer, TPDF dither, which spans two bits, cannot be used in this system. As in PCM, dither in the SDM must be applied right before the quantizer as shown in Figure 12.

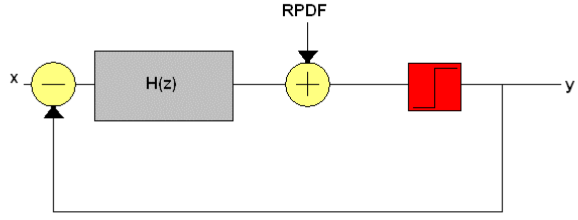

Figure 12: Block diagram of SDM with dither

However, the use of RPDF dither is beneficial and necessary for SDMs. With RPDF dither, one can effectively prevent limit cycles and reduce noise modulation. The tradeoff for using RPDF dither are that the maximum system input amplitude and the SNR are slightly reduced. However, the loss in input amplitude (generally in the range of $10^{-2} to 10^{-3}$ dB) and SNR (generally close to 10^{-1} dB) is marginal when compared to the benefits. It is possible to use TPDF dither albeit with very small amplitudes, but the amplitude has to be so small that there is no benefit of reduced distortion and obviously, the noise floor increase versus RPDF. Other types of dither have been studied [27], for instance single-bit dither [28], which offers hardware benefits with minor SNR loss compared to RPDF dither.

Given that TPDF is not possible in 1-bit SDMs, another method has been developed to attempt to eliminate the distortions present in the output signal: Sigma-Delta Pre-Correction (SDPC) [24]. The principle behind SDPC is the following. When we model a SDM as a non-linear element ΣΔ, the transfer characteristic can be written as

$$\Sigma\Delta(x) = x + \alpha_2 x^2 + \alpha_3 x^3 + \cdots. \tag{25}$$

If we create a model according to

$$s(x) = x - \alpha_2 x^2 - \alpha_3 x^3 - \cdots, \tag{26}$$

then we could create an output signal

$$\Sigma\Delta(s(x)) = x - 2\alpha_2^2 x^2 + \vartheta(x^4) + \cdots, \tag{27}$$

where the second harmonic distortion component has been completely removed, and the third harmonic distortion has been significantly reduced (for the distortions referred to, $\alpha_i << 1$). Equation (26) reveals new higher order distortions but of, in most cases, negligible amplitude. An estimate of the signal $s(x)$ may be obtained using the configuration shown in figure 13.

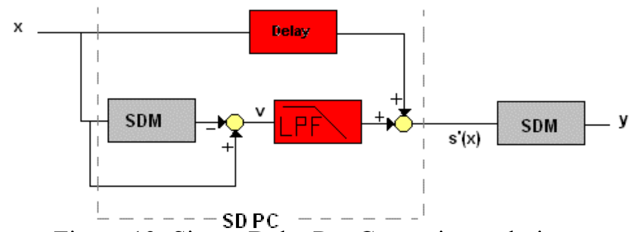

Figure 13: Sigma-Delta Pre-Correction technique

In figure 13, the input signal x is first input to the SDM then, subtracted from the SDM output to create signal v. Signal v contains all the distortion components generated by the SDM, plus the uncorrelated noise added by the noise shaping process. Next, v is low-pass filtered with a cut-off frequency of, for example, 100 kHz (SACDs offer frequency response up to 100 kHz). This filtered signal is then added to the input signal x (properly delayed to compensate for the low-pass filter) to create signal $s'(x)$ (an estimate of $s(x)$). Signal $s'(x)$ is input into an SDM, identical to the used in first stage, which generates output signal y.

The tradeoff for the benefit of SDPC is a 3 dB increase in the noise floor. The reason is that y contains the quantization noise, from both modulators, in the chosen low frequency range.

In practice, the second harmonic is not removed but reduced. Higher harmonics are also favorably reduced. The suppression is not total in part because of the phase distortion from the SDM in frequencies higher than 20 kHz [24]. Figure 14 shows an improved Pre-Correction technique that accounts for the phase distortion in the SDM.

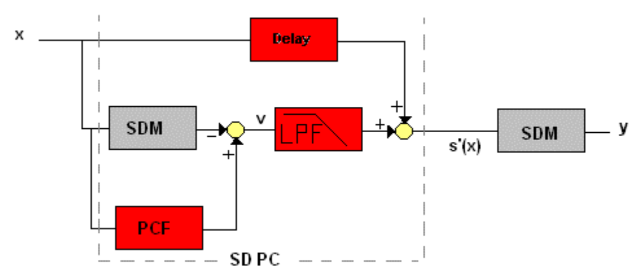

Figure 14: Improved Sigma-Delta Pre-Correction technique

The improved SDPC technique differs from the original in the addition of a phase correcting filter (PCF) that corrects the phase distortion created by the SDM. A cascade of the two structures would offer cancellation of the low order distortions and cancellation of the higher order distortions still present in (27).

C. Super Audio CD and DVD-A

Since the introduction of the compact disc (CD) as the main digital audio carrier, the world associates digital audio recording and playback with the term pulse code modulation (PCM). The heart of a typical PCM system for audio recording involves an oversampling ADC, followed by a digital decimation filter to reduce the sampling frequency and increase the precision to the desired value for recording. For reproduction, the signal is interpolated and converted back to an analog signal. Finally, the signal is low-pass filtered, to get the final analog audio output.

The standard for CD quality audio is set at 44.1 kHz sampling frequency and 16-bit resolution. According to various experts, CD domination is rapidly fading. Two new digital audio formats have arisen to try to take over the digital audio carrier business: the Super Audio Compact Disc (SACD) and the Audio Digital Versatile Disc or DVD-Audio (DVD-A).

The technology used to record and produce audio content of the SACD is known as Direct Stream Digital (DSD). Sony Corporation and Royal Philips Electronics introduced this technology, which uses a new type of disc carrier with various characteristics different from a conventional CD such as dual layers, enhanced capabilities and others which do not influence the signal. DSD uses Σ-Δ modulation to create a 1-bit representation of the audio waveform with a 2.8224 MHz sampling frequency. This sampling frequency results from a 64 times oversampling of the CD standard sampling frequency of 44.1 kHz; $44100 * 64 = 2822400$. This frequency was chosen to provide interoperability between the CD and SACD formats. In addition, Sony claims to have developed a decimation procedure, named *Super Bit Mapping Direct Downconversion*, which uses a “super-power one-stage” FIR digital filter/noise shaper with 32,639 taps to down-convert the DSD signal into a CD quality signal in a single stage [1]. This allows for a CD with the highest possible audio quality.

According to manufacturers, DSD can offer a frequency response from DC to 100 kHz and a residual noise power of -120 dB thanks to its 5th-order noise shaping filters [1]. However, given this noise shaping technique, the residual noise power is not constant throughout the signal bandwidth. By using noise-shaping filters of higher order, it is possible to increase the resolution in the audio band at the expense of resolution at exceedingly (inaudible) high frequencies. These results are valid however only for static, non-transient signals. Transient signals will have poor resolution in a one-bit system. If the signal does not endure for a long enough time, the noise shaper of the one-bit system will not minimize the error.

As indicated by its proponents, DSD offers the advantage of eliminating the decimation and interpolation processes necessary in PCM modulation, thus preventing additional-unnecessary re-quantization noise from polluting the signal. In the SACD "Scarlet Book" Sony and Philips mandate the use of a 100 kHz low-pass filter in SACD mastering so that when the playback volume at standard DSD level is equivalent to 100W, the noise component "outside the audible sound spectrum" is 1W or less. In addition, SACD players must low-pass-filter their analog output above 50 kHz [4]. Figure 15 shows the typical audio chain found in a SACD player.

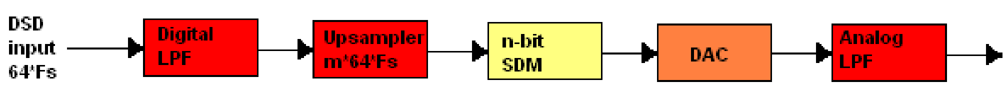

Figure 15: Typical audio chain found in a SACD player

DVD-Audio is basically a CD with higher standards and a larger capacity carrier, as it also uses PCM technology. Notice that the carrier, however, is not the Compact Disc but a Digital Versatile Disc that allows for sampling rates of up to 192 kHz and quantization of up to 24 bits. To date, the industry is still debating over the standard for DVD-A production. Meanwhile various industry leaders push for a standard of 96 kHz sampling frequency and 24-bits word length [16]. Many experts have agreed that values above 96 kHz and 20 bits are a waste of computational processing given that the advantages do not justify the improvement in performance

[10], [16]. For example, using a perfect 24-bit converter would give a signal to noise ratio of 144 dB, which is lower than what any analog component can achieve. Today, the best DVD-A players barely achieve a signal to noise ratio of about -120 dB for bandwidths between 0 and around 100 kHz. Similar to the SACD, DVD-A as a carrier also offers many advantages over the CD such as multi-channel audio, table of contents, lyrics, liner notes, and still pictures. Given the similarities between these extras in both formats, and the fact that either of these features does not affect the purpose of this investigation, these are of no concern here.

Many people believe PCM is the only true way digital audio should be processed [11]--[12]. Among the advantages of PCM are uniform quantization, optimal dithering (addition of random noise to reduce the effect of truncation) and the availability of uniform sampling. In addition, correctly implemented linear PCM implies only distortion attributable to band limitation and non-correlated random noise. In making this statement, it is understood that a uniform quantizer with optimal dither is a completely linear (but noisy) process and that the use of an error feedback loop that encapsulates the pre-quantizer dither sequence to achieve spectral shaping of the noise is also a completely linear process. Indeed, J. Vanderkooy and S.P. Lipshitz in their paper *Digital Dither: Signal Processing with Resolution Far Below the Least Significant Bit* from the Audio Engineering Society's (AES) 1989 conference, stated that there is a right sort of random noise to add, and that when the right dither is used, a digital system can have infinite resolution below the least significant bit (LSB). In such dithered systems, the correlation between the signal and the spectrally shaped noise is significantly reduced, and as such, fully meets the desires of the audiophile community.

For DSD however, linearization must depend on the use of negative feedback (i.e. noise-shaping feedback) to achieve acceptable performance. Even then, performance cannot be guaranteed for all signals, where at low level correlated distortions (idle-channel sequences) can exist although they may be below the system noise level. At higher signal levels, there can be signal-dependent stability constraints, which is a particular problem in higher-order modulators. In such schemes, because of correlation, it is difficult to completely eliminate modulation noise [12]. Consequently, DSD calls for multiple cascading of bitstream converters with the potential for a build-up in distortion compared to PCM.

Returning to the topic of DSD noise shaping, experiments have shown that the noise level in the ultrasound register is more than 100 dB higher (-40dB under maximum output level, using narrow band analysis) than DVD-A [11]. More relevant is that this ultrasound noise from SACD is enough to warm up the tweeter voice coils with some detectable influence on reproduced sound and maybe even affect the system to the point of failure. In addition, the ultrasonic noise may also affect the audible sound by down mixing it in the air, at least at higher sound pressures. Therefore we are left with basically two choices: either use more robust equipment that will handle high levels at very high frequencies, or filter the output signal and thereby remove one of the main alleged benefits of DSD, namely an extended high frequency response, by "turning it down" to any of the PCM levels with lower bandwidth. Recall that a CD player with a low-pass filter will contain no ultrasound information whatsoever.

When commercially released, the main advantage of DSD was that there is no conversion between sampling rates for recording, i.e. no decimation and interpolation filters are needed. In response to direct questions however Sony confirmed during a AES convention that DSD uses multi-bit PCM during recording and mastering processes and that it only uses the one-bit technique in consumer playback systems [11]. This statement eliminates the advantage of no conversion between formats. Also, as in most present cases, Sony/Philips has even officially recommended performing all DSP operations and audio editing of the recorded material in multi-bit format. This is why many agree there is arguably little point in using DSD for recoding, if you are going to turn it into PCM on the way to the master.

In view of the preceding arguments, which show the discrepancies between DSD and PCM, the situation appeals for which, if any, is the best format for the next generation of digital audio. According to the Acoustic Renaissance for Audio (ARA) group, it is sufficient for any upcoming digital audio format to deliver an audio bandwidth of 26 kHz and at least 20-bit word length in a well-implemented linear PCM system [16]. This, even though a specific paper [23] and other recent studies demonstrate that music instruments contain various harmonics with a considerable percentage of power up to 40 kHz. This paper shows that harmonics of a muted trumpet extend to 80 kHz; violin and oboe, to above 40 kHz; and a cymbal crash was still strong at 100 kHz. In these particular examples, the proportion of energy above 20 kHz is, for the muted trumpet, 2 percent; violin, 0.04 percent; oboe, 0.01 percent; and cymbals, 40 percent. This work also cites a paper that states that people react to sounds above 26 kHz even when they cannot consciously hear the sound. In any case, it is clear DVD-A meets this standard, as well as its DSD equivalent. Nevertheless, given the lack of conclusive evidence about higher than 20 kHz audio perception, a 20 kHz and 24-bit standard will be accepted as the standard basis of frequency bandwidth and word length for the purpose of this thesis. 88.2 kHz sampling frequency offers enough bandwidth for this frequency bandwidth basis. In addition, 88.2 is an exact multiple of the CD sampling frequency (44.1 kHz) and the DSD sampling frequency (2.8224 MHz).

D. Perfect Reconstruction Filter Banks

In many applications, a digital signal is split into any number of subband signals by means of an analysis filter bank. If these subband signals are bandlimited to a frequency range at least half that of the original signal, they can be downsampled. After the appropriate procedure (reason for the use of), the subband signals are upsampled and combined by a synthesis filter bank resulting in the desired output signal. Examples of applications that use this procedure include digital coding, noise removing, compression, detection, efficient transmission and signal processing and analysis which benefits from lower sampling frequency.

The whole analysis/synthesis procedure introduces three significant types of distortions: aliasing, short-time phase distortion and short-time frequency distortion [31]. The use of quadrature mirror filters (QMF) allows the aliasing to be removed in the reconstruction stage. Figure 16 shows a basic two-channel QMF bank. Here, the input signal $x[n]$ is passed through the two-band analysis filter bank, $H_0(z)$ & $H_1(z)$, which have low-pass and high-pass frequency responses with cutoff frequency $\pi/2$; the *quadrature* frequency. Figure 17 shows the typical shape of the analysis filters.

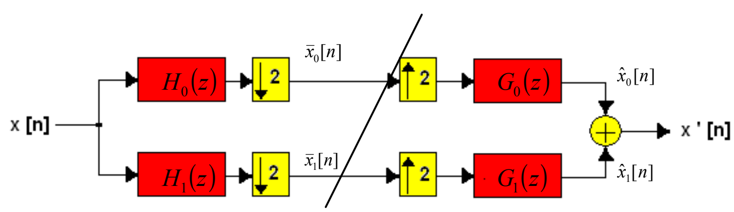

Figure 16: Basic two-channel QMF bank. The line represents the any processing that could take place.

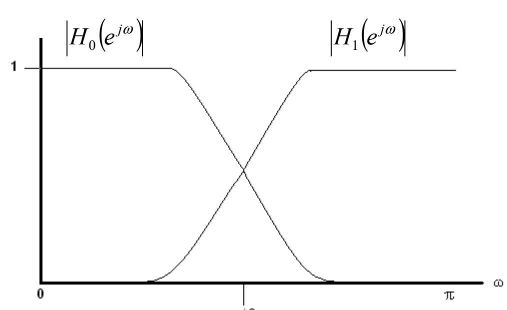

Figure 17: Typical frequency response of low-pass and high-pass analysis filters

After filtering, the subband signals are downsampled by a factor of two. This process of filtering and downsampling is known as the decomposition stage of the system. From figure 17 it is evident that the response of the filters, specifically the cut off region, is not fast and sharp enough to prevent aliasing (more details below). Though this is the case with most wavelets, what happens subsequently depends directly on the application. In any case, the subband signals are then upsampled by a factor of two, filtered through the synthesis filters and added to produce the output signal $x'[n]$. The process of upsampling and filtering is known as the reconstruction stage of the system.

By analyzing figure 16, we can find the z-transform of intermediate signals $\bar{x}_i[n]$ where i = 1, 2 which is,

$$\overline{X}_i(z) = \frac{1}{2}\left[H_0\left(z^{1/2}\right)X_i\left(z^{1/2}\right) + H_0\left(-z^{1/2}\right)X_i\left(-z^{1/2}\right)\right]. \tag{28}$$

After (28) is upsampled and convolved with filters $G_i(z)$, we arrive at the z-transform of the output $x'[n]$, given by

$$X'(z) = \frac{1}{2}\left[H_0(z)G_0(z) + H_1(z)G_1(z)\right]X(z) + \frac{1}{2}\left[H_0(-z)G_0(z) + H_1(-z)G_1(z)\right]X(-z), \tag{29}$$

and defined as

$$X'(z) = T(z)X(z) + A(z)X(-z). \tag{30}$$

The term $A(z)$ is due to the aliasing in the sampling rate alteration. To prevent aliasing in the output $x'[n]$, the analysis and synthesis filters are chosen such that

$$\frac{G_0(z)}{G_1(z)} = -\frac{H_1(-z)}{H_0(-z)}, \tag{31}$$

which gives,

$$G_0(z) = C(z)H_1(-z) \quad and \quad G_1(z) = -C(z)H_0(-z), \tag{32}$$

where $C(z)$ is an arbitrary rational function.

If the filter banks are to produce perfect reconstruction, in addition to condition (31), transfer function $T(z)$ must be magnitude and phase preserving. This can be achieved by imposing a number of conditions on the filters $H_0(z)$ and $H_1(z)$ depending on the filter type implementation, e.g. FIR, time-varying FIR [32], IIR, circular convolution [33], cosine modulation.

For perfect reconstruction FIR realizations, the filters must be power-complementary, i.e.

$$\left|H_0\left(e^{j\omega}\right)\right|^2 + \left|H_1\left(e^{j\omega}\right)\right|^2 = 1\,. \tag{33}$$

However, except for two trivial cases, it is not possible to design a perfect reconstruction two-channel filter bank with linear-phase power-complementary analysis filters [26]. Smith and Barnwell [31], showed a solution to this problem in the form of conjugate quadrature filters (CQF). The method involves removing requirement (33) and imposing power-symmetry,

$$H_0(z)H_0\left(z^{-1}\right) + H_0(-z)H_0\left(-z^{-1}\right) = 1\,, \tag{34}$$

where $H_0(z)$ is an FIR filter of odd order N. Define the modulation matrices

$$\mathbf{G}^{(m)}(z) = \begin{bmatrix} G_0(z) & G_1(z) \\ G_0(-z) & G_1(-z) \end{bmatrix}, \qquad \mathbf{H}^{(m)}(z) = \begin{bmatrix} H_0(z) & H_1(z) \\ H_0(-z) & H_1(-z) \end{bmatrix}. \tag{35}$$

To obtain FIR synthesis filters $G_0(z)$ and $G_1(z)$ from analysis filters $H_0(z)$ and $H_1(z)$, the determinant of $\mathbf{H}^{(m)}(z)$ must be

$$\det[\mathbf{H}^{(m)}(z)] = cz^{-k}\,, \tag{36}$$

where c is a real number and k is a positive integer.

If we choose

$$H_1(z) = z^{-N} H_0(-z^{-1}), \tag{37}$$

the determinant of (35) is

$$\det[\mathbf{H}^{(m)}(z)] = -z^{-N}, \tag{38}$$

which satisfies (36) with $c = -1$ and $k = N$.

Solving and manipulating (30) and (31) with (36) and (37) gives [26], [35]

$$G_0(z) = 2z^{-N} H_0(z^{-1}), \quad G_1(z) = 2z^{-N} H_1(z^{-1}). \tag{39}$$

It is evident that if $H_0(z)$ is causal, the other three filters are also causal. From (36) it follows that $\left|G_{0,1}(e^{j\omega})\right| = \left|H_{0,1}(e^{j\omega})\right|$. Furthermore, $\left|H_1(e^{j\omega})\right| = \left|H_0(-e^{j\omega})\right|$ which for real-coefficient transfer functions implies that $\left|H_1(z)\right| = \left|H_0(-z)\right|$. Thus, if $H_0(z)$ is a low-pass filter, then $H_1(z)$ is a high-pass filter. Accordingly from (39) $G_0(z)$ and $G_1(z)$ will also be low-pass and high-pass filters respectively. In this case, signals $\hat{x}_0[n]$ and $\hat{x}_1[n]$ from Figure 16 are orthogonal to each other [35]. Therefore, this type of filter bank design is referred to as an orthogonal filter bank. CQF design is equivalent to the discrete wavelet transform.

Following (34), one can complete the perfect reconstruction FIR filter bank through zero-phase half-band low-pass filter design. The procedure is to design the zero-phase half-band low-pass filter

$$F(z) = H_0(z) H_0(z^{-1}), \tag{40}$$

with a non-negative frequency response, whose spectral factorization yields $H_0(z)$. The zeros of $F(z)$ appear with mirror-image symmetry in the z-plane and have even multiplicity. Though the spectral factor $H_0(z)$ is designed to contain suitable half of the zeros, it can never be designed to have linear-phase. The stopband edge frequency is the same for $F(z)$ and $H_0(z)$.

A different approach to (39) is to take the causal half-band filter $z^{-N}F(z)$ of length $2N$, and factorize it in the form

$$z^{-N}F(z) = H_0(z)H_1(z^{-1}), \tag{41}$$

where $H_0(z)$ and $H_1(z^{-1})$ are linear-phase filters. The determinant of the modulation matrix **H** $[^{(m)}(z)]$ is now

$$\det[\mathbf{H}^{(m)}(z)] = z^{-N}, \tag{42}$$

which still satisfies the perfect reconstruction condition (36). The two synthesis filters are given by

$$G_0(z) = H_1(-z), \quad G_1(z) = -H_0(-z). \tag{43}$$

This type of filter bank design processes signals with reciprocal bases, thus called, biorthogonal filter banks. Figure 18 shows the frequency response of a biorthogonal low-pass analysis filter and low-pass synthesis filter.

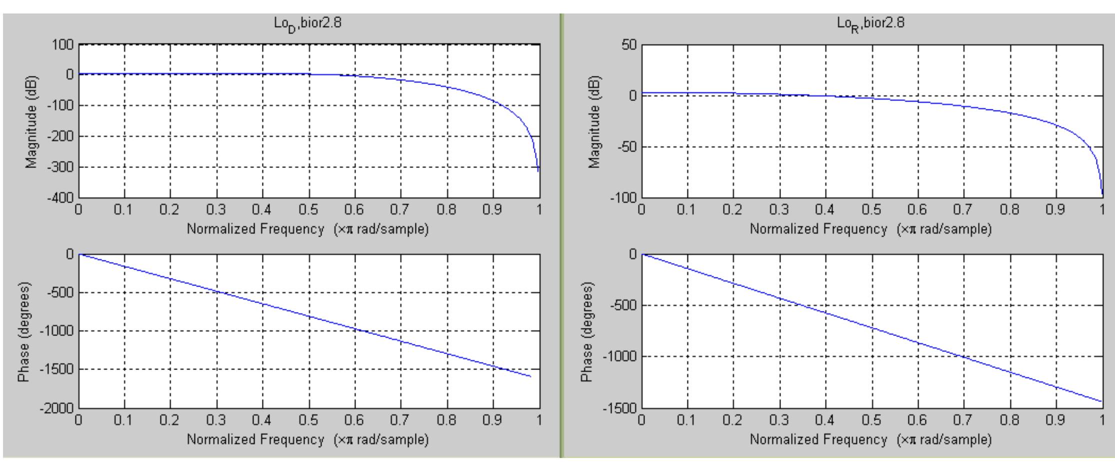

Figure 18: Frequency response of the low-pass analysis filter and synthesis filter of biorthogonal wavelet "2.8" [36]

Note that this type of design has sacrificed the magnitude-preserving feature for an extra degree of freedom, which is used to obtain linear-phase filters. A consequence of this design is that the analysis and synthesis filters do not have the same frequency response. This may lead to energy leakages during the process, which emerge as ring oscillations in the low frequency content of the output.

As previously mentioned, CQF filter design is equivalent to designing a scaling wavelet filter. In addition to orthogonal and biorthogonal wavelets, there are other types of wavelet filters which lead to perfect reconstruction. Just as biorthogonal wavelets sacrifices the magnitude preserving feature for linear phase, each wavelet design offers its unique tradeoff of features. Some examples of these additional wavelets are Coiflets wavelets, Symlet wavelets, Gaussian wavelets and Meyer wavelets. Descriptions of each wavelet and additional examples can be found in [36].

Another example of wavelets is published in a recent paper by Abdelnour and Selesnick [34]. This paper introduced a design of two-band orthogonal near-symmetric CQF. The technique, which uses Gröbner methods for the design, offers orthogonal filters with a subset of exactly symmetric coefficients of various lengths. Nearly symmetric as in, for example, a length 14 filter could have a subset of 9 symmetric coefficients and 5 nearly symmetric coefficients (see Figure 19). These filters can offer improved symmetry for a given support versus typical orthogonal and biorthogonal designs.

$K=3, L=8$	$K=2, L=9$	$K=4, L=4$	$K=3, L=7$
0.000522	0.000042	−0.005941	0.015864
0.004477	0.000776	0.026294	−0.050704
0.006199	−0.009253	0.034885	−0.072207
−0.086052	−0.073222	−0.085213	0.401755
0.085824	0.362766	0.111204	0.812841
0.696542	0.852001	0.688258	0.401755
0.696542	0.362766	0.688258	−0.072207
0.085824	−0.073222	0.111204	−0.050704
−0.086052	−0.009253	−0.131445	0.024837
0.006199	0.000776	−0.035729	0.005638
0.004232	−0.000039	0.010145	−0.002021
0.000096	−0.000002	0.002292	−0.000632
−0.000162	0	0	0
0.000019	0	0	0

Figure 19: Coefficients of various filters of length 14. K is the number of zeros at $z=-1$. L is the subset of symmetric coefficients. Taken from Bodardikar, Raghuveer, Adiga (1997), [33].

For this research, the biorthogonal method for CQF design has been chosen given the advantage of symmetry (linear phase). Symmetry, or constant group delay, is a very important and well-documented constraint for digital audio applications.

III. Simulation Results

A. Experimental Procedure and Graph Notation

All work was done in Matlab unless otherwise stated. All graphs presented hereafter were created with Matlab. Every signal described as an original signal consists of a computer generated wave, with either one or more frequency components. These original signals were created in Matlab using full 8 bytes double array Matlab precision. These signals were then modulated to either multi-bit or single-bit formats using methods described in Chapter 2. All processing was done using full Matlab precision.

For single-bit signals, the signals were modulated to 2.8224 MHz sampling frequency and in accordance with DSD specifications (Chapter 2, Section C), to comply with the Scarlet Book [30] requirements. Every SDM output signal is processed with a Hanning window unless otherwise stated. For multi-bit signals, in accordance with DVD-A specifications (Chapter 2, Section C), the signals were modulated to 24 bits 88.2 kHz sampling frequency; 24 bits to allow maximum DVD-A precision, 88.2 kHz for simplicity of the multi-rate process from DSD to PCM i.e. $2822400 / 88200 = 32$. The PCM output signals were processed with a Rectangular window unless otherwise stated. The PCM signals were not processed through a Hanning window, given this window caused excessive spectral leakage in the signal, thus affecting the graphical interpretation of the signals and the calculation of the SNR.

Even though both high resolution audio formats offer an audio bandwidth which surpasses 30 kHz, there are no explicit results about the effect of higher frequencies on audio perception. Therefore, every analysis of distortions and signal-to-noise ratio (SNR) was done using an audio spectrum of 20 – 20k Hz.

For SDMs, the maximum amplitude of the input signal is ± 0.5, and is used as the 0dB reference for SACD. The maximum amplitude of PCM systems is a full scale ± 1.0, becoming a 0dB signal. For full details of the above, see Chapter 2, Section B and Section C respectively.

Following the norm of the audiophile industry, throughout this work, the analysis of the test signals consisted of measurements and calculations of:

- Signal to noise ratio
- Total harmonic distortion
- Intermodulation distortion
- Transient response
- Phase response

The next two sections depict the performance of the SDM and the PCM respectively, to explicitly quantify their capabilities. Aware of each modulators features, the following sections describes the perfect reconstruction and multirate systems analysis. Last is a commercial signal examination and listening test evaluation.

B. Sigma-Delta Modulator Performance

The first thing to be determined is how good SDM and PCM are. This section describes experiments run to determine the limits of SDM. These include the SDM with and without the necessary added extras needed for proper audio reproduction, i.e. DSD quality. These added extras are the resonators and the pre-correction procedure (SDPC), all detailed in Chapter 2 Section B. With this information and subsequent PCM performance analysis, it is possible to determine the limitations of the modulating systems versus the limitations of the format conversion systems.

Figure 20a and 20b show the spectra of the output of a first-order and second-order SDM respectively. The original signal input to the systems is a 1 kHz 0dB SACD signal. These signals are processed with a rectangular window. Clearly, neither output is acceptable for the audio modulation. From Figure 20 it is evident how the second-order system achieves a lower noise floor than the first-order system, specifically, increased noise shaping. Third and fourth-order systems continue the trend of increasing noise shaping, but not enough to comply with DSD specifications. As a result, with the aim of creating a high-resolution audio signal, one must work with higher order sigma delta modulators, to be exact, fifth or seventh order configurations.

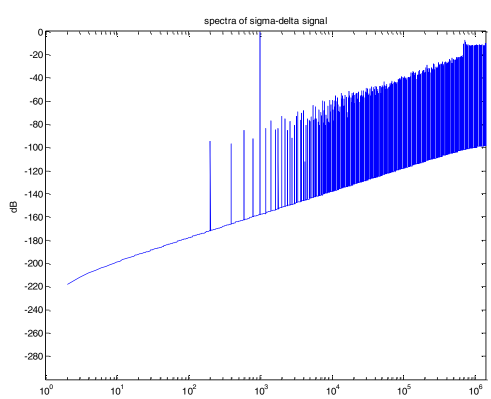

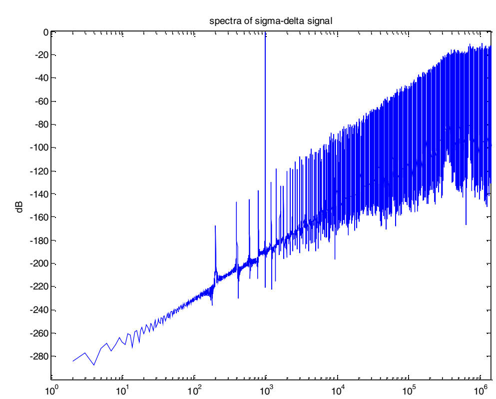

Figure 20: a) Spectra of first-order SDM output signal, b) Spectra of second-order SDM output signal input to both systems is a 1 kHz, 0 dB SACD signal.

Figure 21 shows the output signal of a fifth-order SDM, where the original signal input to the SDM is a 1 kHz, 0 dB SACD signal. The signal to noise ratio of the signal is 116.78 dB. Figure 22 shows a zoom in of Figure 24 in the audio frequency band of interest.

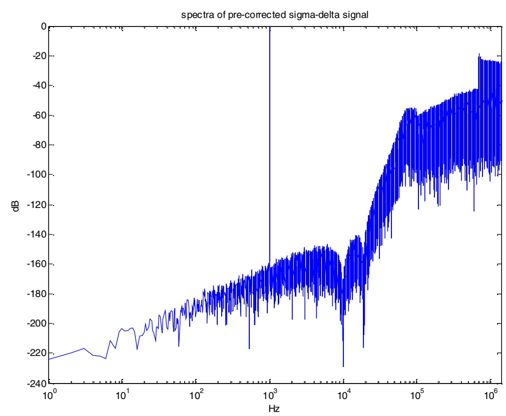

Figure 21: Spectra of fifth-order SDM output signal. Input is a 1 kHz, 0 dB SACD signal.

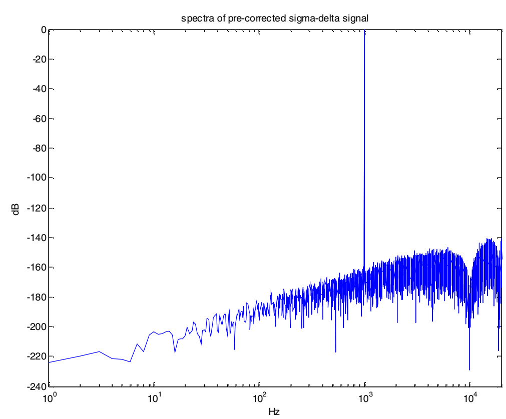

Figure 22: Zoom in of spectra of fifth-order SDM output signal with input 1 kHz, 0 dB SACD.

This fifth-order system was designed following the procedure outlined in Chapter 2, Section B, including pre-correction and dithering. The system is designed starting with a fifth-order Butterworth filter following [24]. The resonators of the system are located at 10 kHz and 19 kHz. This SDM is stable for input amplitudes up to 0.715, which surpasses Scarlet Book indications [30].

Figure 23a and 23b show the fifth-order SDM with and without resonators respectively. The effect of the resonators is clearly identifiable, as two notches in 10 kHz and 19 kHz prevent the high frequency noise from rising too abruptly as is the case in Figure 23a. Therefore, the tradeoff is better resolution in the area of the notches at the expense of less resolution in very low frequency area.

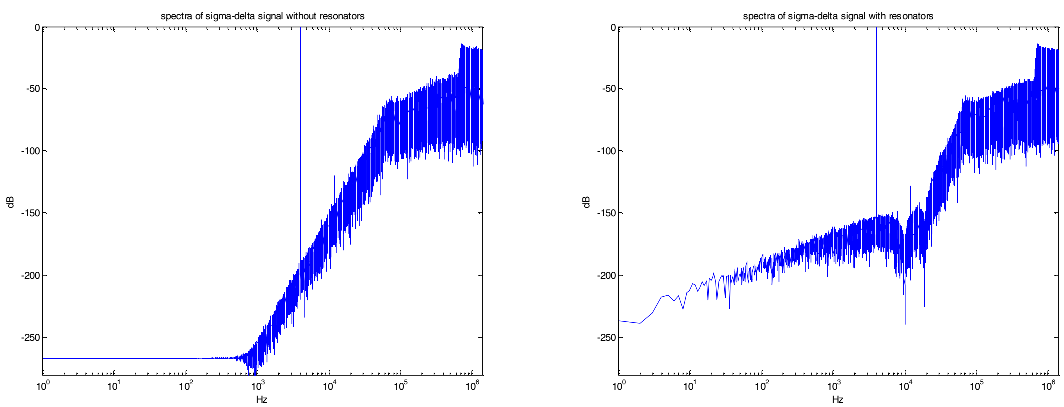

Figure 23: Spectra of fifth-order SDM output signal without pre-correction and with input 4 kHz, 0 dB SACD, a) without resonators, b) with resonators.

To view the effect of the pre-correction, Figure 24a and 24b display the output of the SDM without and with pre-correction respectively. The original signal input to the SDM is a 1 kHz, 0 dB SACD signal. It is evident how the harmonic components created by the sigma-delta modulation are cancelled out by the pre-correction.

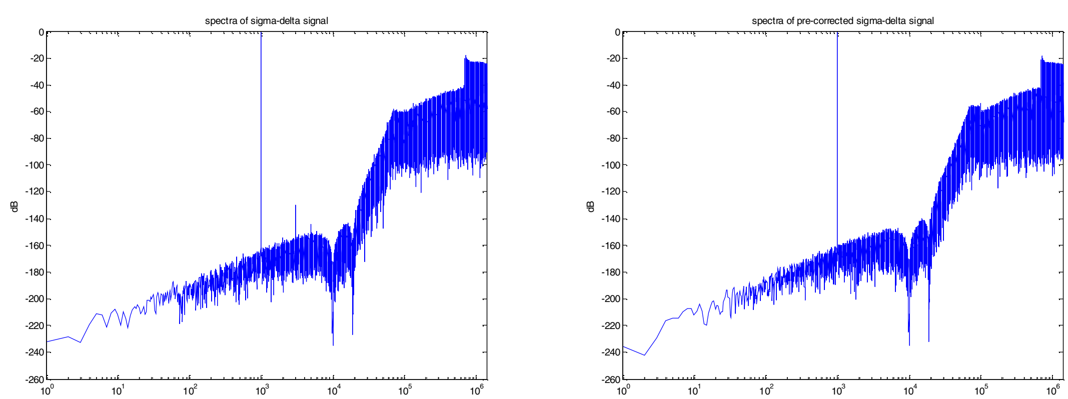

Figure 24: Spectra of fifth-order SDM output signal with input 1 kHz, 0 dB SACD. a) without pre-correction b) with pre-correction.

Figure 25 shows the same output as Figure 24 but after 64 linear averages. The effect of the averages is to lower the uncorrelated signal components and leave the correlated components unaffected. For 64 averages, the noise floor is lowered by exactly 18 dB ($64 = 2^6$; each power of 2 lowers the uncorrelated signal components by 3 dB, $6*3 = 18$). Conversely, remember that the pre-correction process boosts the noise floor by 3dB, while lowering the distortions by about 20 dB. This can be seen in figure 25.

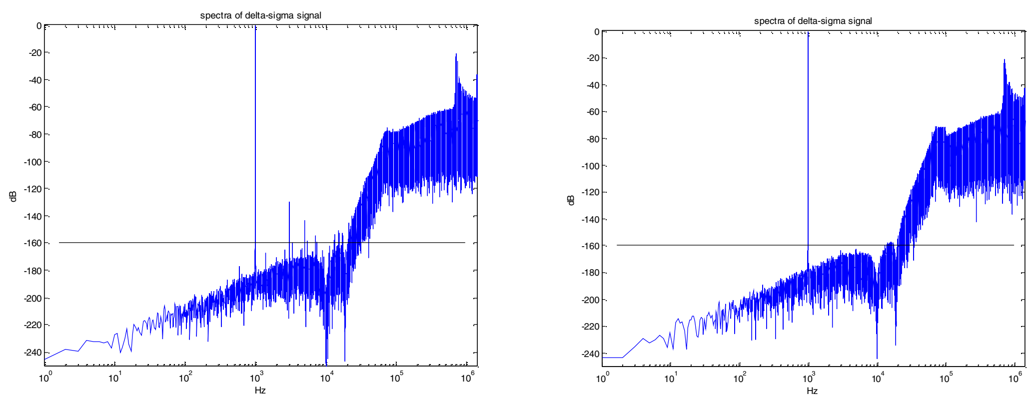

Figure 25: Spectra of 5th-order SDM output signal after 64 linear averages with input 1 kHz, 0 dB SACD. a) without pre-correction b) with pre-correction.

1. SDM Phase Response

Figure 26 shows the phase of the input and output signal of the SDM, where the original signal input to the SDM is a swept-frequency cosine. The frequency swept is from 1 to 30k Hz and lasts 1 second. Figure 26a is the input signal and Figure 26b is the SDM output.

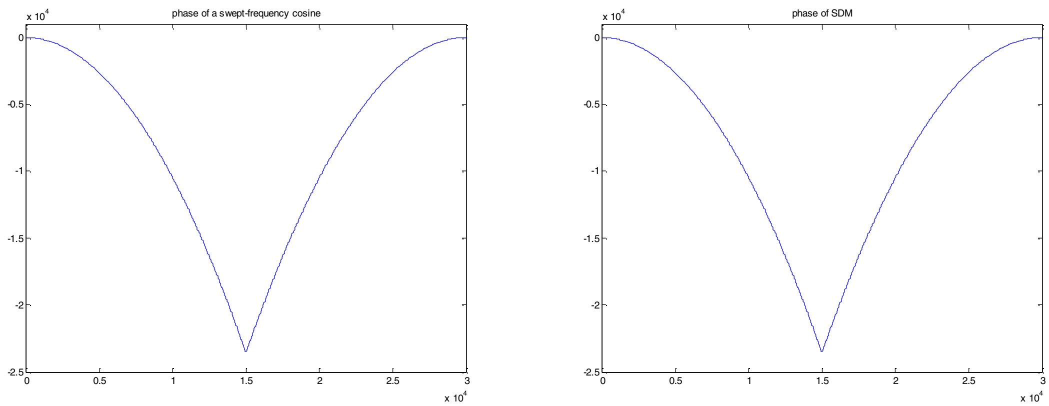

Figure 26: Phase response of, a) Swept-frequency cosine, b) SDM output.

Subtracting the input phase from the output phase gives the results of the system phase, shown in Figure 27. Fig. 27a shows the difference in the frequency band of 0 – 30k Hz. Fig. 27b shows the same result in the frequency band of 0 – 20k Hz. Notice that in the frequency band of 0 – 20k Hz the difference is less than $2\times10^{-4}\,rad$, while in the frequency band of 20k – 30k Hz it is at most $1\times10^{-3}\,rad$.

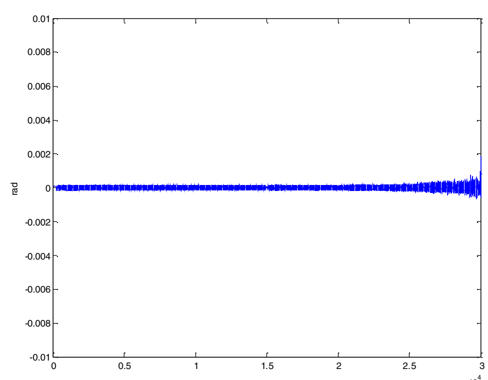

Figure 27: Difference between input and output of SDM with input a swept-frequency cosine:
a) 0 – 30k Hz, b) 0 – 20k Hz.

2. SDM Transient Response

To analyze the transient response of the SDM it is necessary to place a low-pass filter at the output of the system to recuperate a multi-bit signal and accordingly compare the input and the output. Following Scarlet Book [30] specifications, a Butterworth low-pass filter with a -3dB frequency of 50 kHz is placed at the output of the SDM.

Figures 31a and 31b show the transient response of the SDM with the output filter, versus the corresponding input signal. For comparison purposes, figure 29 shows the effect of only the Butterworth filter. Figure 30 shows a zoom in of figure 29 in the area of the step. This comparison allows one to determine the transient response of solely the SDM system and thus conclude it has good performance. As transient performance depends on overshoot and settling time, figure 28 shows the exact numbers for the given Butterworth filter with a step input of amplitude one. The figure reveals an overshoot percent of 14.3% and a settling time of less than 8×10^{-5} seconds. This overshoot accounts for the spike in the output step of the filter, i.e. $.5*1.143 = 0.5715$.

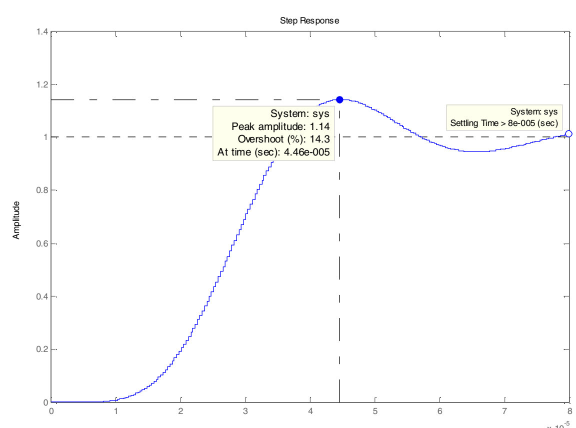

Figure 28: Step response of the 50 kHz Butterworth low-pass filter.

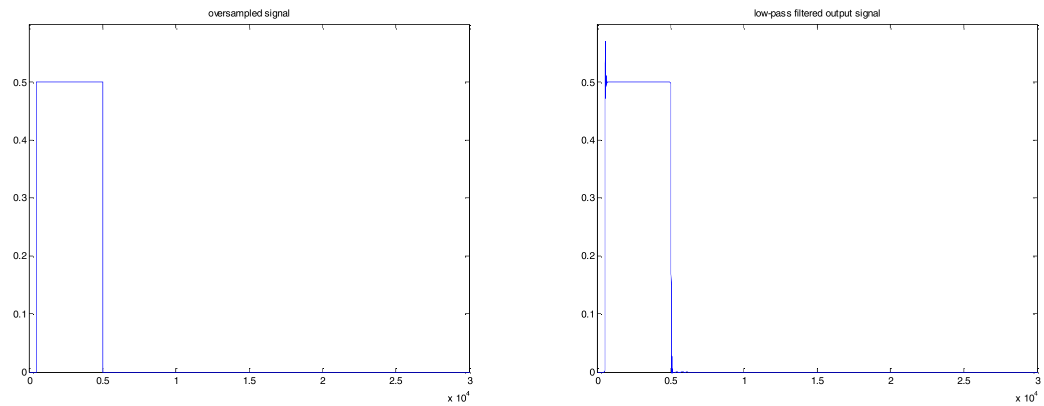

Figure 29: Input and output of Butterworth low-pass filter with input a step pulse a) input, b) output.

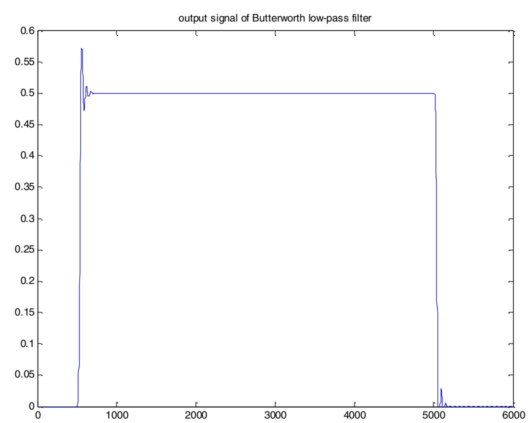

Figure 30: Output of Butterworth low-pass filter with input a step pulse. Zoom in of figure 29b.

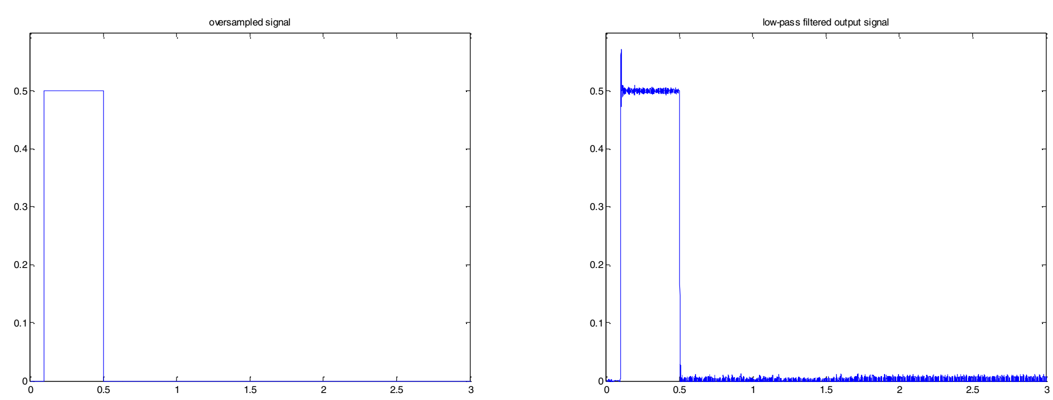

Figure 31: Input and output of SDM with input a step pulse a) input, b) output.

3. SDM Harmonic Distortion

An important analysis aspect when working with signals for audio applications are the frequency harmonics developed by the processing. The most used techniques for harmonic distortions measurements are Total Harmonic Distortion (THD) and Intermodulation Distortion (IMD).

THD figures are derived by feeding a pure sine wave into an audio component and then measuring the amplitude of the fundamental frequency and its harmonics. THD of a signal refers to the ratio of the sum of the powers of all harmonic frequencies above the fundamental frequency to the power of the fundamental frequency, or

$$\%THD = \frac{\sqrt{H_2^2 + H_3^2 + \cdots H_N^2}}{\sqrt{H_1^2}} \times 100, \tag{44}$$

where terms 2 to N are the power levels of the harmonics and term 1 is the power level of the fundamental frequency.

Clearly, from the pre-correction discussion, harmonics derived from the fundamental frequency when the input amplitude is 0dB SACD are not present. On the other hand, smaller signal analysis say, of input amplitude 1×10^{-5} $(-100\,dB)$ do reveal certain harmonics in the output signal (input amplitudes smaller than approximately $-120\,dB$ are too small to show any harmonic components). However, these harmonics are not specific to the input; they depend more on the dithering values. Hence, different simulations give different results; nonetheless, these results are presented for example purposes and to emphasize small signal performance. Figure 32 illustrates the case for an original signal of, a) 1 kHz, -60 dB, b) 1 kHz, -100 dB.

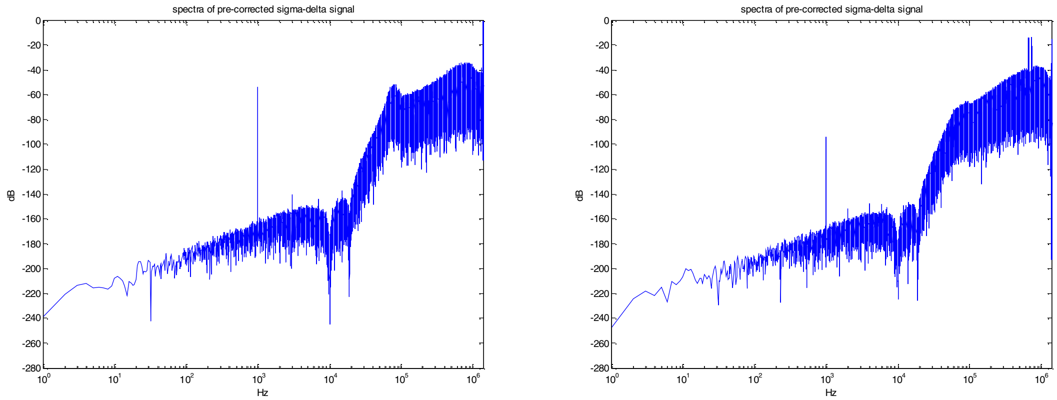

Figure 32: SDM output for an original signal input of: a) 1 kHz, -60 dB, b) 1 kHz, -100 dB.

In figure 32a three harmonics are plainly visible, each at approximately 3 kHz, 7 kHz and 15 kHz with approximate amplitude at -134.3, -137.5 and -131.2 dB respectively. These numbers give a THD of 0.0091%. These measurements are typically done with a full amplitude input signal. As a hypothetical example, a full 0dB SACD signal with the same distortions would have given a THD of less than $.00002\%$. In the signal of figure 32b, there are more visible harmonics with slightly less amplitude. In this figure the THD is approximately 0.5418%.

IMD is a means for measuring a nonlinear distortion occurring when two signals at different frequencies are produced at the same time, creating additional signals at various other frequencies and at various amplitudes. New signals are created at frequencies found by adding the original two frequencies, by subtracting the original two frequencies from one another, and from the sums and differences of the harmonics. Figure 33 shows the output signal of the SDM where the original signal input to the SDM is, a) 19 kHz and 20 kHz, 0 dB SACD signal, and b) 2 kHz and 8 kHz, 0 dB SACD signal. As with the THD examples, for 0dB SACD signals the pre-correction has reduced the IMD to below the noise floor.

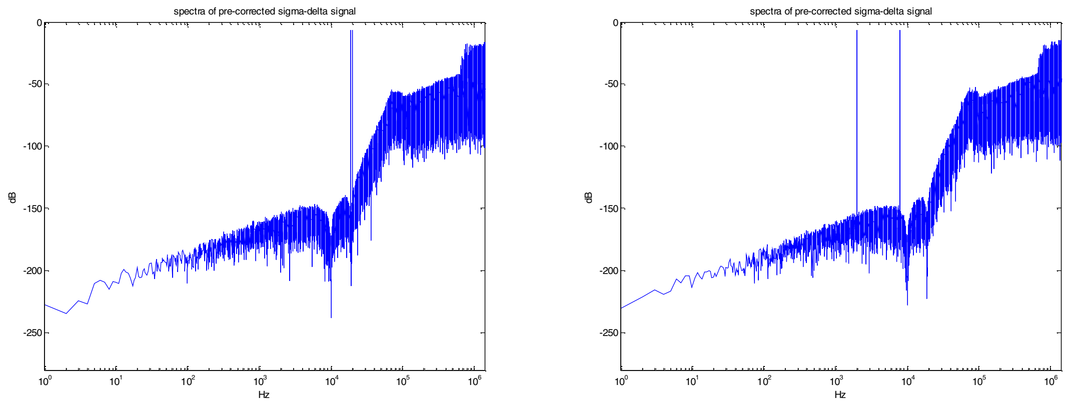

Figure 33: SDM output for an original signal input of: a) 19 and 20 kHz 0 dB SACD b) 2 kHz and 8 kHz, 0 dB SACD signal.

A seventh-order SDM offers better resolution than the fifth-order system for amplitudes less than the maximum modulation depth of 50%. If the system has no clippers and pre-correction is not applied, the system is stable for input amplitudes of up to 0.589, with signal to noise ratio for this amplitude of 133.55 dB. For an input with amplitude of 0.5, the signal to noise ratio is 134.12 dB.

If signal peak amplitudes of 0.71 are desired, to comply with [30], clipper design allows input amplitudes greater than 0.71, however, the signal to noise ratio for input 0.5 is reduced to 104.76 dB. Figure 34 shows the output signal of the seventh-order SDM with clippers and pre-correction for an original signal input of 1 kHz, 0 dB SACD.

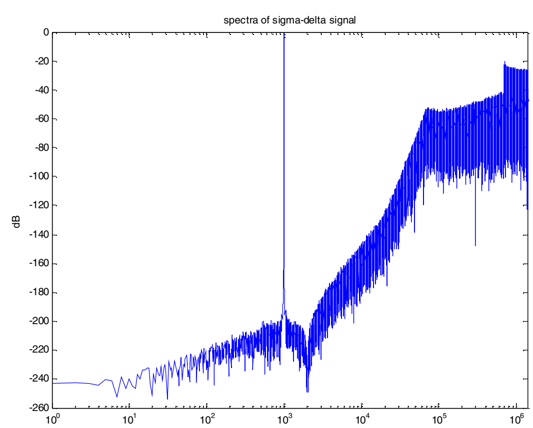

Figure 34: Spectra of seventh-order SDM output signal with clippers. Input is a 1 kHz, 0 dB SACD signal.

For the remainder of this work, the seventh-order system used refers to the specifications of the following. The system is designed from a seventh-order Butterworth filter with cut-off frequency of 70 kHz. The resonators of the system are located in 4 kHz, 12 kHz and 20 kHz. Figure 35 shows the output signal of this seventh-order SDM with the same original signal input of 1 kHz, 0 dB SACD. This system has no clippers, but pre-correction is applied. With pre-correction, the system is stable for inputs up to 0.5, with signal to noise ratio of 131.63 dB, which is exactly 2.49 dB less than the system without pre-correction.

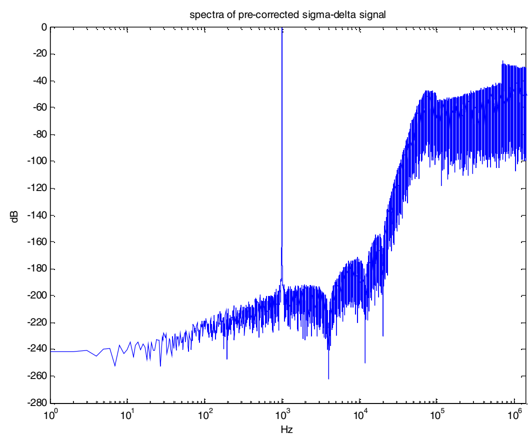

Figure 35: Spectra of seventh-order SDM output signal without clippers. Input is a 1 kHz, 0 dB SACD signal.

Figure 36 shows the spectra of the fifth-order and seventh-order SDM output signals with input 1 kHz, 0 dB SACD signal. The difference is quite noticeable in the noise floors in the audio bandwidth vs. the difference in high frequency noise.

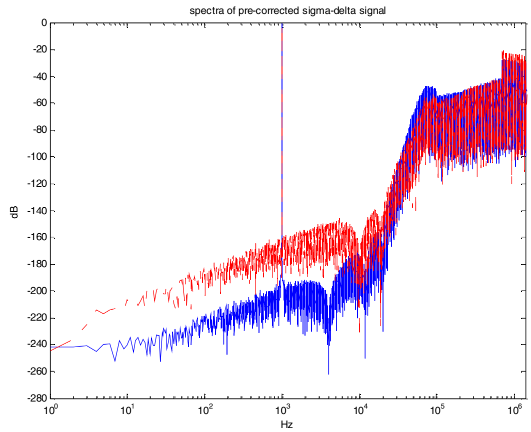

Figure 36: Spectra of fifth-order and seventh-order SDM output signal. Input is a 1 kHz, 0 dB SACD signal. Red (above) is fifth-order, blue (behind) is seventh-order.

To this date, most if not all, hardware DSD recorders make use of fifth-order sigma delta modulators. Therefore, the majority of the simulations and results presented hereafter are from the preceding fifth-order SDM.

As additional examples, the following figures show the output of the SDM with various input signals of different amplitudes and frequency components. The purpose of these figures is to view the performance of both, 5th and 7th order modulators, with input signals different than those used in the previous examples. These figures validate the preceding results are not frequency dependant. However, of particular interest is the SNR of the signals of input amplitudes below 0 dB SACD. Since the noise floor of the system depends on the input amplitude (smaller input = lower noise floor), the reduction in SNR is less than expected. The caption of each figure details SDM order, input signal and signal to noise ratio of the output.

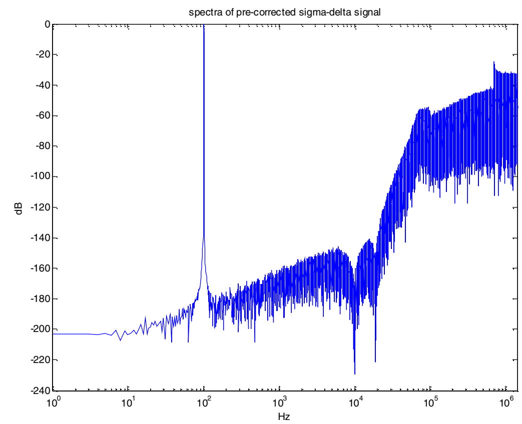

Figure 37: 5th order SDM output for an original signal input of 100 Hz 0 dB SACD. SNR = 116.82 dB.

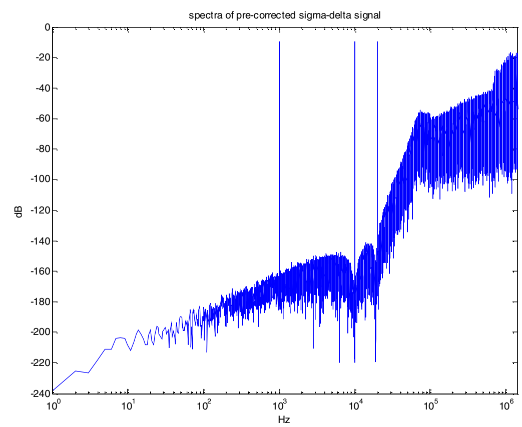

Figure 38: 5th order SDM output for an original signal input of 1 kHz, 10 kHz and 20 kHz, 0 dB SACD. SNR = 116.78 dB.

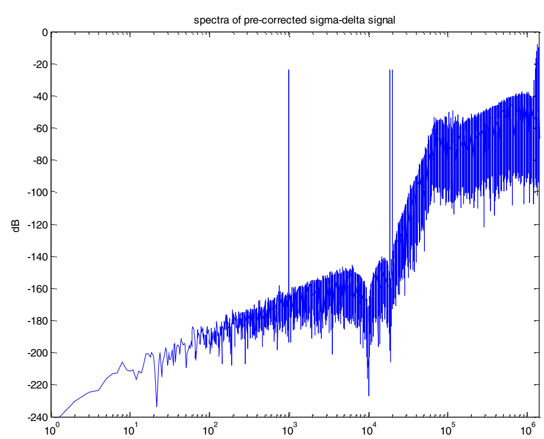

Figure 39: 5th order SDM output for an original signal input of 1 kHz, 19 kHz and 20 kHz, -14 dB SACD. SNR = 103.45 dB.

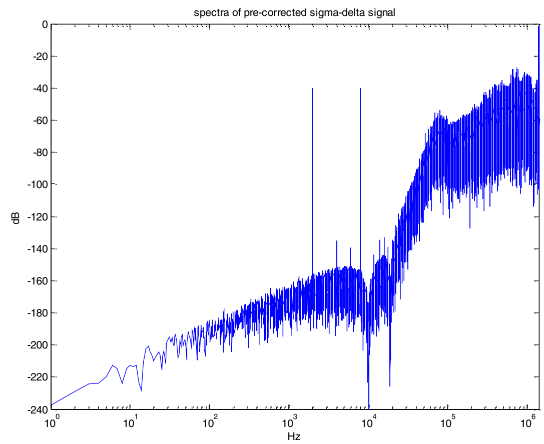

Figure 40: 5^{th} order SDM output for an original signal input of 2 kHz and 8 kHz, -34 dB SACD. SNR = 85.52 dB.

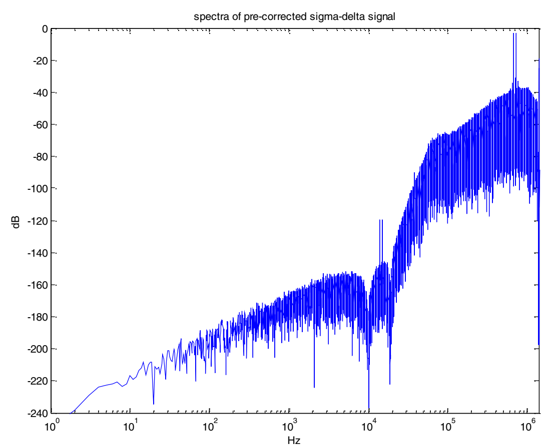

Figure 41: 5^{th} order SDM output for an original signal input of 14 kHz and 15 kHz, -114 dB SACD. SNR = 5.52 dB.

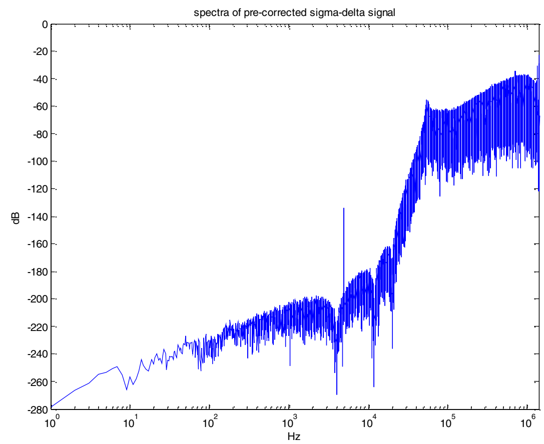

Figure 42: 7th order SDM output for an original signal input of 4 kHz, -134 dB SACD. SNR = 3.27 dB.

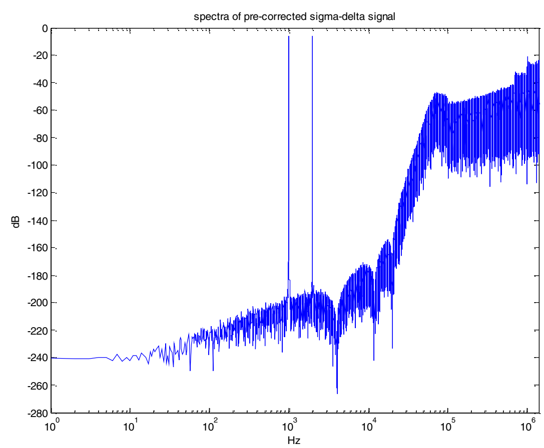

Figure 43: 7th order SDM output for an original signal input of 1k & 2 kHz, 0 dB SACD. SNR = 131.78 dB.

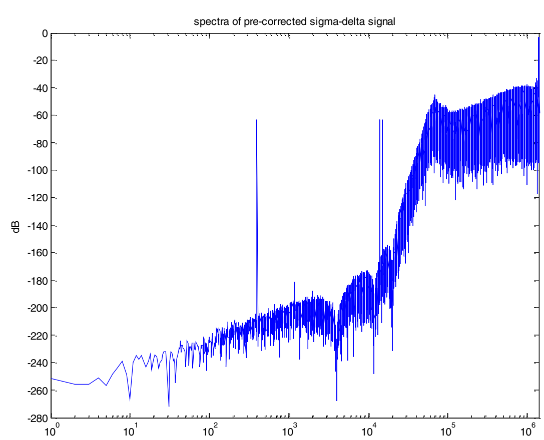

Figure 44: 7th order SDM output for an original signal input of 400 Hz, 14 kHz and 15 kHz, -54 dB SACD. SNR = 79.69 dB.

C. Pulse Code Modulator Performance

The first thing to be determined is how good SDM and PCM are. This section describes experiments run to determine the limits of PCM, specifically 24-bit 88.2 kHz quality. With this information and previous SDM performance analysis, it is possible to determine the limitations of the modulating systems versus the limitations of the format conversion systems.

To compare what is readily available (16-bit CDs) with the high-resolution standard, figure 45a and 45b show the spectra of the output of a) a 16-bit PCM and b) a 24-bit PCM, both with TPDF dithering. The original signal input to the system is a 1 kHz, 0 dB signal. The frequency scale is linear so it is worth noticing the end-to-end flat noise floor of both systems. Theoretically, for a sampling frequency of 88.2 kHz and with TPDF, the noise floor, or average quantization noise power, of a 16-bit system is -139.77 dB, whereas the noise floor of the 24-bit system is -187.88 dB. For the signals of figure 45, the signal to noise ratio for the 16-bit output is 93.29 dB, while the SNR for the 24-bit output is 141.44 dB.

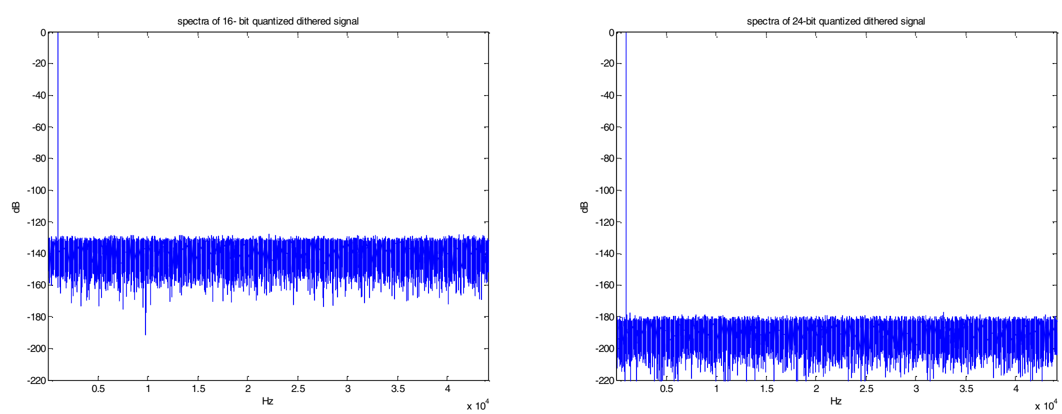

Figure 45: PCM output for an original signal input of 1 kHz 0 dB: a) 16-bit output b) 24-bit output.

Linear PCM has the benefit of linear phase. If an anti-aliasing filter is used, it should also have linear phase to exploit this attribute. Therefore, an analysis of PCM phase performance is not needed.

1. PCM Transient Response

Figure 46a and 46b show the transient response of the PCM system versus the corresponding input signal. Figure 47 shows a zoom in of figure 47b in the area of the step. From these two figures, it is easy to appreciate the high quality transient response performance of PCM. These signals were processed through an anti-aliasing FIR filter, hence the overshoot in the response.

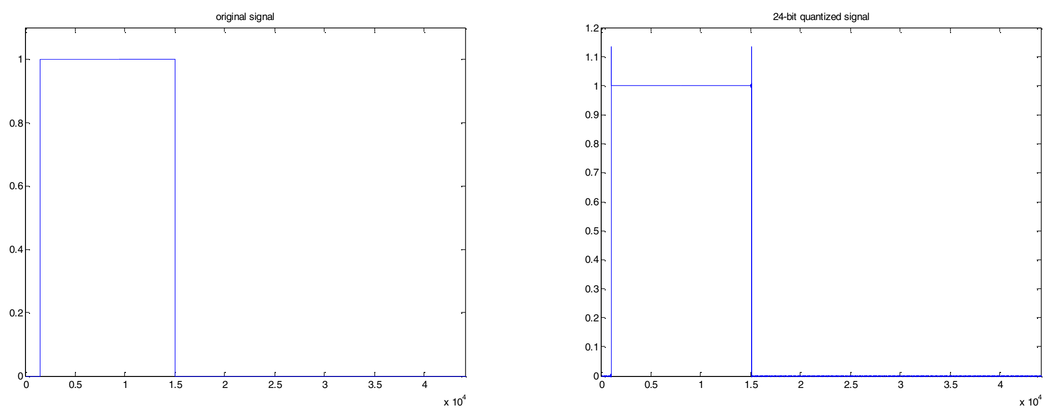

Figure 46: Input and output of PCM with input a step pulse a) input, b) output.

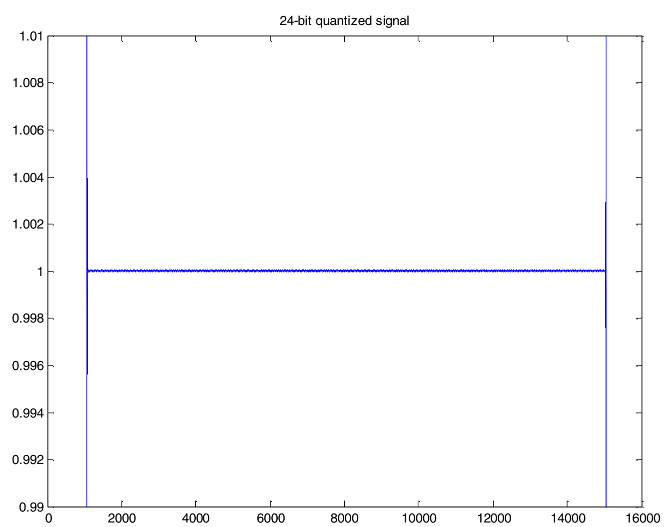

Figure 47: Output of PCM with input a step pulse. Zoom in of figure 46b.

2. PCM Harmonic Distortion

PCM with TPDF dither has the first and second moments of the quantization error independent of the input signal, specifically noise modulation and harmonic distortions; that is, PCM does not have harmonic distortions. Figure 45 confirmed no distortions for a 1 kHz input, having THD = 0%. Furthermore, in contrast to SDM performance, reducing the input amplitude to the PCM does not produce any harmonics in the output for any given frequency signal, i.e. THD = 0%. Regarding IMD, figures 48, 49 and 50 show various scenarios for possible harmonic distortions. The signals in these figures confirm that there is no IMD produced from the modulation process, i.e. IMD = 0%. For enhanced clearness, these figures are plotted in the frequency band of 0 – 26k Hz.

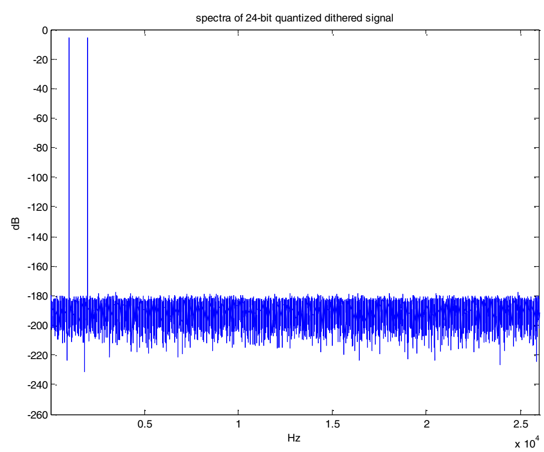

Figure 48: PCM output for an original signal input of 1 kHz and 2 kHz, 0 dB. SNR = 141.46.

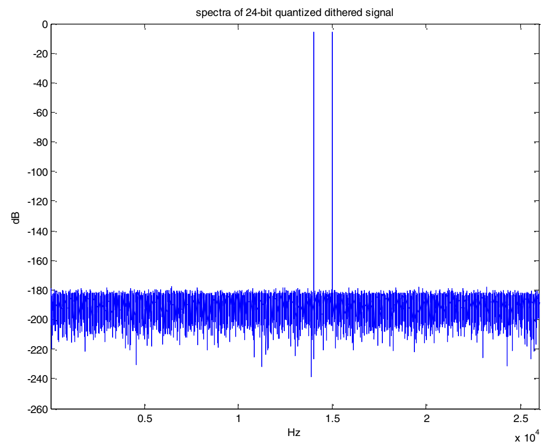

Figure 49: PCM output for an original signal input of 14 kHz and 15 kHz, 0 dB. SNR = 141.48.

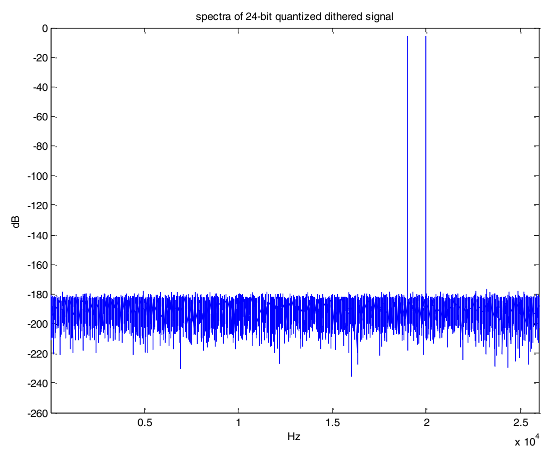

Figure 50: PCM output for an original signal input of 19 kHz and 20 kHz, 0 dB. SNR = 141.44.

D. Perfect Reconstruction

This section describes the methodology and results of a lossless conversion system designed for DSD to PCM and PCM to DSD conversions. The section begins by describing the system and showing perfect reconstruction is possible when all decomposition information is available for reconstruction. Following this are the results of a practical audio converter that converts the DSD signal to a 24-bit 88.2 kHz signal and, using only the multi-bit signal, converts the signal back to DSD format.

Various perfect reconstruction filter banks make it possible to take a 1-bit signal, carry out downsampling and filtering, obtain a multi-bit signal, and subsequently perform upsampling and filtering to recuperate an exact representation of the original 1-bit signal. The thesis of this work is to determine if a lossless conversion from a 1-bit signal to a multi-bit signal, specifically 24 bits, and back is possible. As stated with orthogonal filter banks, most wavelets in general have a very slow and gentle cut off region. As a result, in cases where the sampling rate change allows the original signal's frequency content to appear in the cut off region of the filter, aliasing will occur.

Figure 51 shows the complete system for perfect reconstruction analysis. In this system, the input $x[n]$ is a one-bit sigma-delta modulated signal with a sampling frequency of 2.8224MHz. The system consists of five decomposition stages where in each stage the signal is downsampled by a factor of two. After the fifth stage, the signal has the desired sampling frequency of 88.2 kHz. Afterward the signal is processed through five reconstruction stages to recuperate the one-bit 2.8224MHz signal.

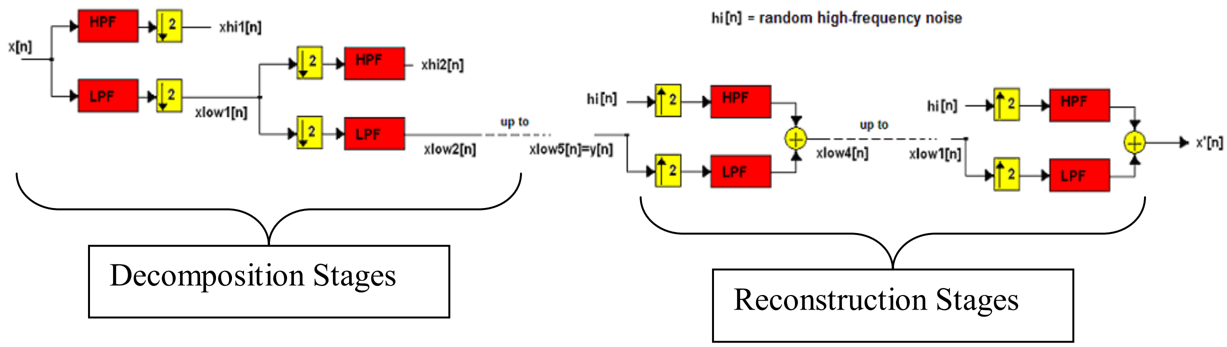

Figure 51: Complete system for perfect reconstruction analysis.

After each decomposition stage, the subband signals (xlow[n] and xhi[n] in figure 51), each have a length equal of half the input signal plus half the length of the filter ($x[n]$ and the filters are all of even length). Consider $x[n]$ of length N and the analysis filters of length M. In order for each subband signal to have exactly half the length of its input signal, N/2, the last M/2 samples of the subband signal are added to the first M/2 samples. The effect of this procedure on the boundaries of the subband signals is negligible for this work.

The perfect reconstruction filter banks that offered the best response for this type of application were a selection of biorthogonal filter banks (see Chapter 2 Section D). As referenced in [36] in the Matlab Wavelet Toolbox, wavelets “2.6”, “2.8”, “3.7”, “3.9” and “6.8” from the family of biorthogonal wavelets, were used in this work. The specific name of the wavelets refers to the effective length of the decomposition and reconstruction filters associated with the respective wavelet. These wavelets minimized aliasing during decomposition. When the sampling rate change was small, that is, when the signal’s frequency bandwidth is near the transition region of the filter, aliasing error is introduced due to insufficient attenuation in the stopband area. For example, in the fifth decomposition stage, where the sampling rate change is from sampling frequency $F_{S1} = 176.4\,kHz$ to $F_{S2} = 88.2\,kHz$, signal content above 44.1 kHz is in the beginning of the transition region of the filter; therefore, it is not sufficiently attenuated.

Figure 52 shows the frequency and phase response of each decomposition and reconstruction filter for biorthogonal wavelet "6.8". These filters do not have a flat response in the pass band. Figure 53 shows a zoom in of each filter, which displays the exact amount of gain each filter generates. This gain is responsible for amplitude errors in the decimated signal when the frequency bandwidth of interest is near that specific region. Each filter offers linear phase response. Out of each biorthogonal filter mentioned in Chapter 4 Sec. B, "6.8" offered the best tradeoff/compromise between fast response, stop band attenuation and pass band gain, thus it was chosen for the perfect reconstruction.

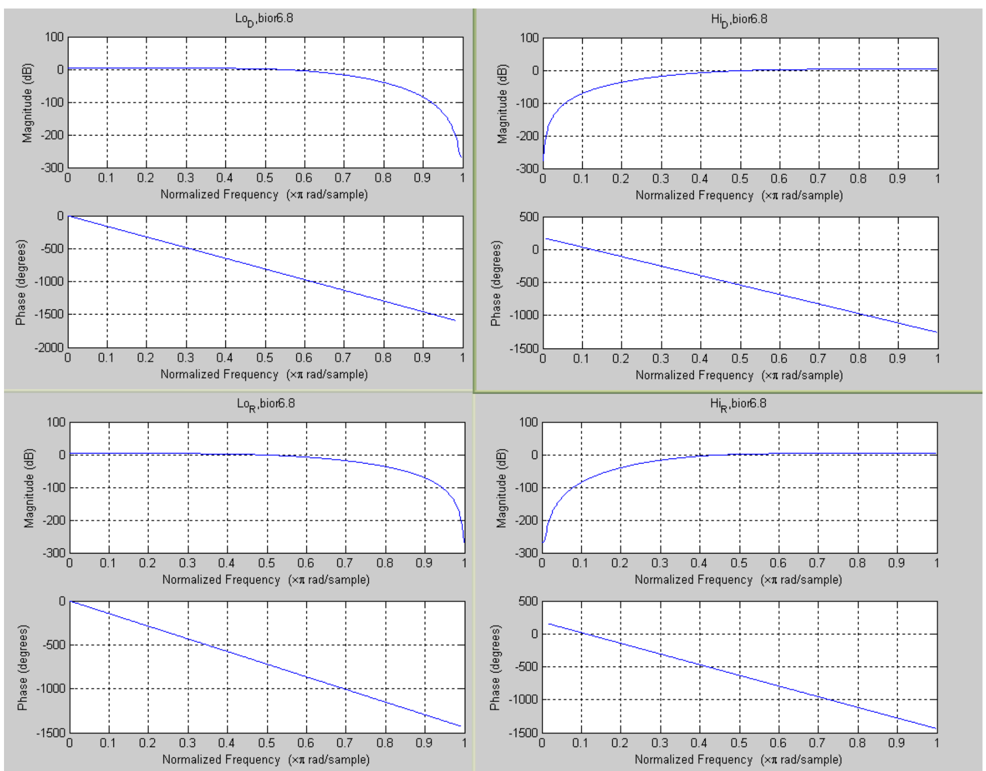

Figure 52: Decomposition and reconstruction filters for biorthogonal wavelet "6.8".

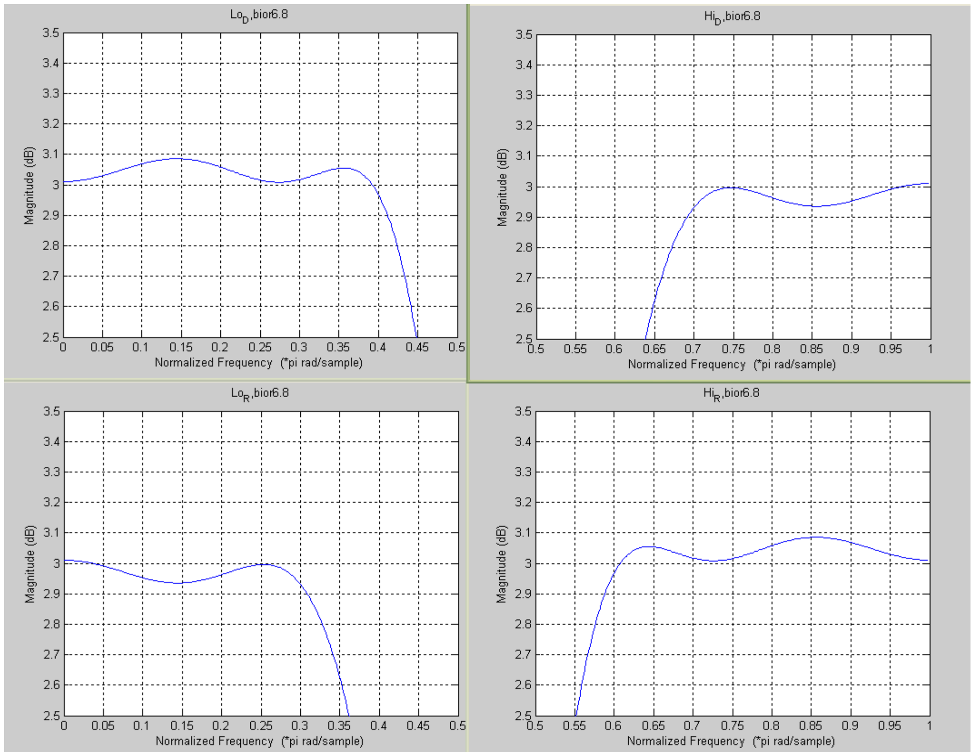

Figure 53: Decomposition and reconstruction filters for biorthogonal wavelet “6.8”. Zoom in of Figure 55.

The following figures show the perfect reconstruction procedure when the original signal input to the SDM is a 1 kHz, 0 dB SACD signal. Figure 54 shows from left to right, the one-bit signal, followed by each signal of interest after each decomposition stage, i.e. a) one-bit signal, Fs = 2.8224 MHz, b) signal xlow1, Fs = 1.4112 MHz, c) signal xlow2, Fs = 705.6 kHz, d) signal xlow3, Fs = 352.8 kHz, e) signal xlow4, Fs = 176.4 kHz, f) signal xlow5, Fs = 88.2 kHz; following notation detailed in figure 51. The signal to noise ratio for each graph is 116.74, 116.73, 103.35, 97.11, 90.15 and 82.55 dB respectively. The first decomposition stage, output signal xlow1, affects the whole signal by just about 3dB; therefore, the SNR has not changed. Subsequent decomposition stages yield decreasing SNR values because of non-uniform magnitude distortion. For these signals not only is there cumulative magnitude distortion, but also aliasing distortions as explained above.

Figure 55 shows the original one-bit signal followed by the output of each reconstruction stage in the same order as figure 54. The last graph is the recuperated one-bit output signal $x'[n]$.

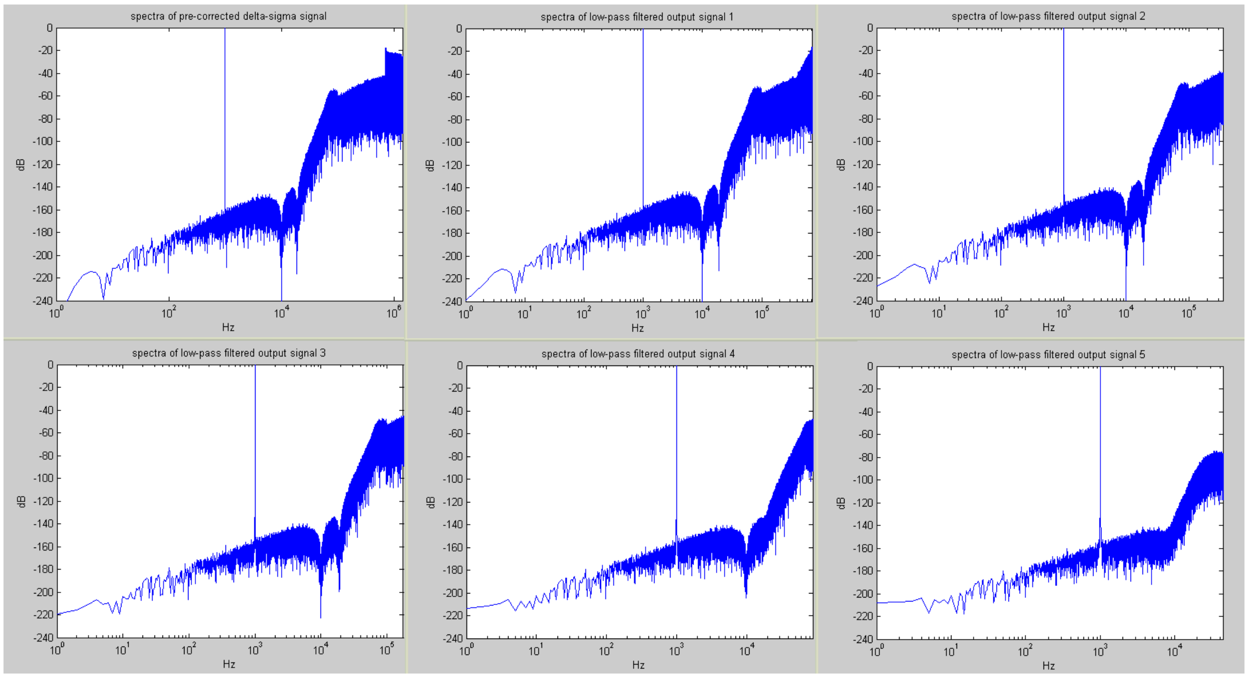

Figure 54: Decomposition procedure for a 1 kHz, 0 dB SACD signal. From left to right: a) 1-bit signal, b) signal xlow1, c) signal xlow2, d) signal xlow3, e) signal xlow4, f) signal xlow5.

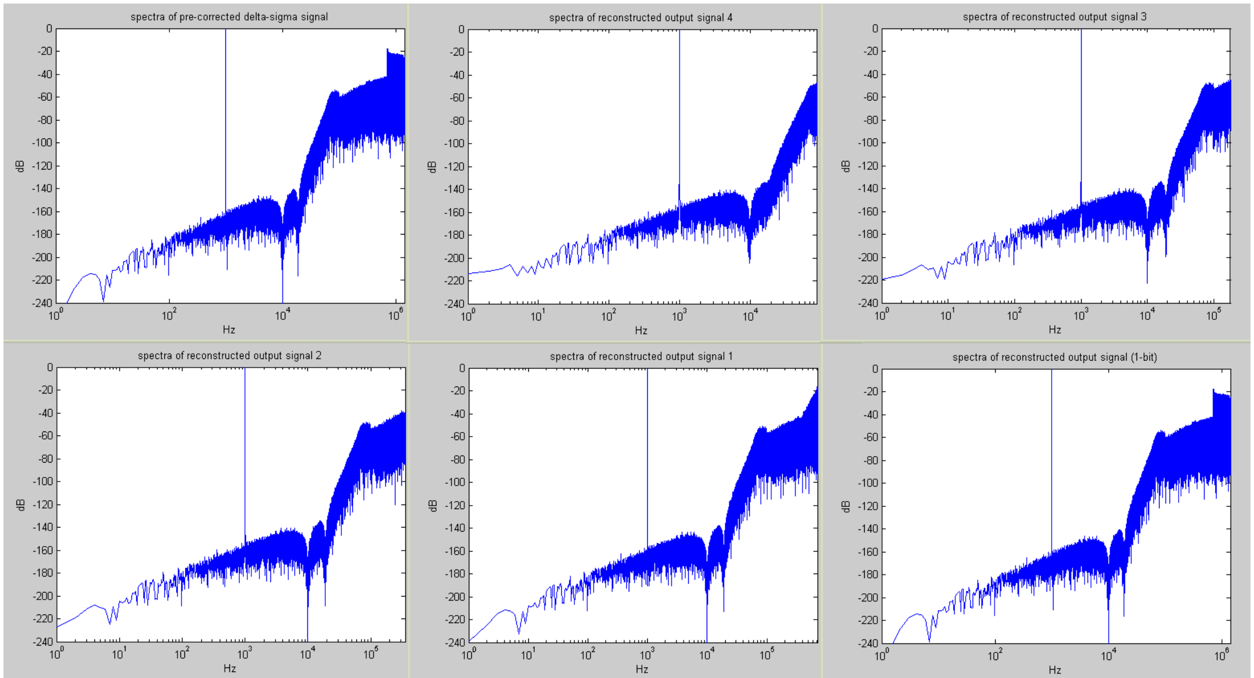

Figure 55: Reconstruction procedure for a 1 kHz, 0 dB SACD signal. From left to right: a) 1-bit signal, b) signal xlow4, c) signal xlow3, d) signal xlow2, e) signal xlow1, f) reconstructed 1-bit signal.

Figures 56 to 59 show additional examples for different input signals. The examples are given to validate the above results as not input dependant. In all these examples the signal to noise ratios at different decomposition stages are very similar to the preceding example.

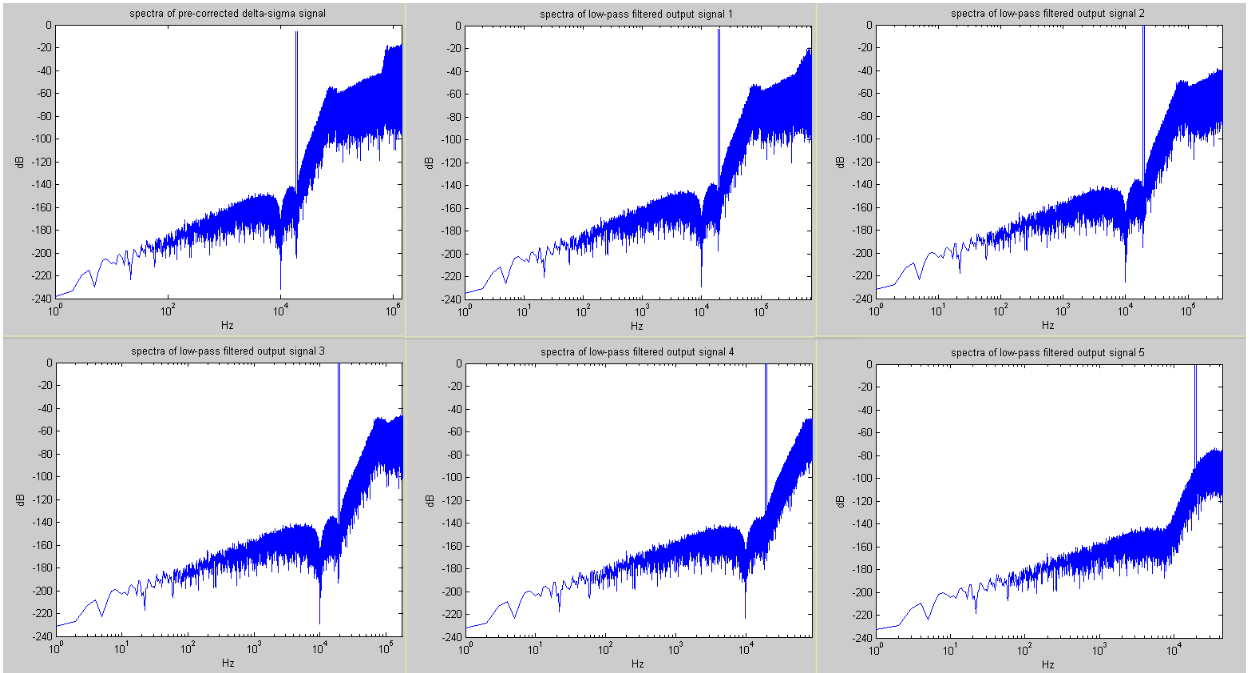

Figure 56: Decomposition procedure for a 19 kHz & 20 kHz, 0 dB SACD signal. From left to right: a) 1-bit signal, b) signal xlow1, c) signal xlow2, d) signal xlow3, e) signal xlow4, f) signal xlow5

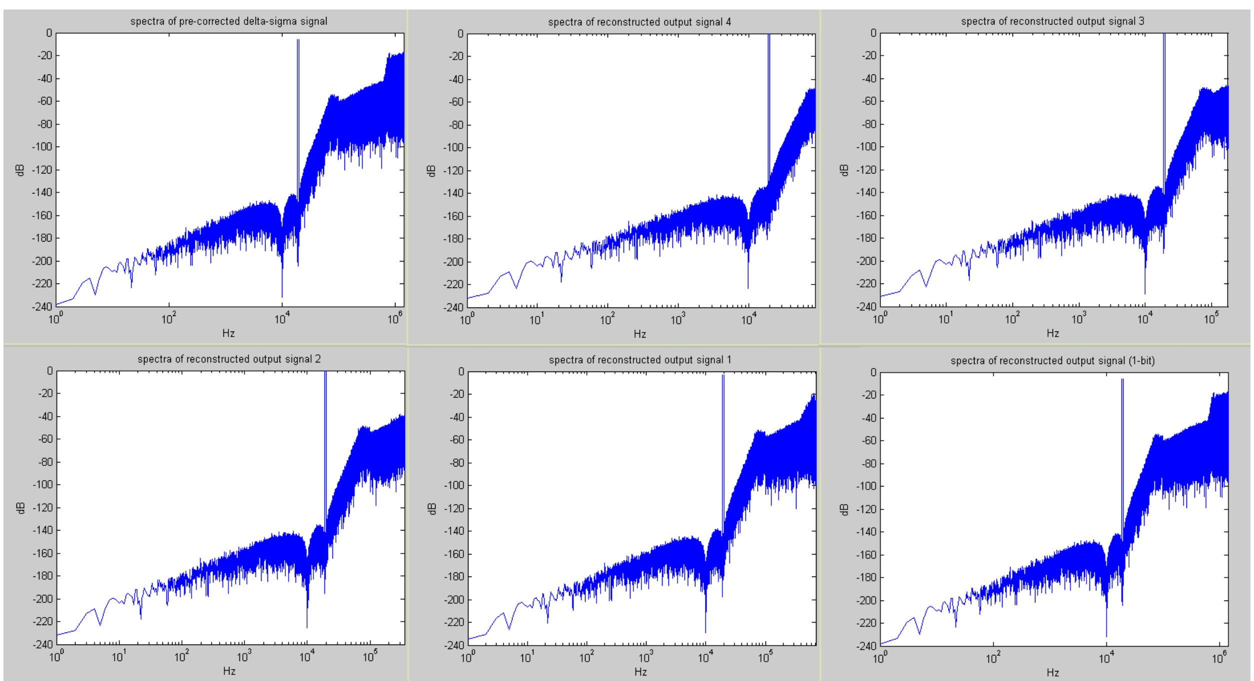

Figure 57: Reconstruction procedure for a 19 kHz & 20 kHz, 0 dB SACD signal. From left to right: a) 1-bit signal, b) signal xlow4, c) signal xlow3, d) signal xlow2, e) signal xlow1, f) reconstructed 1-bit signal

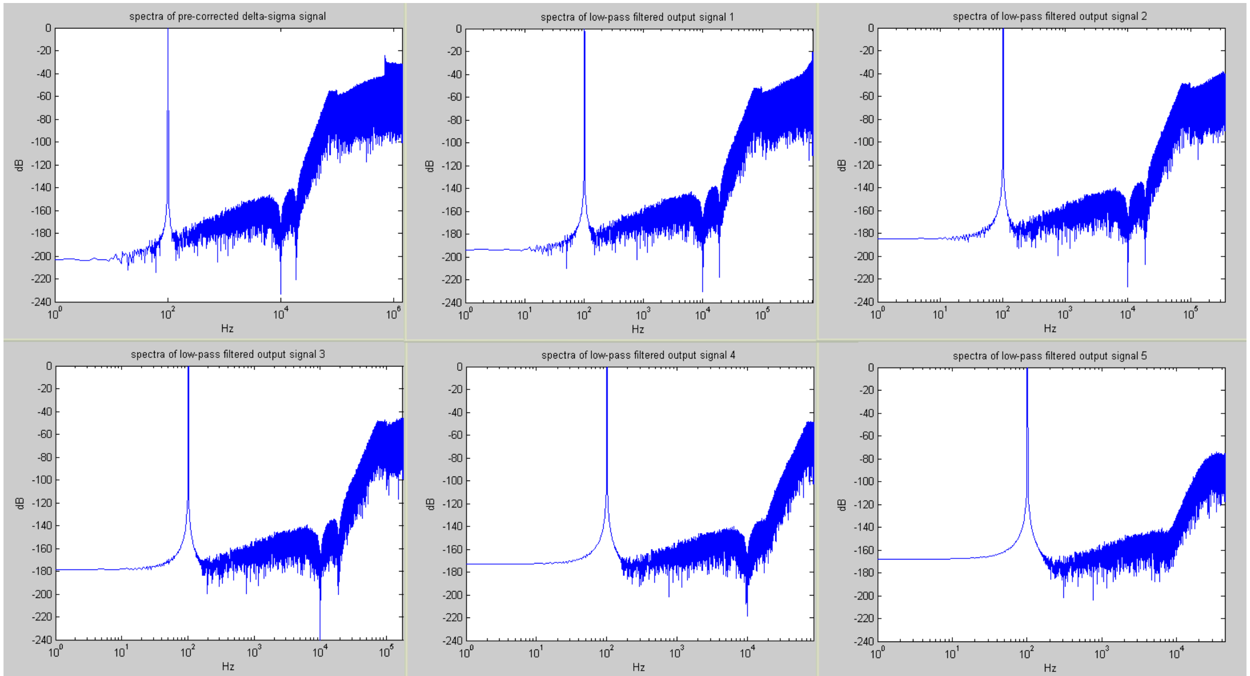

Figure 58: Decomposition procedure for a 100 Hz, 0 dB SACD signal. From left to right: a) 1-bit signal, b) signal xlow1, c) signal xlow2, d) signal xlow3, e) signal xlow4, f) signal xlow5

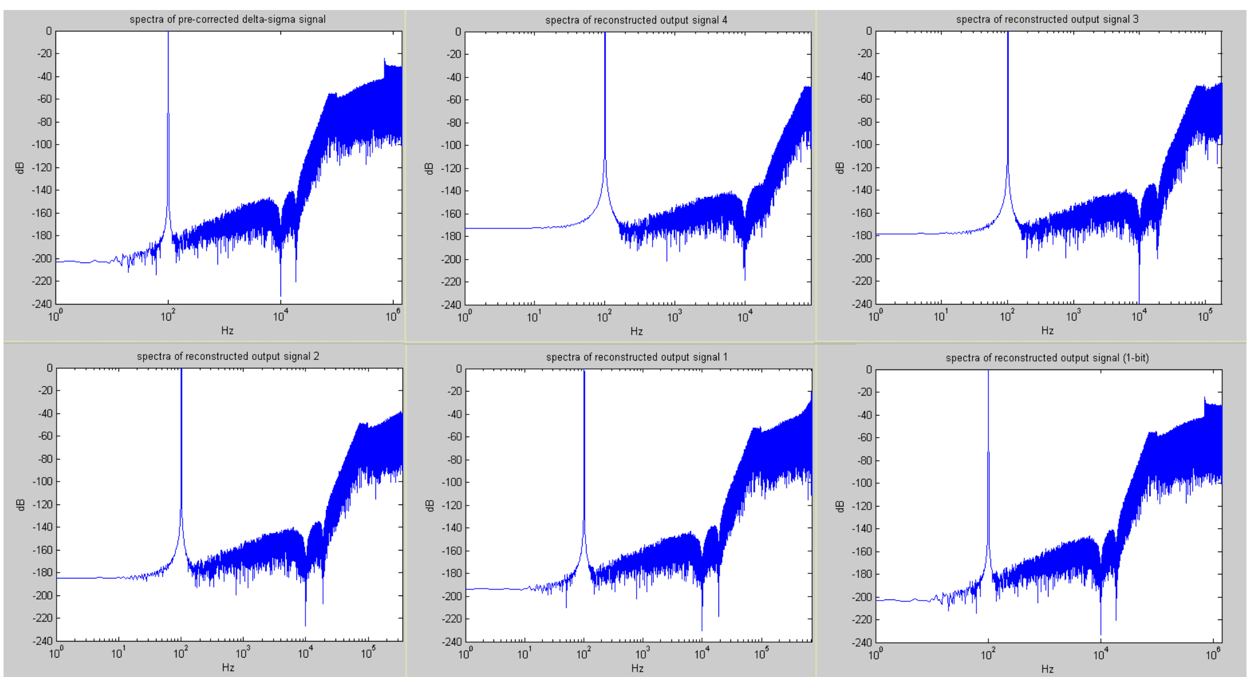

Figure 59: Reconstruction procedure for a 100 Hz, 0 dB SACD signal. From left to right: a) 1-bit signal, b) signal xlow4, c) signal xlow3, d) signal xlow2, e) signal xlow1, f) reconstructed 1-bit signal.

Again, the objective is to determine if a lossless conversion from a one-bit signal to a 24-bit signal and back is possible. In a realistic situation, once the 24-bit signal is obtained, all high frequency information (frequencies above 44.1 kHz, for a Fs = 88.2 kHz) is lost. So, to study the practical significance of this application, the reconstruction procedure was done using random high frequency content (xhi1[n] to xhi5[n] in figure 51). In the following case, again the processed signal is a 1 kHz 0dB SACD signal. This signal is decomposed only once and then reconstructed using the high frequency content from a 4 kHz 0dB SACD signal. Figure 60 shows the initial 1 kHz 0dB SACD signal followed by the reconstructed signal.

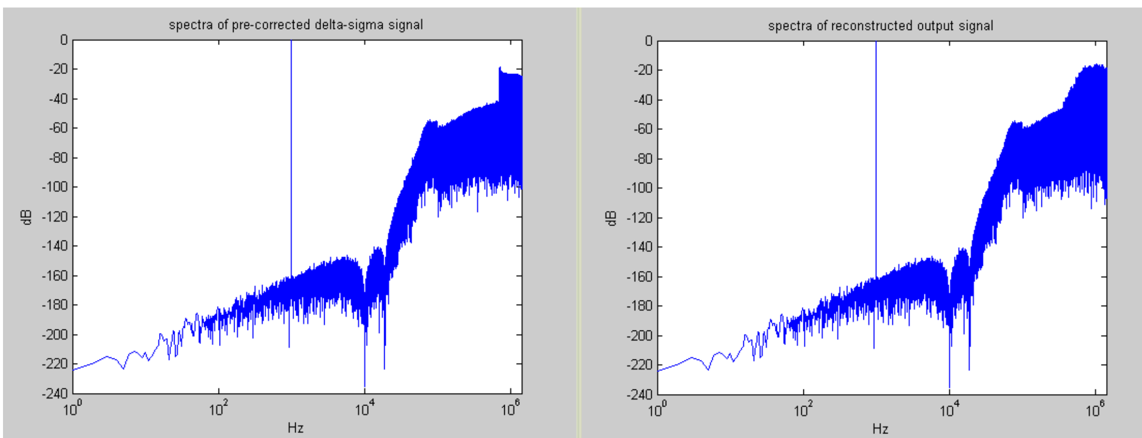

Figure 60: 1 kHz, 0 dB SACD signal followed by a reconstructed signal with random high frequency content.

These signals from figure 60 both have the same signal to noise ratio as the previous example, however, the output signal is not one-bit. A calculation of the difference between the input and output signals gives a maximum and minimum error of 3.76 and -3.67 respectively. This signal cannot be rounded or re-quantized to recuperate a one-bit signal. As more decomposition and reconstruction stages are carried out, an output signal with the same SNR of the input can be achieved, however, calculation of the error would correspondingly give out higher numbers, thus further from the target one-bit format.

E. Multi-rate Modulation System

Having concluded perfect reconstruction filter banks analysis, the main part of this work focused on a multi-rate modulation system (MMS) which could change an original signal to either DSD or PCM. This new signal would then be converted to the other format, one-bit or multi-bit, analyzed and subsequently returned to the original. This system does not produce lossless conversions. It is designed however, to produce minimum distortions.

For most multi-rate conversions, the chosen filters are window-based finite impulse response filters (FIR) designed with a Hanning window. The pass band of these filters is flat to less than +0.6 dB, -0.1 dB.

The only filter not designed this way is the filter used to upsample a 24-bit signal from 88.2 kHz to 2.8224 MHz. This filter is a window-based FIR with a Gaussian window. This specific filtering process was done in the frequency domain given the difficult task of filtering a signal with a noise floor that peaks at less than -180 dB.

The first two sections describe one-way conversions, that is, DSD to PCM and PCM to DSD. With the knowledge of each modulators performance (Chapter 3, Section B and C), it is possible to determine the performance of these systems and thus reach conclusions on the limitations of each modulator in representing the other signal. The last section describes complete conversions, that is, DSD to PCM to DSD and PCM to DSD to PCM. In essence, the complete conversions are the combination of the first two sections. The purpose is to examine how well the original signal is preserved after processing.

1. DSD to PCM Conversions

Figure 61 shows the MMS for DSD to PCM conversions, where $x[n]$ is the one-bit signal and $y[n]$ is the PCM signal. In this system the input signal, with sampling frequency 2.8224 MHz, is processed through the SDM to obtain the one-bit DSD signal $x[n]$. After the applicable measurements and calculations, the signal is low-pass filtered, downsampled and quantized to obtain the 24-bit 88.2 kHz multi-bit $y[n]$. This $y[n]$ is then analyzed along with the DSD signal in order to compare their quality and statistics.

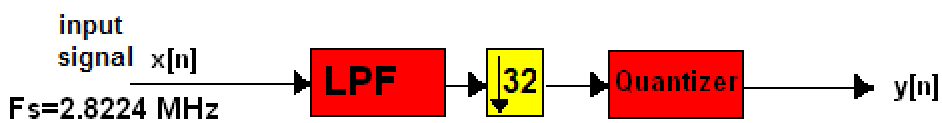

Figure 61: MMS for DSD to PCM conversions.

Figures 62a and 62b show the one-bit signal and 24-bit signal respectively. The input to the system is a 1 kHz, 0 dB SACD signal. The signal to noise ratio of the signals is 116.64 dB and 116.55 dB respectively. Harmonic distortion is zero.

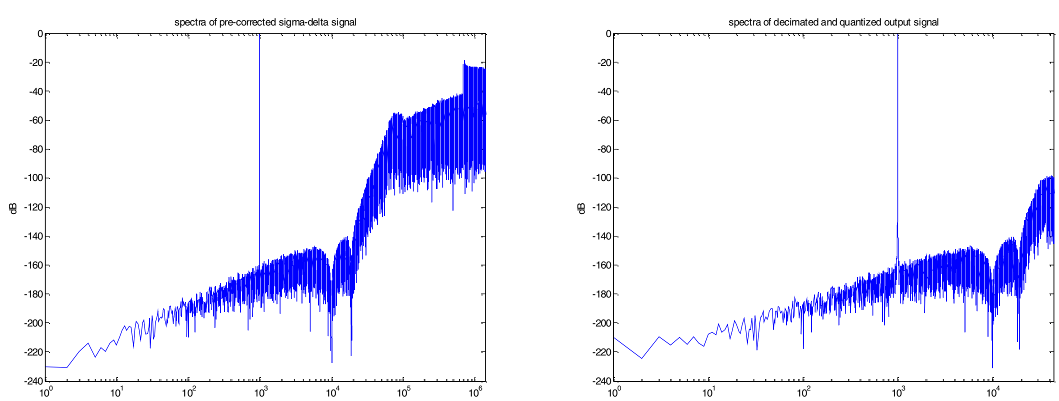

Figure 62: a) 1-bit signal b) decimated 24-bit signal. Input is a 1 kHz, 0 dB SACD signal.

As additional examples, the following figures show the input and output of the system with various input signals of different amplitudes and frequency components. The purpose of these figures is to validate the preceding results are not frequency dependant. For figures 63a and 63b, the input to the system is a 4 kHz, 0 dB SACD signal. The signal to noise ratio of the signals is 116.72 dB and 116.60 dB respectively. Harmonic distortion is zero.

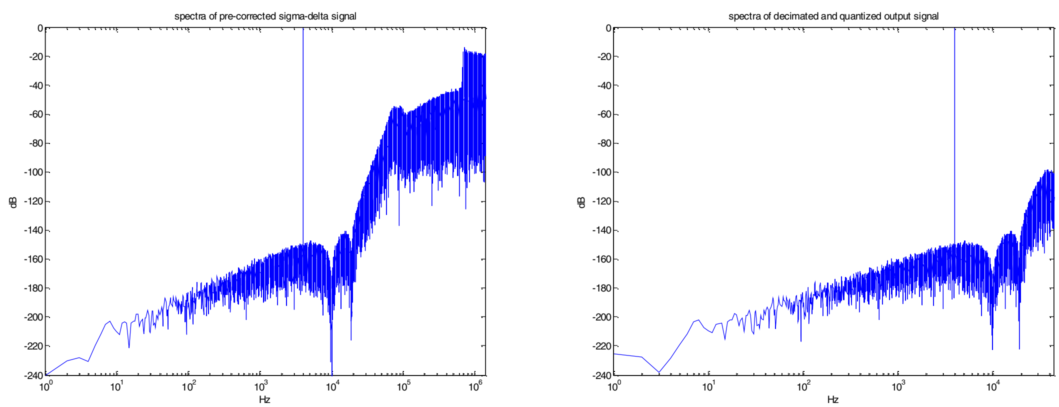

Figure 63: a) 1-bit signal b) decimated 24-bit signal. Input is a 4 kHz, 0 dB SACD signal.

For figures 64a and 64b, the input to the system is a 14 kHz and 15 kHz, 0 dB SACD signal. The signal to noise ratio of the signals is 116.81 dB and 116.64 dB respectively. Harmonic distortion is zero.

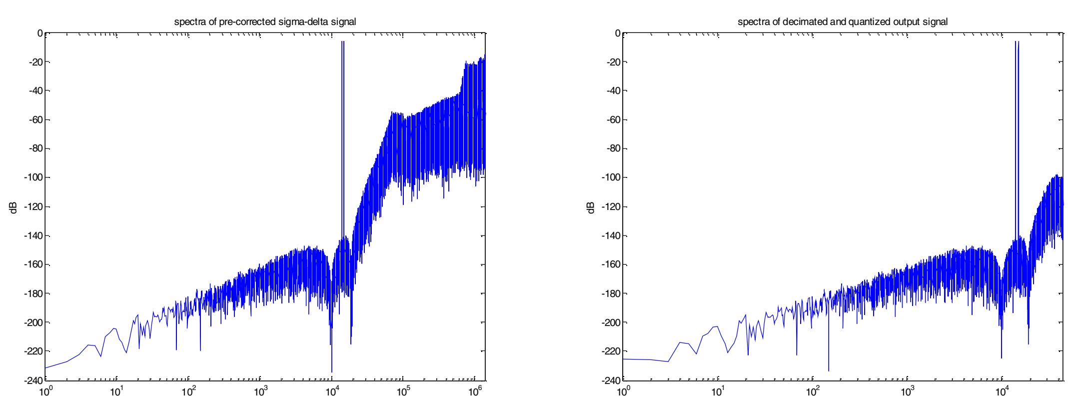

Figure 64: a) 1-bit signal b) decimated 24-bit signal. Input is a 14 kHz and 15 kHz, 0 dB SACD signal.

For figures 65a and 65b, the input to the system is a 19 kHz and 20 kHz, -60 dB signal. The signal to noise ratio of the signals is 68.53 dB and 68.57 dB respectively. Noticeable is how the multi-bit signal accurately preserves all the harmonics produced by the SDM.

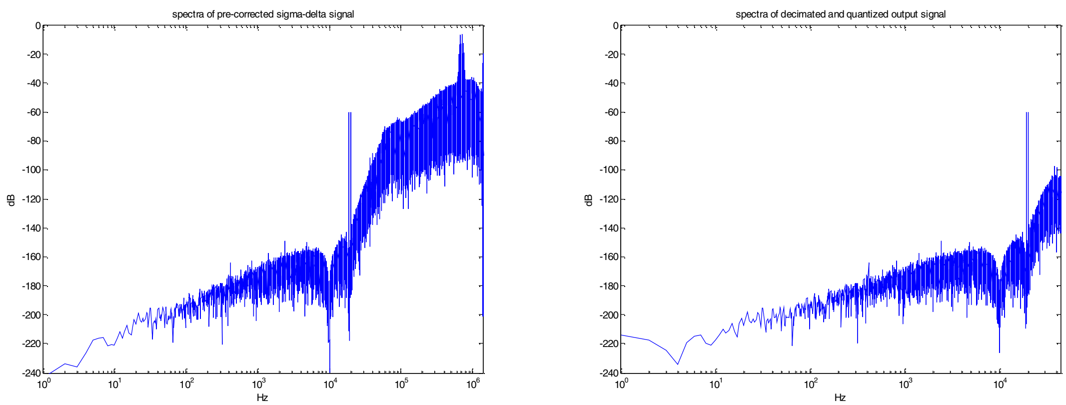

Figure 65: a) 1-bit signal b) decimated 24-bit signal. Input is a 19 kHz and 20 kHz, -60 dB signal.

For figures 66a and 66b, the input to the system is a 1 kHz, 2 kHz and 16 kHz, -20 dB signal. The signal to noise ratio of the signals is 103.73 dB and 103.67 dB respectively. Again, it is evident how the multi-bit signal accurately preserves the harmonics produced by the SDM.

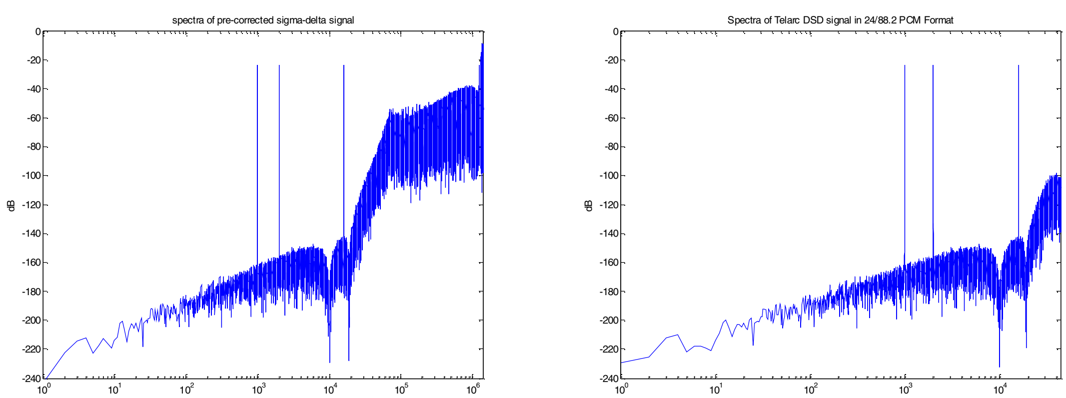

Figure 66: a) 1-bit signal b) decimated 24-bit signal. Input is a 1 kHz, 2 kHz and 16 kHz, -20 dB signal

Figures 67a and 67b show the transient response of this system. While the input to the system is a step of amplitude 0.5, from sample 1500 to sample 4500, the output of the system is a step from sample 150 to sample 1500. Though the step response is displaced in time and reduced in width (the effect of all the filtering processes), what is important is how well reproduced the shape of this input pulse is.

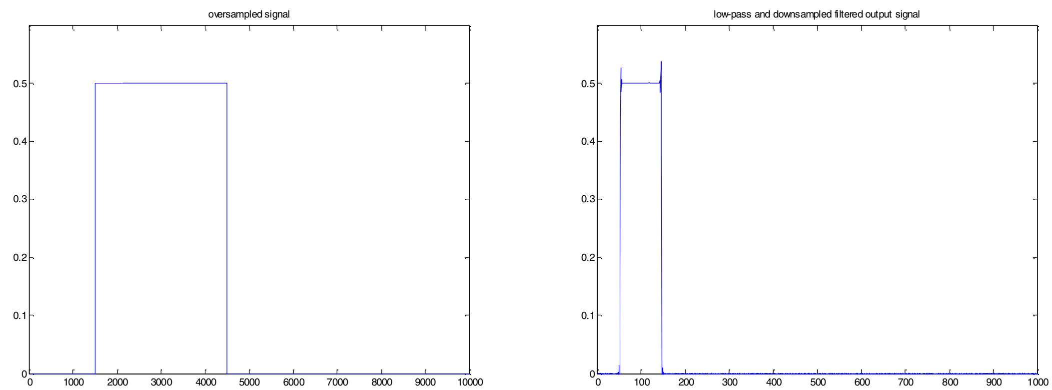

Figure 67: a) input step response b) decimated 24-bit step response.

Figures 68a and 68b show the phase of the SDM and PCM signal, where the original signal input to the system is a swept-frequency cosine. Similar to the preceding examples, the frequency swept is from 1 to 30k Hz and lasts 1 second. The figures show the response from 1 to 30k Hz.

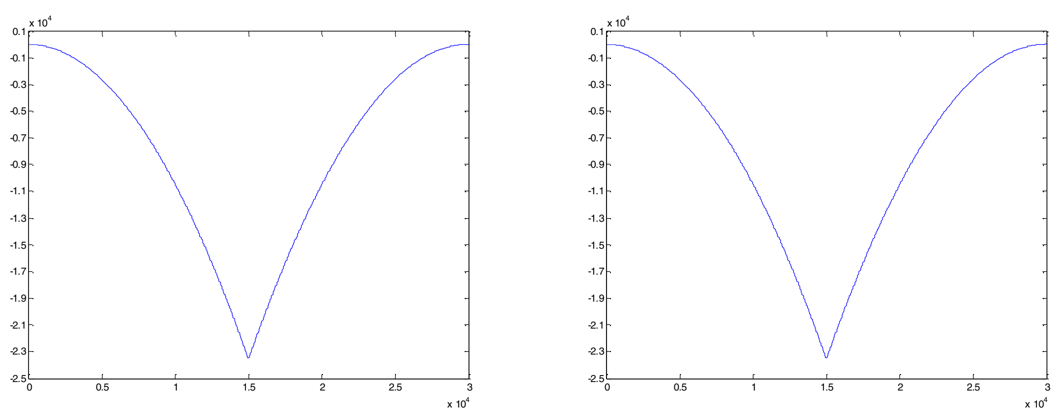

Figure 68: System phase response a) 1-bit phase response b) decimated 24-bit phase response.

Subtracting the one-bit output phase from the multi-bit output phase, in the frequency range of 1 – 30 kHz, gives the results revealed in figure 69. The filtering process is done such that the phase distortion is zero. Figure 69 shows how the phase error, which is linear, increases with increasing frequency. At frequency 1 Hz the error is zero, while at 30 kHz the error is about 10 rad.

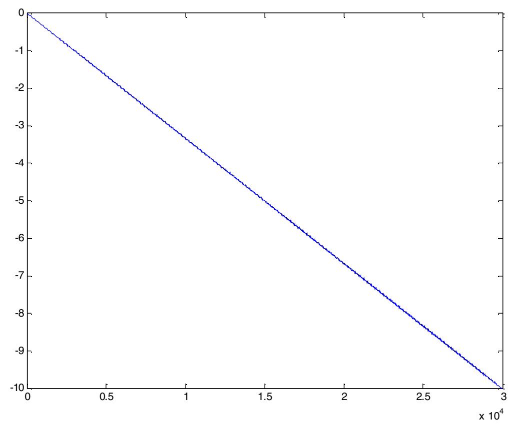

Figure 69: Difference between the 1-bit and 24-bit signals, with input a swept-frequency cosine.

2. PCM to DSD Conversions

Figure 70 shows the MMS for PCM to DSD conversions, where $x[n]$ is the multi-bit signal and $y[n]$ is the one-bit signal. In this system, the input signal is multi-bit PCM, 24 bit 88.2 kHz. The signal is upsampled and low-pass filtered to obtain a signal with 2.8224 MHz sampling frequency. Given that the amplitude of the input PCM signal is greater than the maximum modulation depth for the SDM, the signal's amplitude is reduced by multiplying it by a constant of 0.5. This signal is then processed through the SDM to obtain the DSD signal $y[n]$. This $y[n]$ is then analyzed along with the PCM signal in order to compare their quality and statistics.

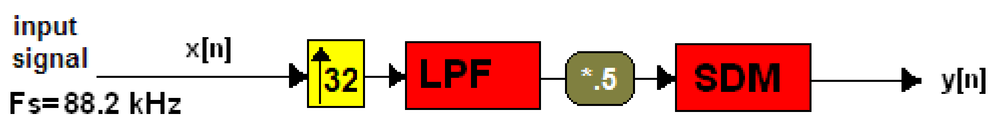

Figure 70: MMS for PCM to DSD conversions.

Figures 71a and 71b show the 24-bit signal and the one-bit signal respectively. The input to the system is a 1 kHz, 0 dB signal. The signal to noise ratio of the signals is 141.44 dB and 116.80 dB respectively. Harmonic distortion is zero.

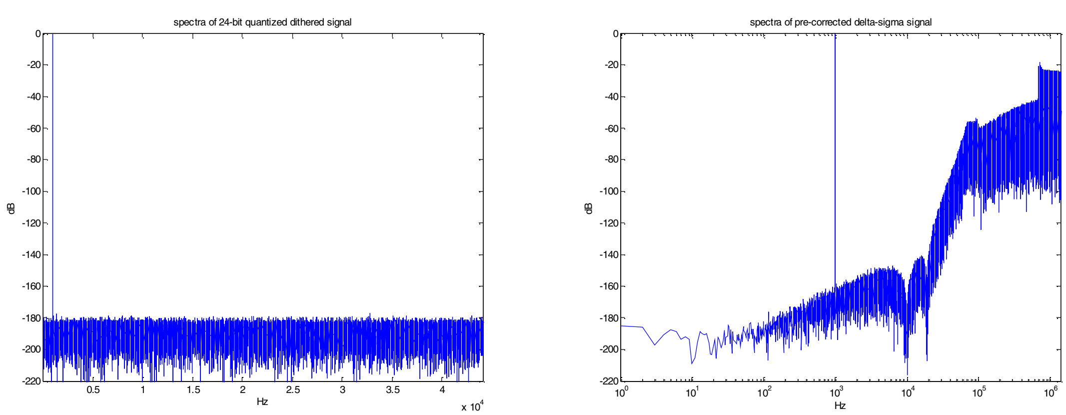

Figure 71: a) 24-bit signal b) interpolated 1-bit signal. Input is a 1 kHz, 0 dB signal.

As additional examples, the following figures show the input and output of the system with various input signals of different amplitudes and frequency components. The purpose of these figures is to validate the preceding results are not frequency dependant. For figures 72a and 72b, the input to the system is a 4 kHz, 0 dB signal. The signal to noise ratio of the signals is 141.47 dB and 116.73 dB respectively. Harmonic distortion is zero.

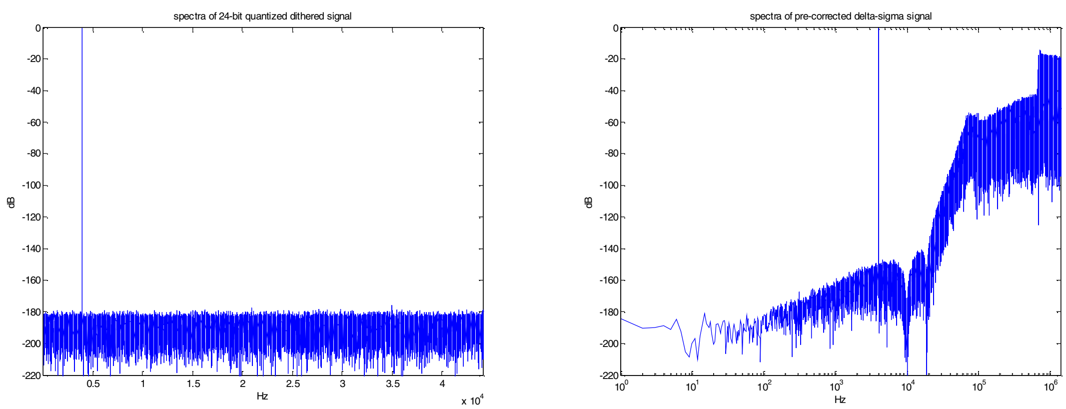

Figure 72: a) 24-bit signal b) interpolated 1-bit signal. Input is a 4 kHz, 0 dB signal.

For figures 73a and 73b, the input to the system is a 14 kHz and 15 kHz, 0 dB signal. The signal to noise ratio of the signals is 141.49 dB and 116.84 dB respectively. Harmonic distortion is zero.

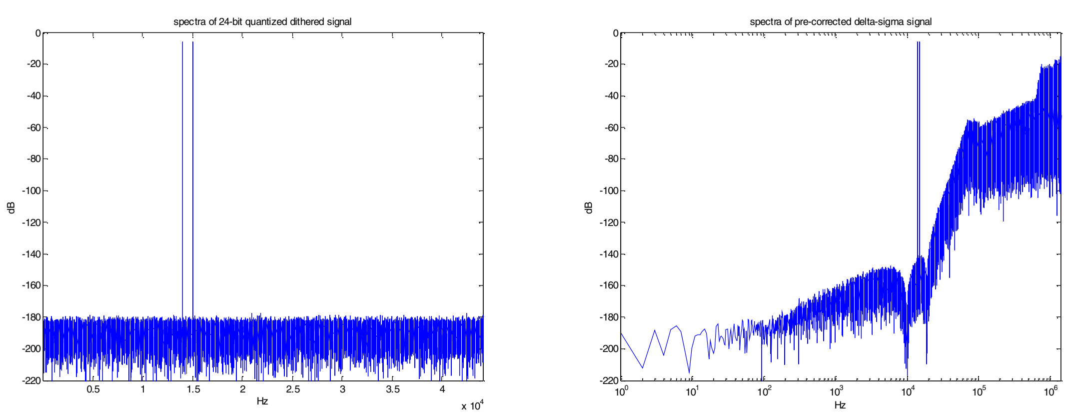

Figure 73: a) 24-bit signal b) interpolated 1-bit signal. Input is a 14 kHz and 15 kHz, 0 dB signal.

For figures 74a and 74b, the input to the system is a 19 kHz and 20 kHz, -60 dB signal. The signal to noise ratio of the signals is 81.44 dB and 68.62 dB respectively. Harmonic distortion is zero.

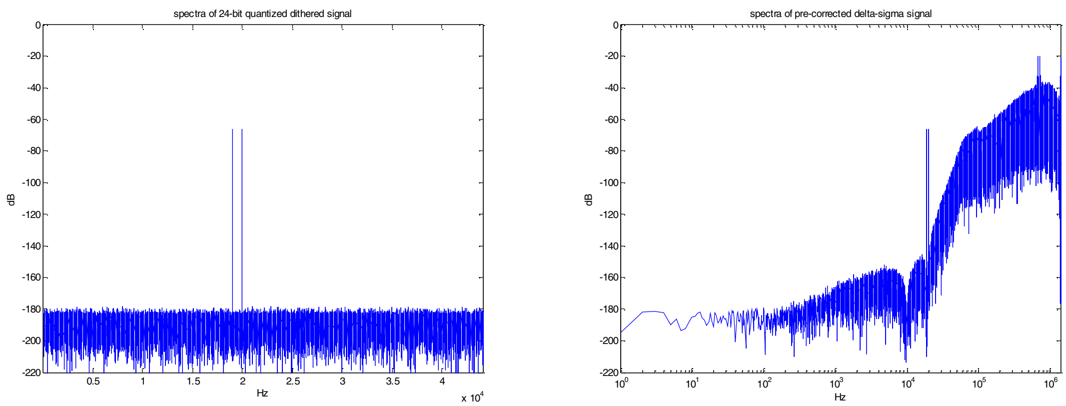

Figure 74: a) 24-bit signal b) interpolated 1-bit signal. Input is a 19 kHz and 20 kHz, -60 dB signal.

For figures 75a and 75b, the input to the system is a 1 kHz, 2 kHz and 16 kHz, -20 dB signal. The signal to noise ratio of the signals is 121.46 dB and 104.30 dB respectively. Harmonic distortion is zero.

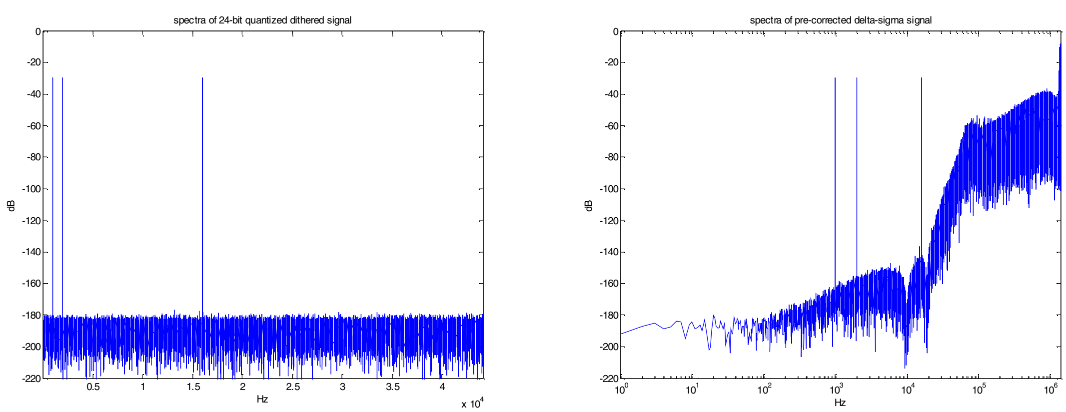

Figure 75: a) 24-bit signal b) decimated 1-bit signal. Input is a 1 kHz, 2 kHz and 16 kHz, -20 dB signal.

Figures 76a and 76b show the phase of the PCM and SDM signal, where the original signal input to the system is a swept-frequency cosine. As in preceding examples, the frequency is swept from 1 to 30k Hz and lasts 1 second.

The figures show the response from 1 to 30k Hz. In this case, the filtering process does not compensate for phase distortion.

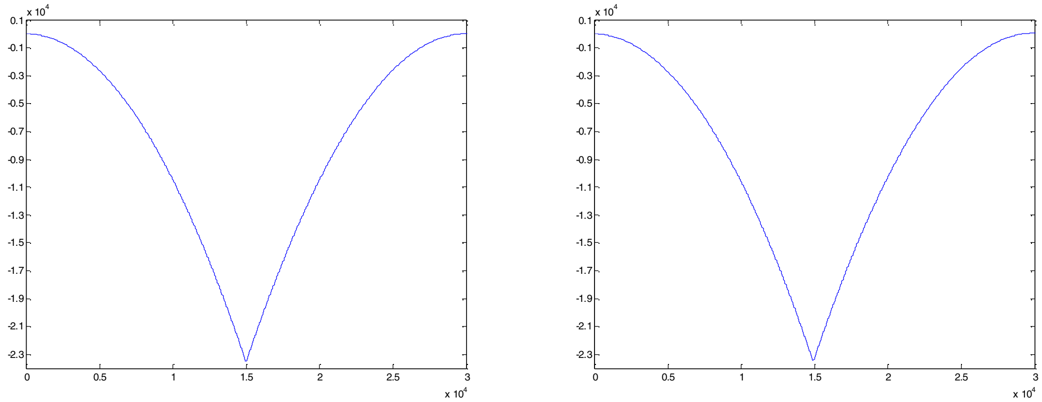

Figure 76: System phase response a) 24-bit phase response b) interpolated 1-bit phase response.

From figure 76, it appears the SDM does maintain the phase response of the PCM signal. Subtracting the multi-bit output phase from the one-bit output phase, in the frequency range of 0 – 30 kHz, gives the results revealed in figure 77. Given the phase delay by the filtering process, which is linear with group delay 6400, the phase error between the input and output signal grows with increasing frequency. At frequency 1 Hz the error is zero, while at 30 kHz the error is about 450 rad.

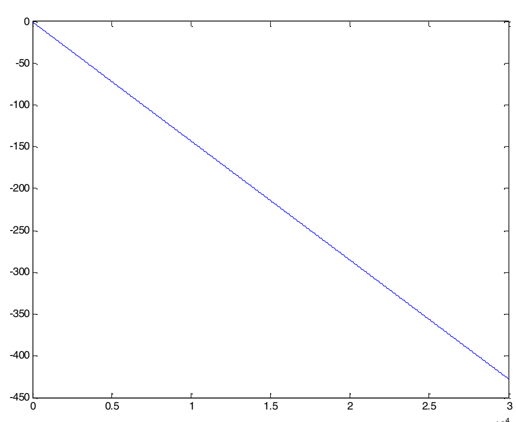

Figure 77: Difference between the 24-bit and1-bit signals, with input a swept-frequency cosine.

3. Complete MMS

The complete MMS consists of the previous stages together as shown in figures 80 and 81. The system of figure 80 was designed to have as input a SDM signal and output this same format. The system of figure 81 was designed to start with a PCM signal and output this same format. Signals $x[n]$ and $y[n]$ are analyzed as done previously.

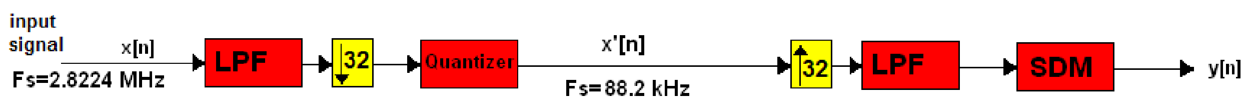

Figure 78: Complete MMS for signal conversions with one-bit input/output signals.

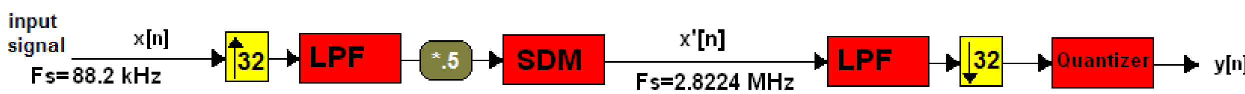

Figure 79: Complete MMS for signal conversions multi-bit input/output signals.

The following illustrations are for the one-bit input and output system. Figures 80a and 80b show the one-bit signal $x[n]$ and the one-bit signal $y[n]$ respectively. The input to the system is a 4 kHz, 0 dB SACD signal. The signal to noise ratio of the signals is 116.78 dB and 113.78 dB respectively. Harmonic distortion is zero.

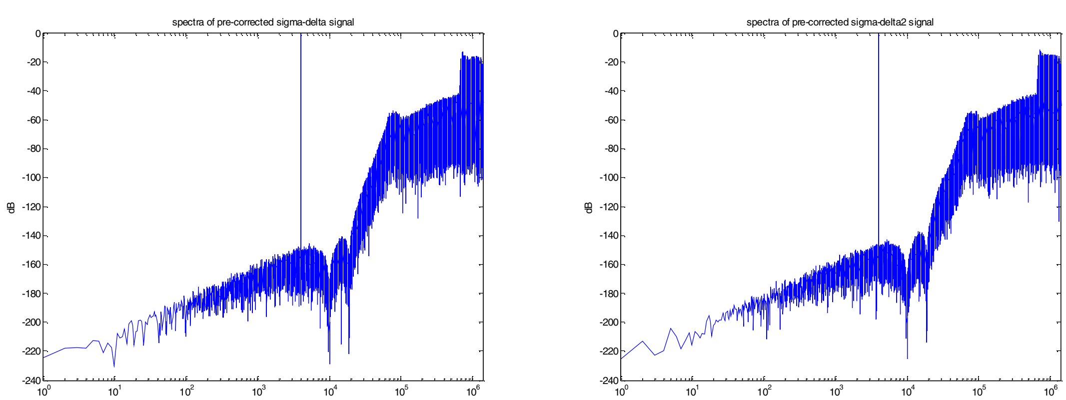

Figure 80: a) 1-bit input signal b) 1-bit output signal. System input is a 4 kHz, 0 dB SACD signal.

As additional examples, the following figures show the input and output of the systems with various input signals of different amplitudes and frequency components. The purpose of these figures is to validate the preceding results are not frequency dependant. Figures 81a and 81b show the one-bit signal $x[n]$ and the one-bit signal $y[n]$ respectively for a 1 kHz and 2 kHz, 0 dB SACD input signal. The signal to noise ratio of the signals is 116.86 dB and 113.85 dB respectively. Harmonic distortion is zero.

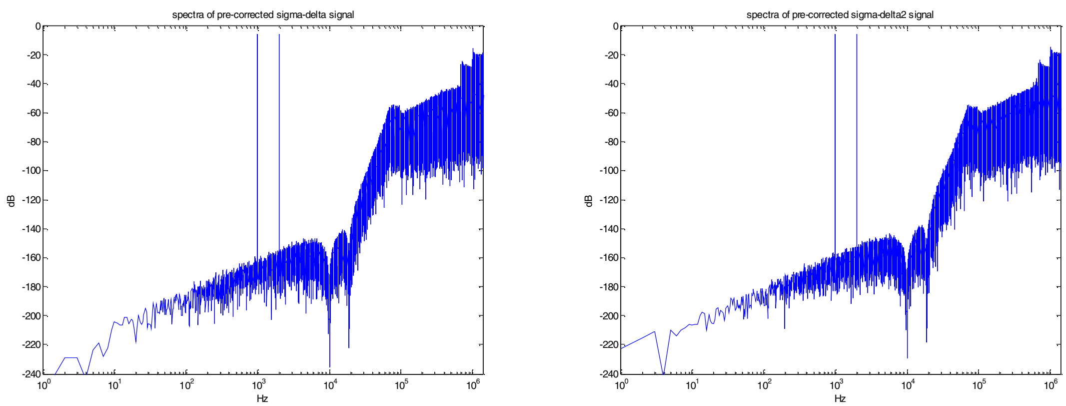

Figure 81: a) 1-bit input signal b) 1-bit output signal. System input is a 1k and 2k Hz, 0 dB SACD signal.

Figures 82a and 82b show the one-bit signal $x[n]$ and the one-bit signal $y[n]$ respectively for a 19k and 20k Hz, -20 dB input signal. The signal to noise ratio of the signals is 103.87 dB and 100.69 dB respectively. Harmonic distortion is zero.

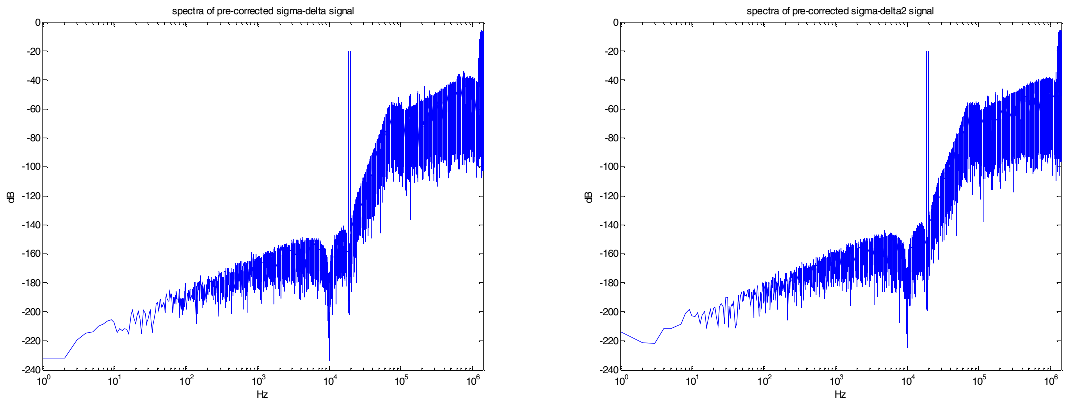

Figure 82: a) 1-bit input signal b) 1-bit output signal. System input is a 19k and 20k Hz, -20 dB signal.

Figures 83a and 83b show the one-bit signal $x[n]$ and the one-bit signal $y[n]$ respectively for a 40 and 18k Hz, -20 dB input signal. The signal to noise ratio of the signals is 103.58 dB and 100.72 dB respectively. Harmonic distortion is zero.

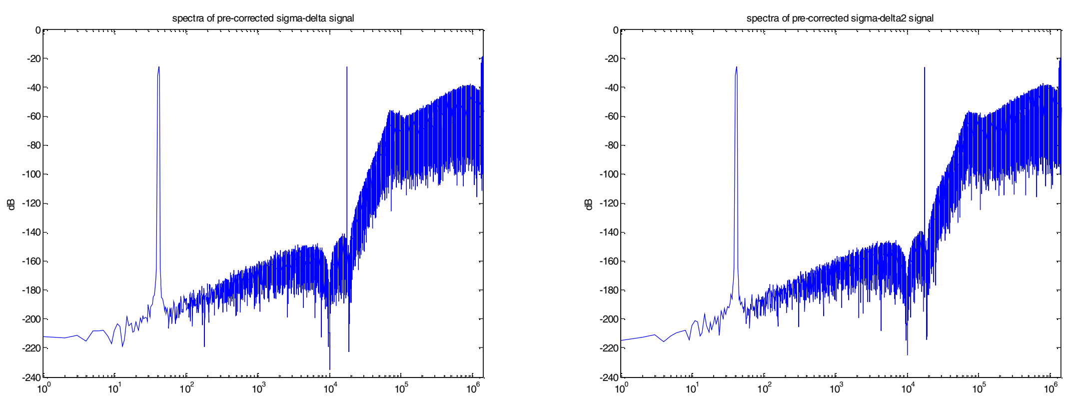

Figure 83: a) 1-bit input signal b) 1-bit output signal. System input is a 40 and 18k Hz, -20 dB signal.

Figures 84a and 84b show the one-bit signal $x[n]$ and the one-bit signal $y[n]$ respectively for a 13k, 14k and 15k Hz, -40 dB input signal. The signal to noise ratio of the signals is 87.77 dB and 84.77 dB respectively. The one-bit input signal presents a $THD \approx 0.00058\%$, however multiple simulations with this same input show a tendency to conclude some of the present harmonics are most likely noise error. The output $THD \approx 0.00038\%$.

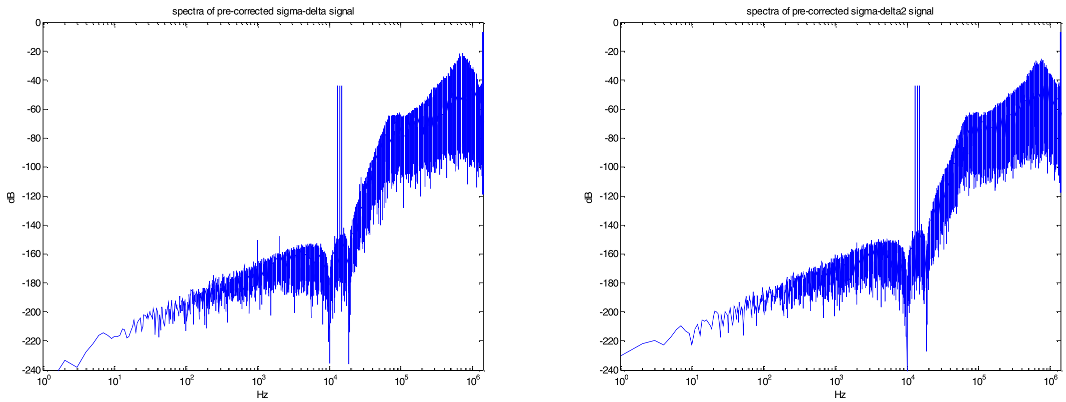

Figure 84: a) 1-bit input signal b) 1-bit output signal. System input is a 13k, 14k and 15k Hz, -40 dB signal.

The following figures are for the analysis of the 24-bit input and output system. Figures 85a and 85b show the 24-bit signal $x[n]$ and the 24-bit signal $y[n]$ respectively. The input to the system is a 4 kHz, 0 dB signal. The signal to noise ratio of the signals is 141.47 dB and 112.98 dB respectively. Harmonic distortion is zero.

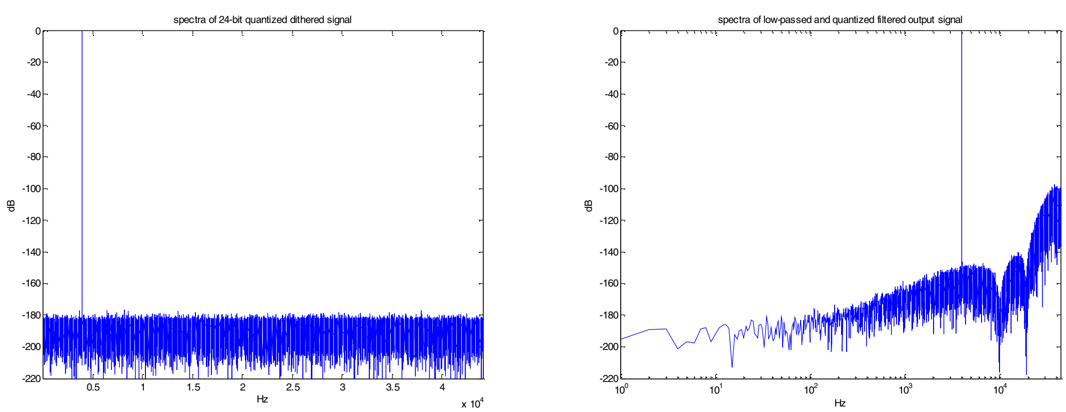

Figure 85: a) 24-bit input signal b) 24-bit output signal. System input is a 4 kHz, 0 dB signal.

Figures 86a and 86b show the one-bit signal $x[n]$ and the 24-bit signal $y[n]$ respectively for a 1k and 2k Hz, 0 dB input signal. The signal to noise ratio of the signals is 141.47 dB and 111.06 dB respectively. Input signal's harmonic distortion is zero. The output signal however has $THD \approx .000012\%$

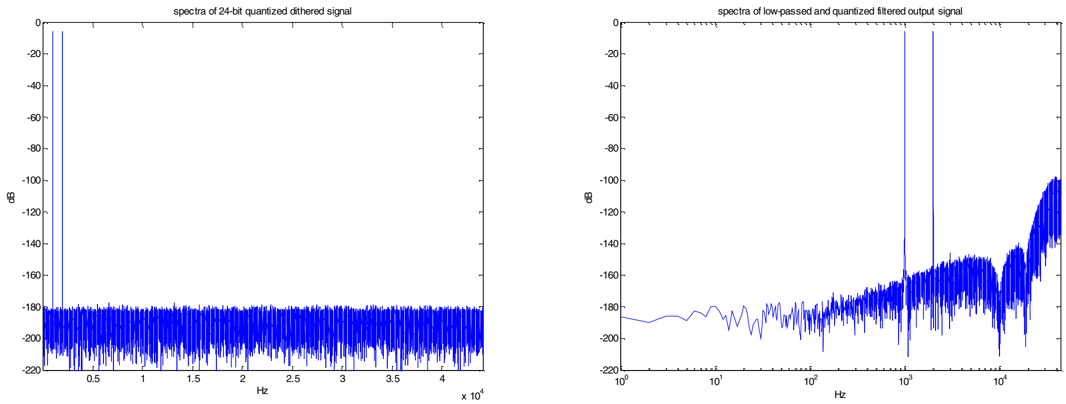

Figure 86: a) 24-bit input signal b) 24-bit output signal. System input is a 1k and 2k Hz, 0 dB signal.

Figures 87a and 87b show the one-bit signal $x[n]$ and the 24-bit signal $y[n]$ respectively for a 19k and 20k Hz, -20 dB input signal. The signal to noise ratio of the signals is 121.44 dB and 104.26 dB respectively. Input signal's harmonic distortion is zero, while the output signal has distortions close to 2kHz, 3kHz, 16kHz, 17kHz, 22kHz, 38kHz and 39kHz resulting in a $THD \approx .00008\%$.

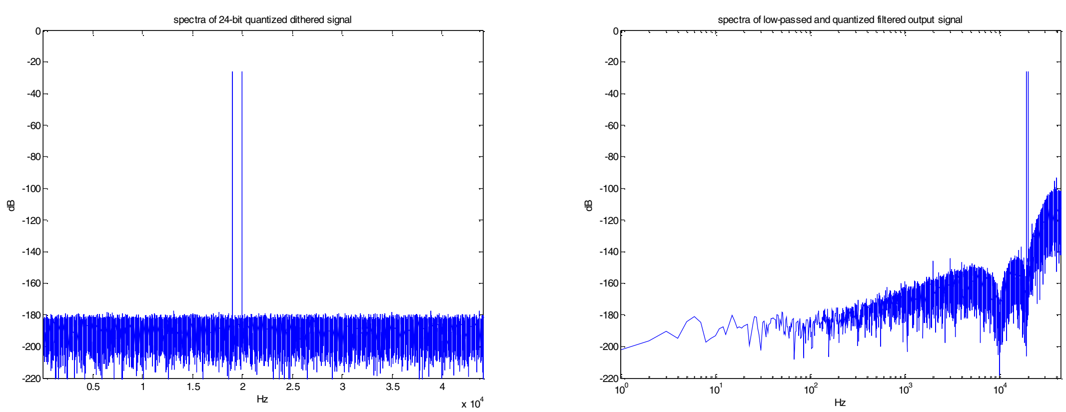

Figure 87: a) 24-bit input signal b) 24-bit output signal. System input is a 19k and 20k Hz, -20 dB signal.

Figures 88a and 88b show the one-bit signal $x[n]$ and the 24-bit signal $y[n]$ respectively for a 40 and 18k Hz, -26 dB input signal. For ease of view, the input signal is plotted in a logarithmic scale. The signal to noise ratio of the signals is 115.46 dB and 98.12 dB respectively. Harmonic distortion is zero.

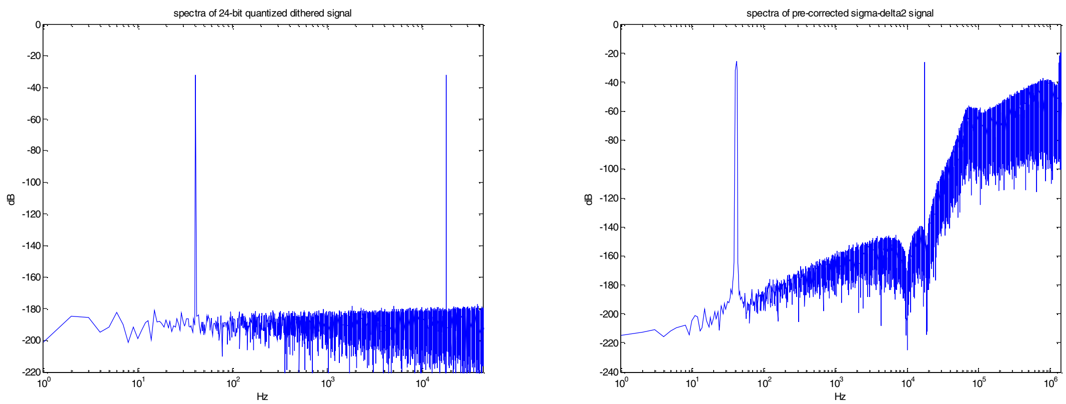

Figure 88: a) 24-bit input signal b) 24-bit output signal. System input is a 40 and 18k Hz, -26 dB signal.

Figures 89a and 89b show the one-bit signal $x[n]$ and the 24-bit signal $y[n]$ respectively for a 13k, 14k and 15k Hz, -40 dB input signal. The signal to noise ratio of the signals is 101.49 dB and 88.10 dB respectively. Harmonic distortion is zero.

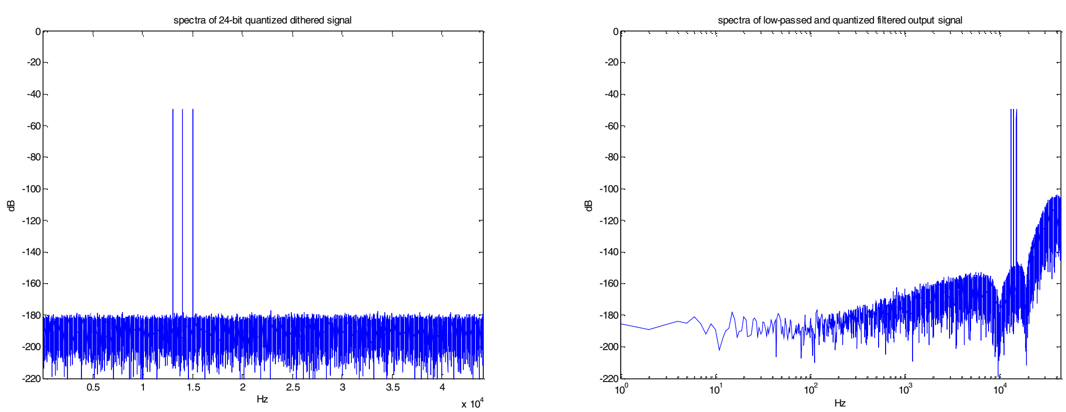

Figure 89: a) 24-bit input signal b) 24-bit output signal. System input is a 13k, 14k and 15k Hz, -40 dB signal.

F. Commercial Signal Analysis

The next part of this work involved commercial audio analysis. The purpose of this analysis is to learn to what extent commercial recordings are taking advantage of the high resolution of DSD. Two audio files were kindly provided by Mr. Todd W. Brown form Telarc® International Corporation, a well recognized music recording company, famous for the exceptionally clear, natural sound of its recordings. One of the audio files is a 1 kHz test tone. This 1 kHz test tone is used for their recordings and the digital signal is produced using their DSD converter. The second audio file is the left channel of the introduction to Stravinsky's Rite of Spring also recorded directly to a DSD system.

Figures 90a and 90b show the spectrum of the Telarc 1 kHz DSD test tone. Figure 90a shows the complete bandwidth of the DSD signal, and figure 90b shows the frequency band from 1 – 30k Hz with a linear scale. The signal to noise ratio of the signal is 103 dB. From figure 90b it is noticeable that, at least up to 30 kHz, the amount of high frequency noise is not excessive at all, reaching a peak of -109 dB at about 29.8 kHz. The graphs show two harmonics with amplitudes of -130.6 dB and -130.8 dB respectively. Given that the harmonics appear at exact multiples of the main frequency component, they are obviously harmonic distortions caused by the one-bit system. It is not clear if these distortions come from the original analog signal, or the DSD conversion.

Of special interest is the noise floor of the system. To show how far off current hardware technology is of digital DSD capability, figure 91 shows the Telarc test tone overlapping a tone of the same frequency created in Matlab.

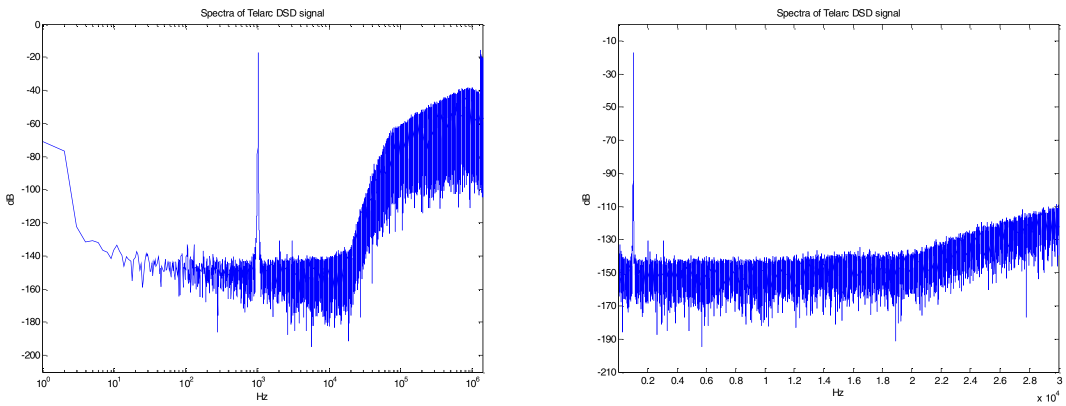

Figure 90: Telarc 1 kHz DSD test tone a) full bandwidth in logarithmic scale b) 1 – 30 kHz in linear scale.

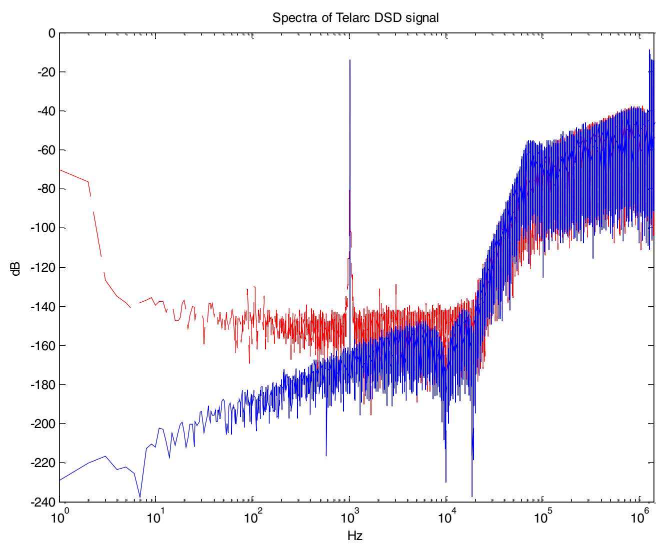

Figure 91: 1 kHz tone created in Matlab (blue) overlapping a Telarc 1 kHz test tone (red).

Figures 92 through 95 show a one second section, at different instances of the Telarc Rite of Spring file in DSD format. The figures on the left, figures a, show the full bandwidth, and the figures on the right, figures b, show the frequency bandwidth from 1 – 30k Hz in a linear scale.

(a) (b)

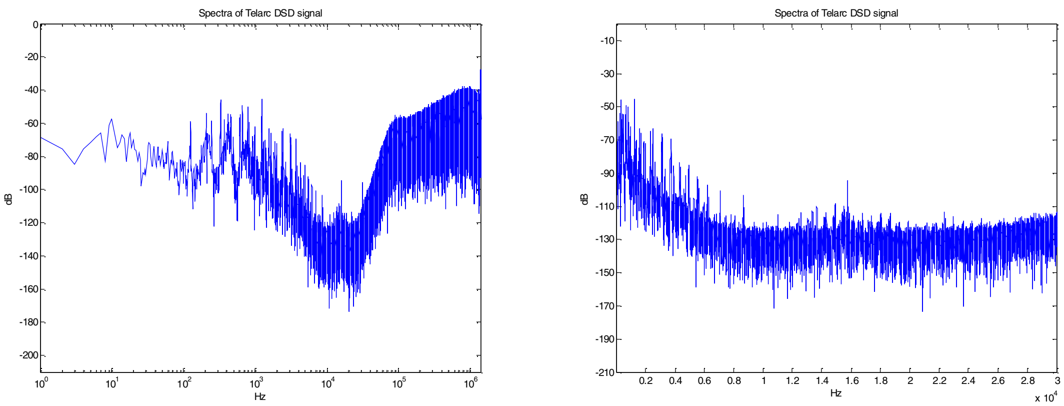

Figure 92: Telarc Rite of Spring file in DSD format a) full bandwidth in logarithmic scale b) 1 – 30 kHz in linear scale.

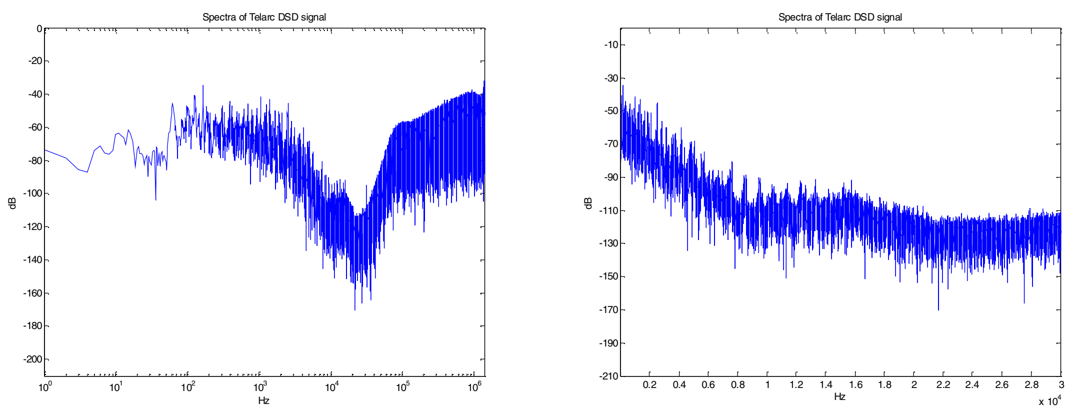

Figure 93: Telarc Rite of Spring file in DSD format a) full bandwidth in logarithmic scale b) 1 – 30 kHz in linear scale.

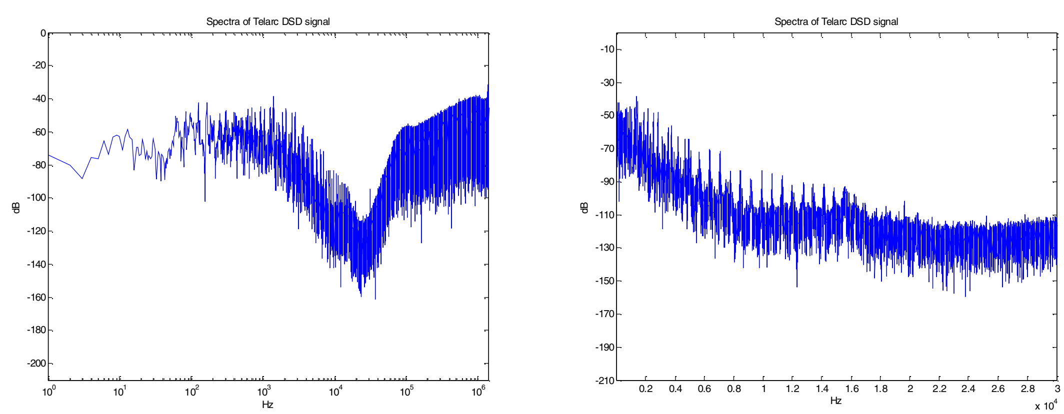

Figure 94: Telarc Rite of Spring file in DSD format a) full bandwidth in logarithmic scale b) 1 – 30 kHz in linear scale.

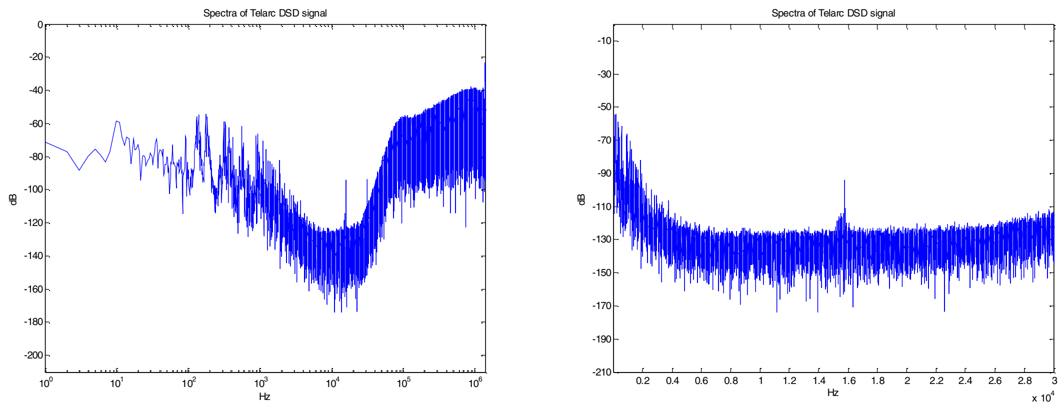

Figure 95: Telarc Rite of Spring file in DSD format a) full bandwidth in logarithmic scale b) 1 – 30 kHz in linear scale.

Figures 96 through 98 show a one second section, at different instances, of the Telarc Rite of Spring file in DSD format and PCM format after processed through the MMS for DSD to PCM conversions. The figures on the left, figures a, show the file in DSD format, while the figures on the right, figures b, show the file in 24-bit 88.2 kHz sampling frequency format. All figures show a frequency bandwidth from 1 – 44.1k Hz in a logarithmic scale.

(a) (b)

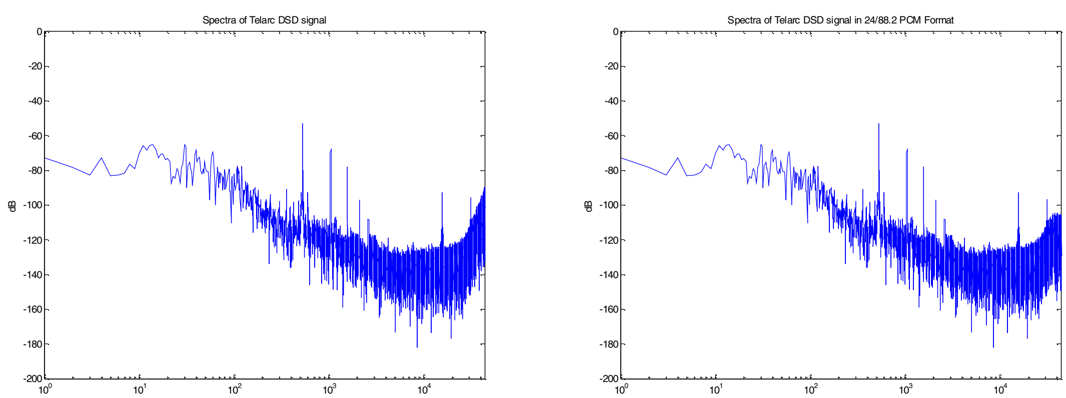

Figure 96: Telarc Rite of Spring file in a) DSD format b) 24-bits 88.2 kHz.

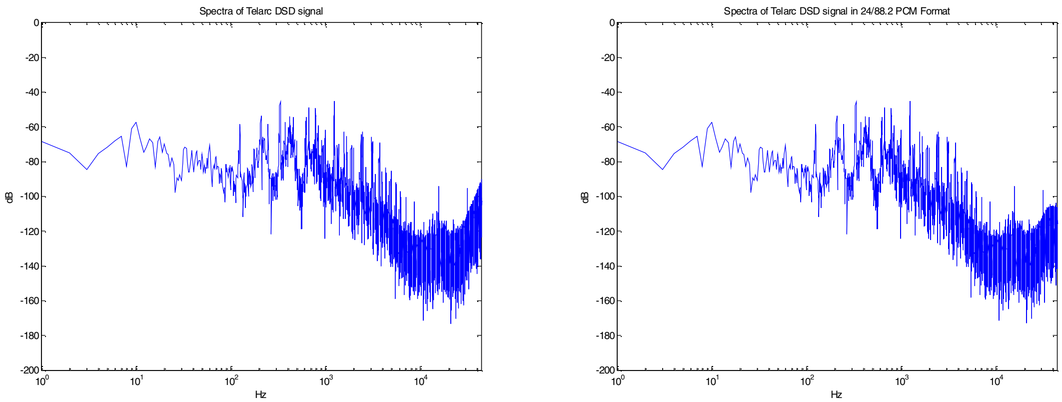

Figure 97: Telarc Rite of Spring file in a) DSD format b) 24-bits 88.2 kHz.

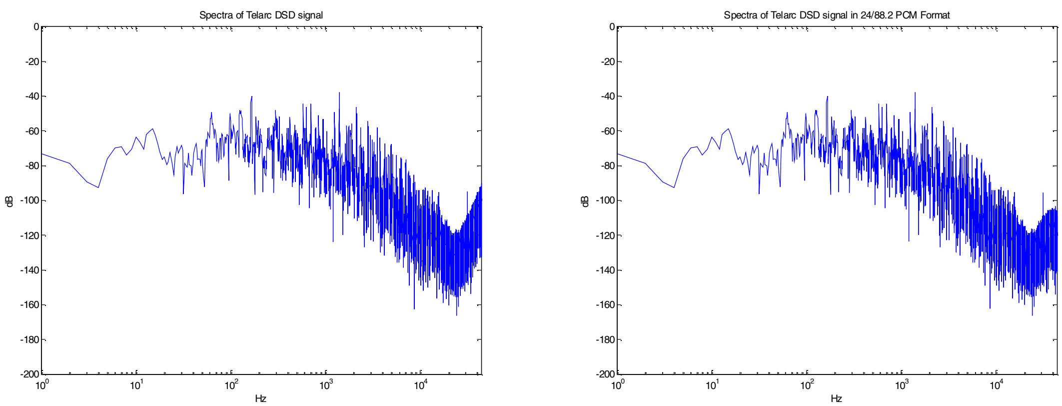

Figure 98: Telarc Rite of Spring file in a) DSD format b) 24-bits 88.2 kHz.

Once again, special interest is taken on the signal noise floor of these signals. Figure 99 shows a nearly silent passage, overlapping two computer generated zero input signals. The zero input signals are a DSD signal and a CD quality signal. The silent passage is chosen to view the frequency response of the complete analog and digital audio recording chain without any audio signal presence, and thus conclude on how far off current hardware technology is compared to digital DSD capability.

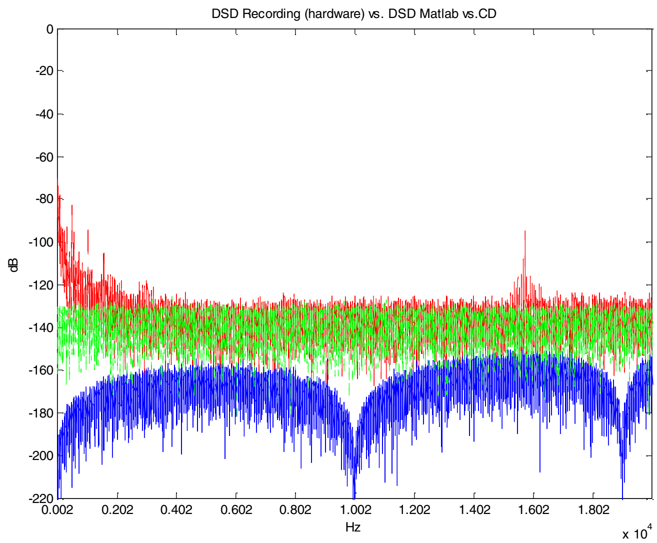

Figure 99: Beginning of Telarc Rite of Spring file (red) overlapped by two silent signals modulated in Matlab. The green signal is CD quality, blue is DSD quality.

G. Listening Tests

The last part of this work involved blind listening tests. The purpose of the listening tests is to determine if the conversions between the formats are audibly lossless. A short audio clip was recorded at UPRM facilities using a 24-bit *M-audio Audiophile* audio card and an *Audix* test microphone. The audio clip is a short melody played by an alto saxophone and drums. The audio file was recorded using Adobe Audition. Three versions of the audio file were prepared:

- the original 24-bit 88.2 kHz sampling frequency.
- 24-bit 88.2 kHz sampling frequency converted to DSD, then back to 24-bit 88.2 kHz sampling frequency.
- 24-bit 88.2 kHz sampling frequency converted to 16-bit 44.1 kHz sampling frequency, then back to 24-bit 88.2 kHz sampling frequency.

The conversion to a one-bit signal was done in C language, following the same procedure as the MMS for DSD to PCM conversions (see Chapter 3, Section E1). The conversion to and from 16-bit 44.1 kHz sampling frequency was done in Adobe Audition.

The tests consisted of two segments, one for each conversion type. A test consisted of each participant completing each test sixteen times. The audio clips were played through headphones with a frequency response from 16 Hz to 22 kHz.

In all, twenty people participated in the tests. The hypothesis is that the difference between the different audio files is not audible; therefore, the estimated mean is 33.3%. Table 1 shows the statistical results of the tests. The table shows the percentage of correct answers each person obtained. For a confidence interval of 99.5%, the percentage μ of each person must be between $2.91\% \leq \mu \leq 63.1\%$.

Table 1: Statistical results from the listening tests

The table shows the percentage μ of correct answers		
subject	Test 1	Test 2
1	37.50%	25.00%
2	31.25%	31.25%
3	50.00%	25.00%
4	37.50%	18.75%
5	31.25%	56.25%
6	31.25%	18.75%
7	56.25%	81.50%
8	18.75%	25.00%
9	37.50%	50.00%
10	37.50%	18.75%
11	37.50%	62.50%
12	12.50%	37.50%
13	50.00%	31.25%
14	43.75%	87.50%
15	43.75%	25.00%
16	37.50%	37.50%
17	18.75%	56.25%
18	18.75%	25.00%
19	37.50%	25.00%
20	37.50%	37.50%
Total percent	35.31%	38.76%

*For a 99.5% confidence interval: $2.91\% \leq \mu \leq 63.1\%$

In Table 1, Test 1 corresponds to the audio files converted to DSD specifications and Test 2 corresponds to the audio files converted to CD quality. Table

1 shows that most results are within the confidence interval. With only three people scoring a correct percentage of 50% or more, it is clear that no one could accurately determine which track was an original recording and which had been modulated as a DSD signal. For Test 2, five people scored 50% or more, with two people scoring over 80% which is outside the confidence interval. These results may suggest that some people could tell the difference between an original 24/88.2 recording and a 16/44.1 recording. The total percentage for each test respectively was 35.31% and 38.76%.

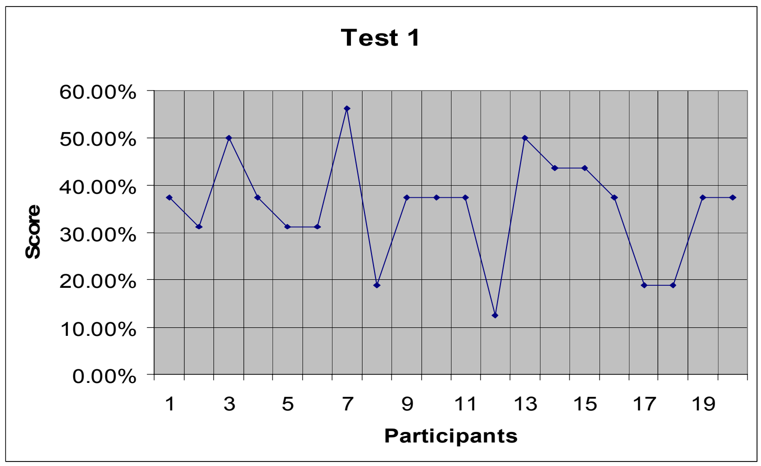

Figure 100: Graphical Results of Test 1.

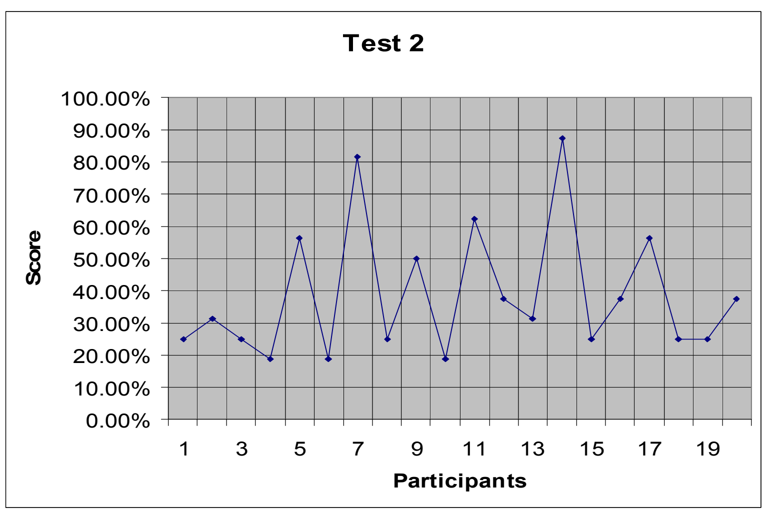

Figure 101: Graphical Results of Test 2.

IV. Discussion of Results

A. Sigma-Delta Modulation vs. Pulse Code Modulation

There is no simple way of comparing PCM with SDM; the theory (Chapter 2) confirms that. If the systems are focused on audio reproduction, it is still not an easy task. If the comparison is between systems with specific configurations for audio, then some fundamentals are worth mentioning. The need to specify system configurations is because, though there is only one way of implementing linear PCM with TPDF, SDM design depends on values such as noise shaping cut-off frequency, resonator values, clipper values, dither level and pre-correction technique, all chosen by necessity and convenience. Of course, all these design parameters depend on the SDM configuration feed-forward or feedback. For this thesis, the parameters were chosen to comply with [30], obtain the smallest amount of distortions and achieve a performance good enough to realize the hypothesis of audibly lossless conversions between this SDM output and 24-bits PCM.

In the frequency band of 1 – 20k Hz, the fifth-order SDM designed for this thesis gave a SNR of 116 dB for a 0 dB SACD input. In the same band, 24-bits TPDF PCM gave a SNR of 141 dB for a 0 dB input. The seventh-order SDM designed for this thesis gave a SNR of 132 dB for a 0 dB SACD input, but this system does not conform to the maximum peak levels of Scarlet Book specifications. Of special importance is the input signal to the systems, as the SDM noise floor levels depends on the input signal. The lower in amplitude the input signal, the lower the noise floor. Partial dithering applied to the SDM only reduces the signal-dependant noise modulation. On the contrary, the noise floor of TPDF PCM does not depend on the presence of an input signal, i.e., there is no noise modulation.

In the frequency band of 1 – 20k Hz, the fifth-order and seventh-order SDMs designed for this thesis gave 0% THD for a 0 dB SACD input. In the same band, 24-bits TPDF PCM also gave 0% THD for any input, again result of the TPDF. Both 5th

and 7th–order SDMs create harmonic distortions for input amplitudes between more or less $-50\,to-120\,dB$, with an example producing $THD = 3.85\%$ for an input amplitude of -100dB.

Linear PCM has linear phase; no possible distortion there. SDM, for the frequency band between 1 – 30k Hz, offered a very good phase response giving a maximum error of $1\times10^{-3}\,rad$ at 30kHz for a swept-frequency cosine input.

Regarding transient response, both systems offered very good response. In fact, both systems proved the weakest link in the process is indeed the anti-aliasing filter before the PCM and low-pass filter after the SDM. Nevertheless, if forced to choose, the better response has to go to the PCM system. This result contributes to the negative effect of the extreme noise shaping SDM incurs. The remarkable low frequency resolution that the SDM has comes at the expense of excessive high frequency noise. Therefore, the excessive amount of noise in the transient response the SDM when compared to the transient response of PCM.

B. Perfect Reconstruction

If a one-bit 2.8224 MHz sampling frequency signal is decomposed with prefect reconstruction filter banks into a multi-bit signal with lesser sampling frequency, say 88.2 kHz, and then reconstructed using the same information decomposed in each stage, perfect reconstruction would be achieved. In an example in Chapter 3 Section D, the recuperated one-bit output signal $x'[n]$ is the same as input signal $x[n]$.

However, if the purpose of the application is a multi-bit 88.2 kHz sampling frequency signal the results are not acceptable. A 24-bit 88.2 kHz sampling frequency signal with TPDF dither attains a SNR of 141.44 dB. A 24-bit 88.2 kHz sampling frequency signal, obtained from five wavelet decompositions of a 2.8224 MHz sampling frequency signal, attains a SNR of more or less 80 dB. For biorthogonal wavelet "6.8", the SNR is exactly 79.91. Therefore, there is no benefit in such an application.

In a practical implementation, the objective is to recuperate the input one-bit signal from the 24-bit 88.2 kHz sampling frequency signal, already decomposed from the original one-bit signal, without any information about frequencies higher than 44.1 kHz. In this case, the task is not possible. With respect to signal specifications, i.e. SNR, dynamic range, harmonic distortions, linear phase and signal amplitude, the reconstruction procedure maintains them all. Still, the recuperated signal is not one-bit. To effectively decompose and reconstruct a one-bit signal, all signal information is necessary. If any of the signal content is replaced with any other information, the reconstructed signal will not be one-bit. Therefore, the objective of accomplishing a lossless conversion from a one-bit signal to a multi-bit signal and back is not possible. Perfect reconstruction techniques derived from present wavelet theory do not allow for such conversions. In any case, as mentioned previously, five times decomposition of the one-bit signal does not produce a distortion free multi-bit signal. The produced distortions in the signals are a consequence of the system filters which in the decomposition stages yield magnitude and aliasing distortion.

C. Multi-rate Modulation System

Given the intention of producing lossless conversion between sigma-delta and PCM was not possible, the next best thing was to develop a multi-rate modulation system, which converts between formats with no additional distortions. The system should not introduce any magnitude or phase distortion to the signals. Therefore, the system would make use of FIR filters with a finely tuned flat passband.

The designed MMS for DSD to PCM conversions proved that, when converting a one-bit 2.8224 MHz sampling frequency signal to a 24-bit 88.2 kHz sampling frequency signal, the PCM signal accurately preserved all the DSD signal specifications; even the unwanted harmonic distortions. Conversely, the designed MMS for PCM to DSD conversions proved that, when converting a 24-bit 88.2 kHz sampling frequency signal to a one-bit 2.8224 MHz sampling frequency signal, the DSD signal could not accurately preserved all the PCM signal specifications. As mentioned, the fifth-order SDM has SNR of 116 dB for a 0 dB SACD input while the 24-bits TPDF PCM has SNR of 141 dB for a 0 dB input. Therefore, it is not possible for the SDM to preserve the SNR of 24-bits PCM. Not even a seventh-order SDM with a SNR of 132 dB can accurately encode a 24-bit PCM signal. Then again, if the analog to digital converter cannot provide such high precision levels, as is current hardware technology, then these results have no impact on the argument of which format sounds better. The listening tests gave more insight about this argument.

The MMS that inputs a DSD signal, converts it to a 24-bit 88.2 kHz sampling frequency signal and then converts it back to a DSD signal showed that the main difference between the input and output signals was the 3dB difference in SNR. Still, this difference is not an error. As explained in the theory (Chapter 2 Section B) re-modulation of the one-bit signal introduces a 3dB rise in the noise floor of the signal. Given, apart from perfect reconstruction techniques, the only way of recuperating a one-bit signal from a multi-bit signal is re-modulating the signal, a 3dB loss in SNR is unavoidable. In rare cases, such as for inputs of small amplitude, this noise floor increase benefited the output signal by burying the harmonic distortions in the noise floor, thus becoming inaudible.

The MMS that inputs a 24-bit 88.2 kHz sampling frequency signal, converts it to DSD signal and then converts it back to a 24-bit 88.2 kHz sampling frequency signal showed a not so good story. First, PCM to DSD conversions proved DSD could not preserve the 24-bit SNR, hence, the greater than 25 dB reduction in SNR in the complete PCM to DSD to PCM conversions. In addition, the SDM in the process introduced intermodulation distortions that did appear in the output PCM signal. This fact is very interesting, as the SDM by itself did not present intermodulation distortions for full amplitude signals. The DSD to PCM conversions and the PCM to DSD conversions also did not present intermodulation distortions for full amplitude signals. Yet the output of PCM to DSD to PCM conversions does present intermodulation distortion for various input amplitudes. Not only that, but the output SNR is about 3 to 5 dB less than that obtained from DSD to PCM conversions. It is well documented that digital TPDF dither completely eliminates all distortion, noise modulation and other signal-dependant artifacts [37]. Nonetheless, TPDF in the last 24-bit quantization does not eliminate the previously mentioned intermodulation distortion created by the SDM. When the signal is input to the second PCM, the distortions are by now signal content.

D. Commercial Signal Analysis

The audio content provided by Telarc® Intl proved that indeed commercial audio hardware does not take benefit of digital noise floors under -140 dB. The presence of harmonics in the test tone graphs implies that the absence of full TPDF dither in one-bit SDM results in the presence of harmful harmonic distortions. However, lack of recording details disallows further conclusions.

The Rite of Spring graphs show actual live orchestral music recorded directly to DSD format. At moments of mostly silence, the signal noise floor does not approach levels achievable with current PCM CD specifications. However, for the 1 kHz test tone, which for other frequencies is silent, the recording shows that the noise floor is at levels beyond those achievable with current PCM CD specifications. Therefore, the constraint in the system is the recording analog hardware, not the DSD converter. An interesting detail from the graphs is the presence of peaks at the video sweep frequency. Significant amounts of commercial recordings, in any format, have suffered this defect, yet no major concern for this fault has been publicized. If high frequency peaks of considerable amplitude (nearly -90 dB in this specific case) have not been documented as cause for signal quality degradation, it is hardly credible any other harmonic distortion under this level should be of concern. As a result, the THD statistics from previous SDM performance analysis should not be a considerable factor of the listening tests results.

When the Rite of Spring file was processed through the MMS for DSD to PCM conversions, the results confirmed this system is successful for commercial audio processing; hence, it not only works with simple sinusoidal signals. With the exception of the obvious filtering effect close to the Nyquist value for a 88.2 kHz signal, 44.1 kHz, the multi-bit signal is, in the frequency domain, visibly identical to its one-bit equivalent. This result once again confirms that a 24-bit signal can accurately preserve a DSD signal.

E. Listening Tests

The listening tests confirmed the hypothesis that no one could accurately determine the difference between a 24-bit 88.2 kHz recording and the same recording converted to DSD quality; therefore, confirming audibly lossless conversions. The results also showed that some people could precisely tell the difference between a 24-bit 88.2 kHz recording and the same recording converted to CD quality. In particular, two people scored over 80% in this second test, but even so, it is not high enough to state the difference was clearly audible.

Given Test 2 involved considerable signal degradation versus Test 1, i.e. from 24-bits 88.2 kHz sampling frequency to 16-bits 44.1 kHz sampling frequency, it was expected that less people would decipher correctly Test 1 versus Test 2. The tests results concurred by showing that the total percentage for the first test was lower than the total percentage of the second test. That the total percentage of Test 2 had a trivial difference between the total percentage of Test 1 can be attributed to the length of the whole tests process, which would cause hearing fatigue in some listeners prior to finishing the second test. This last statement was verified by a quick verbal review of the process with each subject, after finishing the tests. To avoid this last outcome in the results of Test 1, the high-resolution format conversions, every participant completed the tests in the same order.

V. Conclusions

The only downside from DSD to 24/88.2 PCM conversions is the obvious frequency bandwidth limitation, which is arguably not a downside at all. However, PCM 24-bits to DSD conversions do undergo some minor defects, such as reduced dynamic range and possible harmonic distortions. Even so, these so-called minor effects are not audible, as shown by the listening tests.

DSD produced with a fifth order SDM can achieve a signal to noise ratio of about 116 dB. 24-bits PCM with triangular probability density function dithering achieves a SNR of about 141 dB. State of the art recording and playback analog hardware technology barely achieves dynamic range of nearly 120 dB [10]. Of course, there is no venue that could possibly allow such low noise level recordings.

If wavelet/perfect reconstruction synthesis filtering could accurately reproduce a one-bit signal, even if very high frequency content has been replaced by comparable noise, then there would be a system capable of producing lossless conversions between DSD and PCM formats. However, this was not the case, therefore, it was not possible to find methods of lossless conversions. The lack of a perfect reconstruction system obliges the use of lossy conversions, which in the end proved to be audibly lossless. The listening tests, which confirmed this result, were carried out with equipment that is better than the average mainstream audio equipment.

Current DSD cannot surpass 24-bits PCM in with respect to SNR and harmonic distortions; not even a seventh-order SDM system. Higher than seventh-order systems are very unlikely to perform in a stable manner and still improve output specifications. However, the need to surpass 24-bits PCM is, to this date, unnecessary and pointless. What appears to be the case is that current DSP audio modulation systems have a lower than needed noise floor and harmonic distortions amount, therefore reaching a level of which it is irrelevant in which format the music content is stored.

Table 2 shows a précis of the performance of the SDM system for DSD signals and the PCM system for 24-bit 88.2kHz sampling frequency signals designed for this thesis.

Table 2: Précis of the results of the systems designed for this thesis

	DSD	PCM (24-bit Fs = 88.2kHz)
SNR *maximum amplitude input	5^{th} order – 116 dB 7^{th} order – 132 dB	141 dB
SNR for - 40 dB input	5^{th} order –	141 dB
Harmonic Distortions	Present in input amplitudes between ≈ -40 dB & -120 dB	Not present
Transient Response	Very Good, some high frequency noise is present	Very Good
Phase Response *Up to 30 kHz	Very Good	Very Good

As mediums both SACD and DVD-A formats offer dual layers, multi-channel reproduction, copy protection, lossless compression and video content. Moreover, present release of new technology such as Blue-Ray and HD-DVD discs, present extended physical capability of the discs, thus making pointless any possible argument about data rate limitations. However, the improvement in audio quality, though perceptible, does not appear to be enough to drive the CD accustomed world into these high-resolution formats. Advances in digital audio technology should make better analysis of the neurological fundamentals of the complete human listening system. Unless better understanding of this system is realized, it appears we have reached a level of audio quality enough to discriminate between what is needed in a format and overkill.

A. Future Work and Recommendations

Additional analysis of this work would require further development in perfect reconstruction techniques so that decomposition analysis can be achieved without any aliasing and magnitude distortion, while maintaining linear phase. The process should also be able of reconstructing a one-bit signal without the high frequency original signal information (high frequency content depends on the intermediate PCM chosen format).

While of uncertain value, additional listening tests similar to those completed in this thesis could be prepared using state of the art equipment, which could offer an extended bandwidth and lower noise levels, thus taking further advantage of the high-resolution formats. While this equipment does exist, it is still far beyond the financial reach of the average consumer.

A recommendation for future work involves detailed analysis of filtering effects in the processed audio, to determine if details such as transient pre-response, impulse response and ringing cause any harmful effect on the conversions. However, if any effect is considered harmful, it is doubtful the effect will be audible.

VI. Bibliography

[1] Sony Electronics Inc. and Philips Electronics N.V, "Super Audio Compact Disc - A Technical Proposal" [online], 1997 [cited Jan. 29, 2003], available from World Wide Web: <http://www.sel.sony.com/SEL/consumer/dsd/dsd.pdf>.

[2] Sony Corporation and Royal Philips Electronics, "Super Audio Compact Disc - A Technical Overview" [online], Sep. 2001 [cited Jan. 29, 2003], available from World Wide Web: <http://www.superaudio-cd.com/documents/EU-2001_0917.zip>.

[3] Seoul Sound Technology Group, "Direct Stream Digital (DSD)" [online], Seoul Sound Technology Group Ltd., [cited Jan. 27, 2003], available from World Wide Web: <http://www.seoulsound.co.kr/sacdtech4.htm>.

[4] John Atkinson, "Sony SCD-1 Super Audio CD/CD player: Direct Stream Digital - Sidebar 1: Direct Stream Digital" [online], *Stereophile Magazine online archives/reviews*, Nov. 1999 [cited Jan. 27, 2003], available from World Wide Web: <http://www.stereophile.com/showarchives.cgi?180:7>.

[5] Panasonic-Europe, "DVD-Audio Benefits" [online], Matsushita Electric Europe (HQ) Ltd 2003, [cited Apr. 22, 2003], available from World Wide Web: <http://www.panasonic-europe.com/homecinema/main.asp?lang=en>.

[6] Richard Elen, "DVD-Audio Reality" [online], *Audio Media*, Apr. 1999 [cited Mar. 12, 2003], available from World Wide Web: <http://www.audiomedia.com/archive/features/uk-0499/uk-0499-dvd/uk-0499-dvd.htm>.

[7] John Kellogg, "DVD-Audio: A Producer's Primer" [online], Multichannel Audio and Music Production, Dolby Laboratories, 2002 [cited Feb. 20, 2003], available from World Wide Web: <http://www.dolby.com/tech/m.br.0004.DVDAudio.html>.

[8] TimeforDVD.com, "DVD-Audio-Tutorial" [online], http://www.timefordvd.com/, 2002 [cited Feb. 20, 2003], available from World Wide Web: <http://timefordvd.com/tutorial/DVD-AudioTutorial.shtml>.

[9] Richard Elen, "Beyond the Pale – High Resolution Audio" [online], *Audio Media*, Oct. 1999 [cited Mar. 12, 2003], available from World Wide Web: <http://www.ambisonic.net/pdf/hiresaudio.pdf>.

[10] Richard Elen, "Battle of the Discs DVD-A vs. SACD" [online], The Audio Revolution, Inc., Aug. 2001 [cited Mar. 12, 2003], available from World Wide Web: <http://www.audiorevolution.com/equip/index.html>.

[11] Niklas Ladberg, Ing. Öhman, Marten Kihlberg and Rod Elliott, "CD vs. SACD vs. DVD-A" [online], Elliott Sound Products, Aug. 2002 [cited Feb. 20, 2003], available from World Wide Web: <http://www.sound.westhost.com/cd-sacd-dvda.htm>.

[12] M.O.J. Hawksford, "Bitstream versus PCM debate for high-density compact disc" [online], University of Essex, Centre for Audio Research and Engineering © Acoustic Renaissance for Audio, 1995 [cited Mar. 7, 2003], available from World Wide Web: <http://www.meridian-audio.com/ara/bitstrea.htm>.

[13] Jonathan Scull, "Sony SCD-1 Super Audio CD/CD player: Direct Stream Digital - *Table 1: SACD vs. CD*" [online], *Stereophile Magazine online archives/reviews*, Nov. 1999 [cited Jan. 27, 2003], available from World Wide Web: <http://www.stereophile.com/showarchives.cgi?180:15>.

[14] A.V. I. Rosti, "1-bit A/D and D/A Converters" [online], PhD Student in the Machine Intelligence Laboratory, Cambridge University Engineering Department, Nov. 2002 [cited Feb. 12, 2003], available from World Wide Web: <http://www.cs.tut.fi/~rosti/1-bit/>.

[15] M.N. Harris, et al, "Effects in High sample Rate Audio Material" [online], dCS White Papers, 1998 [cited Mar. 12, 2003], available from World Wide Web: <http://www.dcsltd.co.uk/papers/effects.pdf>.

[16] J. Robert Stuart, “Coding High Quality Digital Audio” [online], Meridian Audio Ltd, Stonehill, Stukeley Meadows, Huntingdon, PE18 6ED, United Kingdom, Dec. 1997 [cited Feb. 20, 2003], available from World Wide Web: <www.meridian-audio.com/ara/coding2.pdf >.

[17] M.O.J. Hawksford, “An Introduction to Digital Audio”, IEE Tutorial Colloquium: Audio Engineering, Essex University, March 9, pp. 1/1-114.

[18] J.C. Candy, G.C. Temes, “Oversampling Methods for Data Conversion”, in *IEEE Pacific Rim Conference on Communications, Computers and Signal Processing*, vol.2, May 9-10, 1991, pp. 498 -502.

[19] P.M. Aziz, H.V. Sorensen, J. Vn Der Spiegel, , “An Overview of Sigma-Delta Converters”, AT&T Bell Labs., Murray Hill, NJ*, IEEE Signal Processing Magazine*, vol. 13, Jan. 1996, pp. 61 -84.

[20] R.W. Stewart, “An Overview of Sigma Delta ADCs and DAC devices”, Signal Process. Div., Strathclyde Univ., Glasgow, in *Oversampling and Sigma-Delta Strategies for DSP, IEE Colloquium on*, 23 Nov 1995, pp. 1/1-1/9.

[21] J.C. Candy, O. Benjamin, “The Structure of Quantization Noise from Sigma-Delta Modulation”, Bell Laboratories, Holmdel, NJ, USA, in *Communications, IEEE Transactions on [legacy, pre - 1988]*, vol. 29, Sep. 1981, pp. 1316- 1323.

[22] J.C. Candy, G.C. Temes, “A tutorial discussion of the oversampling method for A/D and D/A conversion”, Sch. of Eng., California Univ., Los Angeles, CA, in *Circuits and Systems, 1990., IEEE International Symposium on*, vol. 2, 1-3 May 1990, pp. 910-913.

[23] James Boyk, “There’s Life Above 20 Kilohertz! A Survey of Musical Instrument Spectra to 102.4 KHz” [online], California Institute of Technology, May 2000 [cited Apr. 26, 2003], available from World Wide Web: <http://www.cco.caltech.edu/~boyk/spectra/spectra.htm>.

[24] Derk Reefman, Erwin Janssen, "Signal processing for Direct Stream Digital – *A tutorial for digital Sigma Delta modulation and 1-bit digital audio processing*" [online], Dec 2002, [cited Jan. 29, 2003], available from World Wide Web: <http://www.superaudiocd.philips.com/Assets/Downloadablefile/wp-2323.pdf>

[25] Robert A. Wannameker, Stanley P. Lipshitz, John Vanderkooy, J. Nelson Wright, "A Theory of Nonsubtractive Dither", in *IEEE Transactions on Signal Processing*, vol. 48, Feb. 2000, pp. 499-516

[26] Sanjit Mitra, "Digital Signal Processing – A Computer Based Approach 2nd ed.", McGraw-Hill Irwin, 2001

[27] M.O.J. Hawksford, "Time-quantized frequency modulation with time dispersive codes for the generation of sigma-delta modulation", in *Proceedings of the AES 112th convention*, Preprint 5618, 2002, Munich

[28] C. Dunn, M. Sandler, "Efficient linearization of sigma-delta modulators using single-bit dither", Department of Electronic and Electrical Engineering King's College, London, *Electronic Letters*, 1995, vol. 31, no.12, pp. 941-942

[29] R.C. Ledzius, J.I. Irwin, "The Basis and Architecture for the Reduction of Tones in a Sigma-Delta DAC", *IEEE Trans. Circuits and Systems – II: Analog and Digital Signal Processing*, 1993, vol. 40, pp. 429 – 439

[30] Royal Phillips Electronics, "Super Audio CD Audio Signal Properties", *Royal Phillips Electronics*, 2003, ver. 1.3, [cited Jan. 23 2003], available from World Wide Web: <http://www.superaudiocd.phillips.com>

[31] Mark J. T. Smith, Thomas P. Barnwell, "Exact Reconstruction Techniques for Tree-Structured Subband Coders", 1986, *IEEE Transactions on Acoustic, Speech and Signal Processing*, vol. 34, no. 3, pp. 434 – 441

[32] Xiang-Gen Xia, Bruce W. Suter, "Construction of Perfect Reconstruction Time-Varying FIR Multirate Filter Banks with Overlaps", 1994, *IEEE*, pp. 120 – 123

[33] Ajit. S. Bodardikar, Mysore R. Raghuveer, B.S. Adiga, “Perfect Reconstruction Circular Convolution Filter Banks and their Application to the Implementation of Bandlimited Discrete Wavelet Transform”, 1997, *IEEE*, pp. 3665 – 3668

[34] A. Farras Abdelnour, Ivan W. Selesnick, “Design of 2-band Orthogonal near-symmetric CQF”, 2001, *IEEE*, Polytechnic University Electrical Engineering, Brooklyn, NY, pp. 3693 – 3696

[35] N.J. Fliege, “Multirate Digital Signal Processing”, John Wiley & Sons, 1995

[36] The MathWorks, Inc., MATLAB Help, Matlab version 6.5.0.180913a (R13), June 2002

[37] Stanley P. Lipshitz, John Vanderkooy, “Why 1-Bit Sigma-Delta Conversion is Unsuitable for High-Quality Applications”, in *AES Convention Paper 5395* Presented at the 110th Convention 2001 May 12–15 Amsterdam, The Netherlands

Appendix A

Matlab source code for the fifth-order Sigma-Delta Modulator

```
%Fifth-order Sigma-delta modulator
function [sd]=sigde5(osin)
%Coefficients and Resonators
c =[2048 768 128 16 1];
f =[0.000496 0.001789];
%Initialization
s = zeros(1,5);        %integrator outputs
sd(1:length(osin))=0;
for n = 1:length(sd)
   summ = c(1)*s(1)+c(2)*s(2)+c(3)*s(3)+c(4)*s(4)+c(5)*s(5);
   %Dithering
          summ = summ + (.007 + (-.007-.007) * rand(1,1));
   %1-bit quantizier
   if summ >= 0                    %1-bit quantizer
      sd(n)=1;
   else
      sd(n)=-1;
   end
   %Main system
   s(5)=s(5)+s(4);                %integrator 5
   if s(5)>2804.5
      s(5)=2804.5;
   elseif s(5)<-2804.5
      s(5)=-2804.5;
   end
   s(4)=s(4)+s(3)-f(2)*s(5);      %integrator 4
   if s(4)>194.5
      s(4)=194.5;
   elseif s(4)<-194.5
      s(4)=-194.5;
   end
   s(3)=s(3)+s(2);                %integrator 3
   if s(3)>39.5
      s(3)=39.5;
   elseif s(3)<-39.5
      s(3)=-39.5;
   end
   s(2)=s(2)+s(1)-f(1)*s(3);      % integrator 2
   if s(2)>11
      s(2)=11;
   elseif s(2)<-11
      s(2)=-11;
   end
   s(1)=s(1)+(osin(n)-sd(n));   %integrator 1
   if s(1)>3.2
      s(1)=3.2;
  elseif s(1)<-3.2
      s(1)=-3.2;
  end
end
```